REEL – C
349
A.T.I.
8949

UNCLASSIFIED

ARR No. 5A03

D52.1/Curtiss/1266

NATIONAL ADVISORY COMMITTEE FOR AERONAUTICS

WARTIME REPORT

ORIGINALLY ISSUED

February 1945 as
Advance Restricted Report 5A03

AN INVESTIGATION OF A THERMAL ICE-PREVENTION SYSTEM FOR A C-46 CARGO AIRPLANE

I - ANALYSIS OF THE THERMAL DESIGN FOR WINGS, EMPENNAGE, AND WINDSHIELD

By Carr B. Neel, Jr.

Ames Aeronautical Laboratory
Moffett Field, California

NACA

WASHINGTON

NATIONAL ADVISORY COMMITTEE FOR AERONAUTICS

ADVANCE RESTRICTED REPORT

AN INVESTIGATION OF A THERMAL ICE-PREVENTION SYSTEM FOR A C-46 CARGO AIRPLANE

I - ANALYSIS OF THE THERMAL DESIGN FOR WINGS, EMPENNAGE, AND WINDSHIELD

By Carr B. Neel, Jr.

SUMMARY

This report, the first of a series on an investigation to develop a thermal ice-prevention system for the C-46 cargo airplane and to provide fundamental information concerning the performance and operation of the system, presents an analysis of the design of the thermal anti-icing equipment for the wings, the empennage, and the windshield. The purpose of the analysis was to establish the thermal requirements for the C-46 ice-prevention equipment on the basis of a certain temperature rise for all points on the heated surfaces of the wings and the empennage, and of a specified heat flow through the outer panel of the windshield. The rate of heat transfer from the wing and empennage surfaces was calculated by utilizing the airfoil pressure distributions for these surfaces measured in flight.

The design analysis showed that the thermal requirements for the anti-icing systems of the wings, the empennage, and the windshield were within the limits of practicability, although complete protection of the windshield might not be realized in the specific application when utilizing a secondary heat exchanger.

INTRODUCTION

For several years the NACA has been engaged in a research program to investigate the feasibility of utilizing the waste heat of airplane engine exhaust gases to heat those parts of an airplane that require protection from the formation of ice in order to provide safe and efficient operation of the airplane in icing conditions. In this thermal anti-icing method, the heat of the exhaust gases is transmitted to air in suitable heat exchangers located adjacent to the engines, and the heated air is then circulated through the airplane so that it passes along the inner surfaces of affected parts. The method has been demonstrated to be sound in successful applications to a Lockheed 12A airplane, a Consolidated B-24D airplane, and a Boeing B-17F airplane (references 1, 2, and 3, respectively). These applications were made at the Committee's Ames Aeronautical Laboratory, Moffett Field, Calif.

As a continuation of this general research program on aircraft ice prevention, the laboratory has undertaken a comprehensive investigation to develop a thermal ice-prevention system for a Curtiss-Wright C-46 cargo airplane. The investigation consists of a design analysis of the heat anti-icing system, design and construction of the exhaust-gas-to-air heat exchangers, fabrication and instrumentation of the complete system, and performance tests of the C-46 airplane equipped with the thermal ice-prevention system under dry air and natural icing conditions.

This report is the first of a series describing the investigation, and presents the design analysis of the thermal ice-prevention system for the wings, the empennage, and the windshield. Emphasis was placed on this phase of the investigation because it was believed necessary to establish a satisfactory theoretical basis for the design of the system before extensive application of the system could be accomplished. The investigation has been undertaken at the request and with the cooperation of the Air Technical Service Command of the U. S. Army Air Forces and with the assistance of the Curtiss-Wright Corporation.

TENTATIVE DESIGN OF THE THERMAL ICE-PREVENTION SYSTEM

A standard C-46 cargo airplane, shown in figure 1, was provided for the investigation. The tentative design of the thermal ice-prevention system, on which the subsequent analysis was made, was based on previous experience (references 1, 2, and 3). The important elements of the design are shown in figures 2, 3, 4, 5, and 6. The existing structure of the airplane and other practical considerations limited various factors of the design.

In this design the required supply of heated air for the ice-prevention system was provided by four exhaust-gas-to-air heat exchangers, two in each engine nacelle. The heat exchangers were located on the inboard and outboard sides of the nacelles so that the two exhaust-gas pipes from the collector rings on the engines led to the exhaust-gas entrances of the heat exchangers. On the basis of the design the outside air was passed through the exchangers and thence circulated through ducts to the wings, the empennage, and the windshield. The exchangers on the outboard sides of the nacelles supplied heated air to the wing outer panels, and the two inboard exchangers supplied heated air to the wing inboard panels, the empennage, and the windshield. The disposition of the heated air as considered in the analysis is shown in figure 2.

The proposed construction of the outboard wing leading-edge regions, which in this report include the airfoil sections forward of the 10-percent chord points, is illustrated in figure 3. Available dies made the corrugation-type passage shown in figure 3 most expedient for the internal circulation of heated air over the surfaces to be protected. The upper and lower corrugations were divided by a continuous spanwise slot at the 0-percent reference chord point in order to allow the entrance of heated air, which flowed chordwise between the corrugations and the outer wing skin. The location of essential wing structure at 10-percent chord required that the corrugations be terminated at that point. The baffle plate, which was located between the 5- and 6-percent chord points (because this location was most advantageous from the standpoint of fabrication) formed, with the leading-edge inner surface, the spanwise duct to distribute heated air to the corrugations.

Structural considerations required that most of the nose ribs be retained. However, the installation of a corrugated inner skin is known to add a certain amount of rigidity to wing and empennage structures, and accordingly the nose ribs outboard of station 292 (fig. 2) were omitted. A liner was installed along the inner edges of the nose ribs in order to give a smoother contour to the wing leading-edge duct than would be possible if the nose ribs were exposed to offer resistance to the flow of heated air. The liner was terminated at station 292 because the design called for omission of the nose ribs outboard of that point. Holes were cut in the nose-rib liner as shown in figure 3 to allow the passage of heated air from the leading-edge duct to the corrugation entrances. Thus the heated air passed along the leading-edge duct (region 1 of fig. 3), through the corrugation gaps (region 2) into the space between the baffle and front spar (region 3), through the holes in the spars, and from the afterbody of the wing (region 4) out through exit holes in the aileron and flap-hinge regions (region 5).

The distribution of heated air for the empennage and details of the leading-edge region construction of these surfaces, as considered in the analysis, are shown in figures 4 and 5, respectively. The proposed horizontal-stabilizer and vertical-fin thermal systems are similar to that of the wing outer panels. However, the nose ribs were eliminated entirely and the leading-edge ducts were formed by the corrugations and the baffle plate.

The tentative windshield thermal system design is illustrated in figure 6, which shows the pilot's windshield only. This design consists of two glass panels spaced with a constant gap between them. The existing windshield outer panels are made up of two layers of semi-tempered plate glass separated by a layer of vinyl plastic. In the tentative anti-icing-system design the heated air entered the plenum chamber at the base of the windshield panels, passed upward through the gap between the outer and inner glass panes, and exited at the top into the cabin, thus heating the pilot's compartment as well as protecting the windshield from icing. Because of this special design feature, however, it was necessary to include in the windshield anti-icing system a secondary heat exchanger in order to prevent carbon monoxide from entering the cabin in the event of a failure of the exhaust-gas-to-air heat exchanger. The secondary heat exchanger transferred heat from the primary heating air, supplied by the inboard exhaust-gas-to-air heat exchangers, to the secondary air from the ambient stream. The windshield ice-prevention system included valves by means of which the secondary heated air could be discharged directly into the pilot's compartment during periods when windshield heating is not necessary.

TEST PROCEDURE

The airfoil pressure distributions over the wings and the empennage were obtained experimentally in flight in order to provide a basis in the analysis for calculating the heat transfer from the heated surfaces of the airplane to the outside air. This method of analysis is believed to be a more rational procedure for obtaining the heat requirements of these surfaces than the methods used in previous designs of aircraft thermal ice-prevention systems.

The pressure distributions were measured by means of pressure belts, as described in reference 4. Data were obtained for stations 82, 157, 292, and 382 on the outer panel of the right wing; stations 72, 127, and 172 on the right stabilizer; and stations 122 and 172 on the fin. The airfoil sections of the wing consist of an NACA 23017 section of 16.5-foot chord at station 0, tapering to an NACA 4410.5 section of 7.1-foot chord at station 393, which is 19 inches inboard of the wing tip joint (station 412). The wing at station 393 has three degrees of washout with respect to station 0. The horizontal stabilizer and the vertical fin both have NACA 0010 airfoil sections throughout.

The pressure belts were wrapped around the leading edges of the wing and empennage surfaces and extended back approximately to the 20-percent chord point. Typical installations are shown in figures 7 and 8, and the water manometer used for indicating pressures at the empennage pressure belts is shown in figure 9.

Previous experience with similar thermal ice-prevention installations has indicated that a satisfactory assumed design flight condition is cruising engine power for maximum range at a pressure altitude of 18,000 feet. The first two flights were made at a pressure altitude of 18,000 feet with engine-power setting to approximate maximum range of the airplane, and the pressure distributions for the two outboard stations of the wing and the horizontal stabilizer were obtained. The indicated airspeed was established at 155 miles per hour under level-flight conditions. The required indicated airspeed having been determined, the remaining pressure distributions were secured at 5000 feet pressure altitude and approximately 155 miles per hour indicated airspeed. It was assumed that at the same indicated airspeed the angle of attack of the airplane and the airfoil pressure distribution are unchanged with variations in altitude for level flight at a constant load condition. The gross weight of the airplane and crew, in flight, for all the pressure-belt tests was approximately 39,000 pounds. During the flights, the water manometers indicating the pressures at the pressure belts were allowed to reach equilibrium, and the manometers were photographed to record the readings. Adter each flight, the pressure belts were moved to the next station and the procedure was repeated.

SYMBOLS

For the purpose of analysis, the following symbols were used:

A cross-sectional area, square feet

c length of airfoil chord, feet

c_p specific heat of air, British thermal units per pound, degree Fahrenheit

D_e equivalent diameter of a duct, equal to $4m$, feet

f friction factor for air flow in ducts

g gravitational acceleration, taken as 32.2 feet per second, second

G weight rate of air flow per unit of cross-sectional area, pounds per second, square foot

h surface heat-transfer coefficient, British thermal units per hour, square foot, degree Fahrenheit

k thermal conductivity of air, British thermal units per hour, square foot, degree Fahrenheit per foot

L distance around airfoil surface, measured chordwise from 0-percent-chord point, feet

m hydraulic radius, or ratio of cross-sectional area to wetted perimeter in a duct, feet

N length of air duct or corrugation, feet

Nu Nusselt number, equal to hD_e/k

p calculated static pressure, pounds per square foot or inches of water

p_f measured pressure differential from free-stream static pressure, inches of water

p_e free-stream static pressure, pounds per square foot

P pressure coefficient, equal to p_f/q_o

q_o free-stream dynamic pressure, inches of water

Q rate of heat flow, British thermal units per hour

R gas constant for air, taken as 53.3 feet per degree Fahrenheit

R_c body Reynolds number, equal to cV_o/ν

Re Reynolds number, equal to GD_e/μ

s distance around airfoil surface, measured chordwise from stagnation point, feet

S surface area, square feet

t temperature, degrees Fahrenheit

T temperature, degrees Fahrenheit absolute

v specific volume, cubic feet per pound

V local ambient-air velocity outside the boundary layer, feet per second

V_i airplane indicated airspeed, miles per hour

V_o free-stream velocity, feet per second

w weight rate of air flow per corrugation, pounds per hour

W_a weight rate of air flow, pounds per hour

x distance along chord line, measured from 0-percent-chord point

γ density of air, pounds per cubic foot

δ boundary-layer thickness, feet

λ constant dependent on shape of boundary-layer velocity profile

μ absolute viscosity of air, pounds per second, feet

ν kinematic viscosity of air, equal to μ/γ, square feet per second

For the sake of clarity, other symbols, not presented here, will be defined when introduced.

The values of c_p, μ, and k for air, subsequently used in the calculations, were taken from figure 10, which contains plots of data obtained from reference 5.

Use of Subscripts

The temperature, pressure, and specific volume subscript numbers refer to the temperature, the pressure, or the specific volume of the region to which the numbers apply (figs. 3 and 5). Thus, the temperature of the air in a corrugation, region 2, will be designated as t_2, the static pressure as p_2, and the specific volume as v_2.

Two subscript numbers refer to the flow of heat from one region to another. Thus, the heat-transfer coefficient for the air in a corrugation to the wing surface will be designated as h_{2-e}.

The subscript av refers to average conditions.

ANALYSIS OF WING AND EMPENNAGE THERMAL SYSTEMS

Past experience has indicated that a satisfactory design specification to insure ice prevention is the maintenance of the heated surfaces at approximately 100° F above ambient-air temperature during flight in dry air (no visible moisture) at a pressure altitude of 18,000 feet with cruising engine power for maximum range. Therefore, for the purpose of this analysis, the requirement of a minimum temperature rise of approximately 100° F for all points on the surface of the wing and the empennage between the 0- and 10-percent-chord points was established for the design flight conditions of 0° F ambient-air temperature, 18,000 feet pressure altitude, and 155 miles per hour indicated airspeed.

Preliminary investigation of the structure in which the system was to be installed indicated that essential wing structure precluded freedom of design. An analysis indicated, however, that a satisfactory thermal design could be obtained without altering this essential primary structure, and use could be made of existing die equipment for fabricating the inner skin. As a result, certain design factors were considered fixed at the start of the analysis, such as the extent of the heated region or the length of the corrugations, which was fixed by the location of essential structure at the 10-percent-chord point, and the corrugation size, which was determined by available dies. With those factors fixed, the analysis resolved itself into the adjustment of such variable factors as the heated-air flow rate and the pressure drop to satisfy the design specification. The analysis therefore consisted of the determination of (1) the boundary-layer characteristics from which the external heat-transfer coefficients could be calculated, (2) the adjustment of the heated-air flow rate to obtain the required surface temperature rise, and (3) the calculation of the resulting air-pressure drops to ascertain that equilibrium had been established. These phases are discussed hereinafter under appropriate sections of the report.

A trial-and-error process was employed in the calculation of the thermal and pressure values. A more elegant analysis was precluded by the great number of variables involved and the complicated relationships resulting when expressed in analytic form.

The analysis was made for the wing outer panel from station 11 to station 412, for the horizontal stabilizer from station 47 to station 190, and for the vertical fin from station 112 to station 192. The analytical study did not include consideration of the wing inboard panel or the tips of the wing, the stabilizer, or the fin.

Boundary-Layer Characteristics

The determination of the external heat-transfer coefficients is dependent upon knowledge of the characteristics of the boundary layer surrounding the heated surfaces. The pressure-belt data recorded during flight tests were used to calculate the coefficients of heat transfer from the airfoil surface to the boundary layer at each belt location. The differences between the measured static pressures at the belt orifices and the free-stream static pressure were determined and are designated as p_f. Table I presents all calculated values of $(1 - P)$ where $P = p_f/q_0$. A plot of $(1 - P)$ as a function of the chord in percent for wing station 82 is given in figure 11. Similar plots of airfoil pressure distribution were made for each set of pressure-belt data, but are not presented in this report. Values of (1 - P) were taken from these curves for convenient chord stations and corresponding values of the velocity ratio, V/V_0, were calculated by the equation

$$V/V_0 = \sqrt{1 - P} \tag{1}$$

which is derived from Bernoulli's equation for fluid flow. Figure 12 gives a curve of the velocity ratio thus obtained for flow over the wing at station 82.

The location of the laminar-separation point was determined as a function of the slopes of the velocity profile. The curves of velocity ratio were replaced by two straight lines (referred to as double-roof profiles in reference 6) the slopes of which closely approximated the slopes of the actual velocity profile. The ratios of the slopes of the double-roof profiles were calculated, and the ratios of the local velocity at separation to the maximum local velocity were obtained from figure 13, where b is the slope of increasing velocity and β is the slope of decreasing velocity. Figure 13 is a plot of the following equation which was obtained from footnote 1 on page 21 of reference 6,

$$\frac{U_s}{U_1} = \sqrt{1 - r\,(\theta_s - 1)} \tag{2}$$

where

U_s local velocity at laminar separation

U_1 maximum local velocity

r ratio of β to b

θ_s a function of r

For the upper surface at wing station 82,

$$\beta = 0.278$$

$$b = 6.00$$

Then

$$r = \frac{\beta}{b} = \frac{0.278}{6.00} = 0.0463$$

and from figure 13,

$$\frac{U_s}{U_1} = 0.906$$

From figure 12,

$$\frac{V_{max}}{V_o} = \frac{U_1}{V_o} = 1.52$$

then

$$U_1 = 1.52\ V_o$$

and

$$\frac{U_s}{V_o} = 0.906 \times 1.52 = 1.378$$

Thus, by extending the decreasing velocity curve beyond the limits of the graph shown in figure 12, it was found that separation occurred at $s/c \times 100 = 27$.

Transition from laminar to turbulent flow over the airfoil surfaces was considered to take place at the laminar-separation point. In all cases, the separation point was established well aft of the region to be heated. Since the boundary layer was found by the calculations to be laminar over the heated areas, the method presented in reference 7 was used to determine the boundary-layer thickness. The equation for boundary-layer thickness δ in the laminar-flow region, as given in reference 7, is

$$\delta^2 = \frac{5.3c^2}{R_c}\left(\frac{s_1/c}{V_1/V_o}\right)\left[\frac{\int_0^{s_1/c}\left(\frac{V}{V_o}\right)^{8.17} d\left(\frac{s}{c}\right)}{\left(\frac{V_1}{V_o}\right)^{8.17}\left(\frac{s_1}{c}\right)}\right] \qquad (3)$$

where the subscript 1 denotes the point on the airfoil surface at which the boundary-layer thickness is being computed.

The evaluation of $\int_0^{s_1/c} \left(\frac{V}{V_o}\right)^{8.17} d\left(\frac{s}{c}\right)$ was made graphically in each case, using curves of the functions of velocity ratio similar to those shown in figure 14. The values of the constant $5.3c^2/R_c$ were determined from the true airspeed and the chord length.

For wing station 82,

$$c = 14.51 \text{ feet}$$

The indicated airspeed deviated slightly from the desired value of 155 miles per hour during each flight when the pressure-belt data were recorded. The indicated airspeed was 151 miles per hour during the flight when belt data were obtained for station 82. Correcting the indicated airspeed to free-stream velocity, using the reciprocal square root of density ratio at 18,000 feet pressure altitude, gives

$$V_o = 1.325\ V_i = 1.325 \times 151 = 200 \text{ miles per hour}$$

$$= 293.5 \text{ feet per second}$$

At 18,000 feet pressure altitude and 0° F free-air temperature,

$$\gamma = \frac{p_o}{RT} = \frac{1058}{53.3 \times 460} = 0.0431 \text{ pounds per cubic foot}$$

From figure 10,

$$\mu = 1.104 \times 10^{-5} \text{ pound per second, feet at } 0^\circ \text{ F}$$

Then

$$\nu = \frac{\mu}{\gamma} = \frac{1.104 \times 10^{-5}}{0.0431} = 0.000256 \text{ square foot per second}$$

$$R_c = \frac{cV_o}{\nu} = \frac{14.51 \times 293.5}{0.000256} = 16.64 \times 10^6$$

and

$$\frac{5.3c^2}{R_c} = \frac{5.3 \times 14.51^2}{16.64 \times 10^6} = 0.0000671$$

Since the value of δ is indeterminate at the stagnation point, the following approximation recommended in reference 7 was used:

$$\delta^2_{stag} = \frac{c^2}{5R_c}\frac{\bar{r}}{c} \tag{4}$$

where $\bar{r}$ is the radius of curvature at the stagnation point.

For wing station 82,

$$\bar{r} = 5.26 \text{ inches}$$

and

$$\delta^2_{stag} = \frac{14.51^2}{5 \times 16.64 \times 10^6} \times \frac{5.26}{14.51 \times 12} = 7.65 \times 10^{-8}$$

$$\delta_{stag} = 2.76 \times 10^{-4} \text{ feet}$$

The values of $\bar{r}$ were approximated from the airfoil-section loft lines. A curve of the calculated boundary-layer thickness for wing station 82 is shown in figure 12.

Calculation of Heat-Transfer Coefficients

The coefficient of convective heat transfer from a heated surface to the laminar boundary air layer can be expressed as a function of the boundary-layer thickness by the equation

$$h_{6-7} = \frac{k\lambda}{\delta} \tag{5}$$

The value of λ was considered to be a constant (0.765) from the stagnation region to the minimum pressure point, and then was considered to decrease linearly from 0.765 to 0 at the laminar-separation point. (See reference 7.)

Since the indicated airspeed varied slightly for each flight when pressure-belt data were obtained, the calculated values of h_{6-7} were corrected to give corresponding values at the design airspeed, 155 miles per hour, by the equation

$$(h_{6-7})_{corr} = h_{6-7}\sqrt{\frac{155}{V_i}} \qquad (6)$$

A tabulation of the results of intermediate steps taken to calculate the boundary-layer thickness and the external heat-transfer coefficient for wing station 82 is presented in table II. The curves of calculated values of corrected external heat-transfer coefficients from the pressure-belt data are presented for all wing and empennage stations investigated in figures 15 to 23. Because the flow was assumed to be symmetrical over the vertical fin, the heat-transfer coefficients were calculated for one side only, as shown in figures 22 and 23. The curves show that in all cases the external heat-transfer coefficient increases as the chord and the leading-edge radius decrease, with the exception of station 127 of the horizontal stabilizer, at which point the calculated heat-transfer coefficient is highest for the stabilizer. It is believed that this increased heat-transfer coefficient for station 127 of the stabilizer is due to the effect of the higher air velocities in this region caused by the propeller slipstream.

Air-Flow and Heat-Flow Calculations

The weight of air required to produce the desired skin-temperature rise was evaluated on the basis of tentatively fixed dimensions and coverage of the corrugations and the allowable inlet-air temperature. The conditions, which must exist for the establishment of a satisfactory flow distribution through the system, are that the pressure losses along all streamlines must be equal and that the skin-temperature rise must provide ice protection. Pressure equilibrium for the system was established by calculating the losses in the corrugations at the wing-root and wing-tip sections and adjusting the baffle position to provide spanwise duct loss equal to the difference between the two chordwise corrugation losses.

For the calculations to determine the required heated-air flow to produce a desired temperature rise, the leading-edge region was divided into three segments as follows: 0- to 3-percent chord, 3- to 7-percent chord, and 7- to 10-percent chord. Since the corrugation passages were of constant cross section, the exact value of the design skin-temperature rise (100° F) could not be established at all points on the leading edge - that is, some variation was unavoidable. The procedure followed was to assume 100° F rise for the skin from 0- to 3-percent chord, calculate the required heated-air flow, and then determine the temperature rise aft of 3-percent chord produced by that air flow. After satisfactory air flows were established for the corrugation passages at the wind root and tip, the baffle location was determined. The establishment of pressure equilibrium, which was accomplished by a trial-and-error method, required slight changes in the heated-air distribution which, in turn, produced changes in the skin-temperature distribution. These changes, however, were not excessive and the final skin temperatures all were approximately equal to the design requirement. The detailed application of the general procedure outlined above for the wing outer-panel and empennage leading-edge systems is presented in sufficient detail to illustrate the process; the remainder of the analysis is presented in tabular form.

First approximation of required heated-air distribution.- The first calculation consisted in establishing the heated-air flow required at two stations, one at the wing root and one at the wing tip, to produce a skin-temperature rise of 100° F from 0- to 3-percent chord. Considering the flow in a passage formed by a single corrugation on the upper surface at station 82, the heat flow from a 1-inch strip of skin to the ambient air must be balanced by an equal flow of heat from the air in the passage to the skin, or

$$h_{6-7}\ S(t_6 - t_7) = h_{2-6}\ S(t_2 - t_6) \qquad (7)$$

On the basis of previous experience, it is believed that the maximum safe operating temperature for air in contact with aluminum-alloy structures is between 300° and 400° F. Consequently, the air-temperature rise above ambient air from the heated-air source was assumed to be 300° F. If a 10° air-temperature drop is assumed between the heated-air source and station 82, the temperature of the air at the corrugation entrance will be 290° F. The air-temperature drop through the upper corrugation from 0- to 3-percent chord was found by trial and error to be 87° F. Therefore, the average temperature of the air in the corrugation will be

$$(t_2)_{av} = 290 - \frac{87}{2} = 246^\circ \text{ F}$$

Since the design free-air temperature t_7 is 0° F, the required skin temperature t_6 will be 100° F. The average external heat-transfer coefficient h_{6-7} for the 0- to 3-percent-chord upper surface, obtained by graphical integration from figure 15, is 15.1 Btu per hour per square foot, degree Fahrenheit. The required internal heat-transfer coefficient, as obtained from equation (7), is as follows:

$$h_{2-6} = \frac{h_{6-7}\,(t_6 - t_7)}{t_2 - t_6} \qquad (8)$$

Substituting the above values into equation (8) gives

$$h_{2-6} = \frac{15.1 \times (100 - 0)}{246 - 100} = 10.34 \text{ Btu per hour, square foot, degree Fahrenheit}$$

The equivalent diameter for a corrugation is 0.0192 foot. Using the value of thermal conductivity for air at 246° F obtained from figure 10, the Nusselt number is

$$Nu = \frac{h_{2-6}\,D_e}{k} = \frac{10.34 \times 0.0192}{0.0193} = 10.30$$

The corresponding Reynolds number is taken from figure 24, which gives the Reynolds and Nusselt number relationship obtained from figure 76, page 171, of reference 8 for the flow of air inside pipes.

$$Re = \frac{GD_e}{\mu} = 2.50 \times 10^3$$

Using the value of absolute viscosity for air at 246° F as obtained from figure 10 gives

$$G = 2.50 \times 10^3 \times \frac{1.51 \times 10^{-5}}{0.0192} = 1.965 \text{ pounds per second, square foot}$$

The cross-sectional area of a single corrugation is 0.000651 square foot. The weight-rate flow of heated air required to raise the temperature of the strip of skin analyzed 100° F, then, is

$$w = G \times A = 1.965 \times 3600 \times 0.000651 = 4.61 \text{ pounds per hour per corrugation}$$

To check the heat balance, the total heat transferred from the strip of skin to the ambient air is assumed to be equal to the total heat removed from the heated air in passing through the corrugation from 0- to 3-percent chord:

$$h_{6-7}\ S(t_6 - t_7) = wc_p\ \Delta t_2 \tag{9}$$

where $S = L/12$ for a single corrugation. The value of L is obtained from figure 25. Then

$$h_{6-7}\ \frac{L}{12}\ (t_6 - t_7) = 15.1 \times \frac{0.774}{12} \times 100 = 97.4 \text{ Btu per hour}$$

and

$$wc_p\ \Delta t_2 = 4.61 \times 0.242 \times 87 = 97.0 \text{ Btu per hour}$$

Similar calculations were made for the wing upper surface at station 382. The air-temperature drop from stations 82 to 382 was assumed to be 30° F, which on the basis of flight data from similar designs appeared to be a reasonable value. Based on this assumption, the temperature of the air entering the corrugation then will be 260° F. The air flow necessary to raise the skin temperature 100° F for the 0- to 3-percent-chord section was found to be 7.01 pounds per hour per corrugation. The analysis was completed for the upper corrugations of wing stations 82 and 382, using the previously established air-flow rates to determine the temperature rise of the skin aft of the 3-percent-chord point.

The air-pressure drops through the upper corrugations at stations 82 and 382 were calculated for these air-flow rates, using the equation

$$p_1 - p_3 = \frac{G^2\ (v_3 - v_1)}{g} + \frac{f_{av}\ NG^2\ v_{av}}{2gm} \tag{10}$$

which is a form of equation (22c), page 138 of reference 8, where the subscripts 1 and 3 represent the regions shown in figures 3 and 5. The values of the friction factor f_{av} were obtained from figure 26, which is taken from figure 51, page 118 of reference 8. It was found that the pressure loss through the corrugation at station 382 was greater than that at station 82, and therefore this air distribution never could be obtained with the same size of corrugations at the two stations. Consequently, the surface temperature for the section from 0- to 3-percent chord could not be raised exactly 100° F simultaneously at the two stations. Previous experience has shown that after an approximate required value of air-flow rate has been found, based on the design skin-temperature rise, the actual air-flow rate which will give pressure equilibrium is most readily established by assuming air-flow rates, checking pressure drops by an approximate method, and then calculating the skin-temperature rises. This procedure, therefore, was followed for the remaining wing-outer-panel calculations.

Recalculation of heated-air distribution.- The approximate method of determining the pressure loss in the corrugation passages consisted in using the second term only of equation (10), since the first term is of minor importance and can be introduced as a refinement of the final calculations without affecting the results to any appreciable extent.

For the upper corrugation at wing station 82 an air-flow rate, based on the preliminary calculations, of 5.00 pounds per hour was assumed. Then

$$G = \frac{W}{A} = \frac{5.00}{0.000651 \times 3600} = 2.13 \text{ pounds per second, square foot}$$

Based on this air-flow rate, the air-temperature drop in the corrugation from 0- to 3-percent chord was found by trial to be 84° F. Then the average air temperature is

$$(t_2)_{av} = 290 - \frac{84}{2} = 248^\circ \text{ F}$$

Using the value of absolute viscosity for air at 248° F, obtained from figure 10, the Reynolds number is

$$R = \frac{GD_e}{\mu} = \frac{2.13 \times 0.0192}{1.52 \times 10^{-5}} = 2.69 \times 10^3$$

and from figure 24

$$Nu = \frac{h_{2-6}\, D_e}{k} = 10.9$$

Using the value of thermal conductivity at 248° F, obtained from figure 10, the available internal heat-transfer coefficient is

$$h_{2-6} = \frac{10.9 \times 0.0193}{0.0192} = 10.96 \text{ Btu per hour, square foot, degree Fahrenheit}$$

From figure 15,

$$h_{6-7} = 15.1 \text{ Btu per hour, square foot, degree Fahrenheit}$$

The average skin-temperature rise is calculated from the following equation:

$$t_6 = \frac{h_{2-6}\ t_2}{h_{2-6} + h_{6-7}} \qquad (11)$$

which is reduced from equation (7) when $t_7 = 0^\circ$ F. Thus,

$$t_6 = \frac{10.96 \times 248}{10.96 + 15.1} = 104^\circ \text{ F}$$

To check the heat balance, the total heat transferred from the 1-inch strip of skin to the ambient air is assumed to be equal to the heat transferred from the heated air in traveling from 0- to 3-percent chord (equation (9)). Substituting appropriate values gives

$$h_{6-7} \frac{L}{12} (t_6 - t_7) = 15.1 \times \frac{0.774}{12} \times 104 = 101.4 \text{ Btu per hour}$$

and

$$wc_p\ \Delta t_2 = 5.00 \times 0.242 \times 84 = 101.6 \text{ Btu per hour}$$

which show that thermal equilibrium has been established for this section.

Repeating the calculations for the sections aft of 3-percent chord, using the values of external heat-transfer coefficient from figure 15, the skin-temperature rises shown in table III for the upper surface at station 82 were obtained.

For an upper corrugation at station 382 the entering air temperature was assumed to be 260° F and the air-flow rate to be 6.20 pounds per hour per corrugation. The resulting skin-temperature rises were calculated and are presented in table III.

Pressure-loss calculations were made for the upper corrugations at stations 82 and 382 to determine if the pressure drop at station 382 was sufficiently less than the pressure drop at station 82 to allow a reasonable pressure drop through the leading-edge duct. In the succeeding pressure-drop calculations it will be shown that the required pressure equilibrium is attained with these established air-flow rates.

Before final pressure-loss calculations could be made, it was necessary to determine the air-flow rates through the lower corrugations at stations 82 and 382 and through the corrugations at the intermediate stations. The lower-corrugation air-flow rates are dependent upon the upper-corrugation flow rates, since the air-pressure drops through the upper and lower corrugations must be equal. After determining the necessary lower-corrugation air-flow rates by the process of trial and error, the resulting skin-temperature rises were calculated by the method previously outlined, using the values of L obtained from figure 27.

Arbitrary curves of heated-air-flow distribution, the general shape of which was based on experience, were then drawn through the points representing the flow rates established for stations 82 and 382. The assumed curves of the flow distribution through the wing leading-edge corrugations are shown in figure 28. The correct shape of these curves is governed by the interdependency of the flow of heated air through the leading-edge duct and corrugations and the air-pressure drops through the leading-edge duct and corrugations, and will be discussed later. On the basis of these curves, skin-temperature rises were calculated for stations 157 and 292, using the values of heat-transfer coefficients from figures 16 and 17. The calculated wing skin-temperature rises for all four wing stations are given in table III. By integrating the areas under the heated-air-flow distribution curves, the total required flow of heated air was obtained. In determining the total heated-air-flow rate the fact that nose ribs would be spaced 15 inches apart in the wing, thereby eliminating a corrugation every 15 inches, was taken into consideration. There are approximately 370 corrugations in the wing outer panel from station 11 to station 412.

Calculate from figure 28 the weight rate of air flow

$$(W_a)_{total} = 4130 \text{ pounds per hour}$$

Using the assumed air-temperature rise through the heat exchanger (300° F), the required exchanger thermal output can be established as follows:

$$Q_{exch} = W_a c_p \Delta t = 4130 \times 0.243 \times 300 = 301{,}000 \text{ Btu per hour}$$

Curves of the total heat removed from the wing leading-edge surface, obtained by plotting summations of the heat removed from each corrugation analyzed, are shown in figure 28. The total heat removed, obtained by integrating the areas under the curves, was found to be 115,500 Btu per hour, or 38 percent of the total heat supplied.

Air-pressure drops in corrugation passages.- The following air-pressure-drop calculations are the results of a trial-and-error development which was made in conjunction with the previous air-flow and heat-flow calculations.

The air-pressure drops in the corrugations were calculated, using equation (10). The air-pressure drop through the upper corrugation at wing station 82 was found as follows:

The air-flow rate for the upper corrugation at station 82, as determined previously, is 5.00 pounds per hour and G = 2.13 pounds per second, square foot. The air temperature at the corrugation inlet was assumed to be 290° F. The air temperature at the corrugation outlet was computed in the heat-flow calculations for the 0- to 10-percent-chord section and was found to be 147° F. Thus

$$T_1 = t_1 + 460 = 290 + 460 = 750^\circ \text{ F absolute}$$

and

$$T_3 = t_3 + 460 = 147 + 460 = 607^\circ \text{ F absolute}$$

$$v_1 = \frac{RT_1}{p_0} = \frac{53.3 \times 750}{1058} = 37.8 \text{ cubic feet per pound}$$

and

$$v_3 = \frac{RT_3}{p_0} = \frac{53.3 \times 607}{1058} = 30.6 \text{ cubic feet per pound}$$

Then

$$v_{av} = \frac{v_1 + v_3}{2} = \frac{37.8 + 30.6}{2} = 34.2 \text{ cubic feet per pound}$$

The value of $\left(\frac{GD_e}{\mu}\right)_{av}$ for the upper corrugation at station 82 was assumed equal to the value of $\left(\frac{GD_e}{\mu}\right)$ for the central region, 3 percent to 7 percent, which from table III is

$$\left(\frac{GD_e}{\mu}\right)_{av} = 2.88 \times 10^3$$

From figure 26,

$$f = 0.0114$$

The value of N in the case of the corrugations is equal to L, and is taken from figure 25. For a single corrugation m = 0.0048 foot. Then the pressure drop from region 1 to region 3, neglecting entrance and exit losses, from equation (10) is

$$p_1 - p_3 = \frac{2.13^2\ (30.6 - 37.8)}{32.2} + \frac{0.0114 \times 1.893 \times 2.13^2 \times 34.2}{2 \times 32.2 \times 0.0048}$$

$$= -1.015 + 10.85$$

$$= 9.84 \text{ pounds per square foot or } 1.89 \text{ inches of water}$$

Similar calculations were made for the lower corrugation at station 82 with a flow rate of 5.20 pounds per hour per corrugation. The air-pressure drop through the corrugation was found to be 1.90 inches of water, which is substantially the same as the value for the upper corrugation, indicating that pressure equilibrium for the upper and lower corrugations has been established.

Repeating the calculations for wing station 382, the pressure drop through the upper corrugation was found to be 1.32 inches of water with a flow rate of 6.20 pounds per hour, and 1.35 inches of water through the lower corrugation with a flow rate of 6.70 pounds per hour. A tabulation of the pressure-drop calculations for the four wing stations analyzed is presented in table IV.

Air-pressure drop through wing leading-edge duct.- The air-pressure-drop calculations for the wing and empennage leading edges were based on the assumption that the air traveled through a smooth duct formed by the baffle plate and the leading-edge corrugations. In the case of the wing, the leading-edge duct was considered to be formed by the baffle plate and the nose-rib liner for the section of span inboard of station 292.

Using figure 28, the average air-flow rate from station 11 to station 82 for the wing is 5.00 pounds per hour per corrugation for the upper surface and 5.15 pounds per hour per corrugation for the lower surface, or a total average of 10.15 pounds per hour per corrugation. Since there are five nose ribs between stations 11 and 82, the total air lost through the corrugations from station 11 to station 82 is

$$10.15 \times [(82 - 11) - 5] = 670 \text{ pounds per hour}$$

Then the air-flow rate in the leading-edge duct at station 82 is

$$W_a = 4130 - 670 = 3460 \text{ pounds per hour}$$

The wing leading-edge-duct dimensions are given in figure 29. At station 82,

$$A = 0.458 \text{ square foot}$$

$$m = 0.160 \text{ square foot}$$

Then

$$G = \frac{W_a}{A} = \frac{3460}{3600 \times 0.458} = 2.10 \ \frac{\text{pounds per second}}{\text{square foot}}$$

$$D_e = 4m = 0.64 \text{ foot}$$

When

$$t_1 = 290^{\circ} \text{ F}, \quad \mu = 1.59 \times 10^{-5} \text{ pound per second, foot}$$

and

$$Re = \frac{GD_e}{\mu} = \frac{2.10 \times 0.64}{1.58 \times 10^{-5}} = 8.50 \times 10^4$$

From figure 26,

$$f = 0.00483$$

$$(v_1)_{av} = \frac{RT_1}{p_0} = \frac{53.3 \times 750}{1058} = 37.8 \text{ cubic feet per pound}$$

To calculate the air-pressure drop, equation (10) was used. Since the air-temperature change is small through the increments of duct analyzed, the first term may be neglected. Then the pressure drop at station 82 for 1 foot of span is

$$\Delta p_1 = \frac{fNG^2 v_{av}}{2gm} = \frac{0.00483 \times 1 \times 2.10^2 \times 37.8}{2 \times 32.2 \times 0.160}$$

= 0.0781 pound per square foot per foot or 0.01501 inch of water per foot

Repeating the calculations for several other stations, as shown in table IV, plotting the results (fig. 30), and integrating the area under the curve from stations 82 to 382 results in a total air-pressure drop through the leading-edge duct between these stations of 0.52 inch of water. For equilibrium conditions, the air-pressure drop through the corrugations at station 82 must be equal to the air-pressure drop through the leading-edge duct from stations 82 to 382 plus the air-pressure drop through the corrugations at station 382.

$$(p_1 - p_3)_{82} = (\Delta p_1)_{82 \text{ to } 382} + (p_1 - p_3)_{382}$$

From the calculations,

$$(p_1 - p_3)_{82} = 1.90 \text{ inches of water}$$

$$(\Delta p_1)_{82 \text{ to } 382} + (p_1 - p_3)_{382} = 0.52 + 1.34 = 1.86 \text{ inches of water}$$

which show that pressure-equilibrium conditions have been adequately established. Since $(p_1 - p_3)_{82}$ is slightly greater than $(\Delta p_1)_{82 \text{ to } 382} + (p_1 - p_3)_{382}$, a slightly greater air flow through the corrugations near station 382 might be expected, with a corresponding slight increase in skin-temperature rise in the region near the wing tip which, as seen from table III, is desirable.

A comparison of the pressure-drop difference of the air passing through the corrugations at the four wing stations with the air-pressure drop through the leading-edge duct, with station 82 as reference, is shown in figure 31. The shape of the air-flow-distribution curves (fig. 28) depends on these two curves. When pressure-drop equilibrium has been established, the two curves of figure 31 should coincide, since the air-pressure-drop difference of any two corrugations must equal the air-pressure drop through the leading-edge duct between these two points. From the curves shown in figure 31, it is evident that the air-flow-distribution curves should be slightly less concave in order to establish equilibrium.

The method of calculating the air and heat flows and pressure drops for the horizontal stabilizer and vertical fin was the same as for the wing. A leading-edge-duct air temperature of 270° F was assumed at horizontal-stabilizer station 72 and at vertical-fin station 122. The general dimensions of the horizontal-stabilizer leading-edge thermal system as used in the calculations are given in figures 32 and 33. The stabilizer air and heat flows and skin-temperature rises are presented in table V and figure 34, and the air-pressure drops are presented in table VI and figure 35. The general dimensions of the vertical fin as used in the calculations are given in figures 36 and 37. The fin air and heat flows and skin-temperature rises are presented in table VII and figure 38, and the air-pressure drops are presented in table VII and figure 39.

AIR-HEATED-WINDSHIELD DESIGN

The approach to the air-heated-windshield design was different from that used in the analysis of the airfoil sections. Since the value of the external heat-transfer coefficient for the windshield surface was not known, the method outlined in reference 9 was used and a specified heat flow through the windshield outer panel was established as the heat requirement for ice prevention.

As in the analysis of the wings and empennage, certain factors were fixed and an attempt was made to vary the remaining factors to satisfy the design requirements. The fixed factors consisted of the windshield area and shape, while the variable factors consisted of the heated-air temperature, the flow rate, and the gap thickness. Consideration of the strength of the glass and the comfort of the pilots limited the heated-air temperature to a maximum value of about 200° F.

The necessary heat flow through the windshield outer panel was taken as 1000 Btu per hour per square foot, as recommended in reference 9. The outer panel consists of two layers of semi-tempered plate glass 0.1095 inch thick each, separated by a layer of vinyl plastic 0.125 inch thick. The thermal conductivity of the glass was taken as 6.67 Btu per hour, square foot, degree Fahrenheit per inch and the thermal conductivity of the plastic was assumed to be 1.25 Btu per hour, square foot, degree Fahrenheit per inch, although this value is not considered accurately established. The thermal conductance C for the outer panel was calculated from equation (3) of reference 9:

$$C = \frac{1}{\frac{l_1}{K_1} + \frac{l_2}{K_2} + \frac{l_3}{K_3}} \tag{12}$$

where l designates the thickness and K the thermal conductivity of each of the three layers. Then

$$C = \frac{1}{\frac{0.1095}{6.67} \times 2 + \frac{0.125}{1.25}} = 7.54 \text{ Btu per hour, square foot, degree Fahrenheit}$$

In order to obtain the required heat flow through the outer panel at the outer-surface temperature of 50° F, as specified in reference 9, the inner-surface temperature must be

$$t_1 = \frac{1000 + 50\,C}{C} \tag{13}$$

which for the subject windshield is 183° F. As was stated previously, the heated-windshield design included a secondary heat exchanger which would transmit the heat of primary heating air from the exhaust exchangers to secondary air for windshield and cockpit heating. Calculations using the method of reference 9 indicated that no practical double-panel design which would give the required heat flow was possible with the heat available from a secondary heat-exchanger installation that used the remaining heated air from the inboard exchangers after supplying the empennage system. The secondary exchanger installation was necessary, however, in order to supply cockpit heated air free from carbon-monoxide contamination in the event of leakages in the exhaust exchangers. The windshield installation finally adopted consisted of (1) the double-panel arrangement which would provide the optimum heating for the allowable pressure drop through the gap, and (2) a means of discharging the primary air from the secondary exchanger over the outer surface of the windshield. In order to provide for

In the air-pressure-drop calculations, the corrugation entrance and exit losses were neglected. In the case of the wing, the pressure drop of the air traveling from the nose-rib-liner duct to the corrugation entrances was neglected as well. Since the purpose of the pressure-loss calculations was to determine the air-flow distribution which would result during flight, neglecting the entrance and exit losses would change the air- and heat-flow calculations only slightly. The air velocities in the corrugations at the tip regions are higher than in the corrugations at the root regions; consequently the entrance and exit losses would be higher in the tip regions than at the root sections. The air-flow rates through these corrugations, therefore, would probably be less than calculated. The curve of friction factor f as used in the calculations of pressure drop is intended for isothermal flow, as stated in reference 8, but was assumed to be suitable for the polytropic flows of the analysis.

BLOWER TESTS OF WING LEADING-EDGE THERMAL SYSTEM

Upon completion of the right-wing leading-edge thermal system, blower tests of the leading edge were conducted to obtain isothermal air-flow data to determine the desirability of installing a nose-rib liner.

A blower was connected to the leading-edge duct with a venturi meter installed to obtain the air-flow rate. With approximately the required air-flow rate of the analysis supplied to the leading-edge system by the blower, the total pressure of the air out of representative upper and lower corrugations between each nose-rib bay was measured by means of a survey tube connected to an open-end manometer. From these total pressures, the air-flow rates in the corrugations were calculated.

A blower test was first made without the nose-rib liner installed in order to determine if a liner would be necessary. It was found that the pressure drop along the leading-edge duct was excessive and prevented the desired flow of air through the corrugations in the region of station 382. The nose-rib liner was then installed and holes were cut in the liner to give approximately the same area as the corrugations they supplied. Tests were made and the air-flow-distribution curve then compared favorably with the calculated distribution curve. A comparison of the curves of the two tests with the calculated curves is shown in figure 44.

circulation of air through the secondary exchanger and windshield system by the dynamic pressure of the free stream, the allowable pressure drop through the windshield gap was 4 inches of water. Based on the equations of reference 9, it was indicated that the optimum heating of the windshield outer panel with a 4-inch pressure drop in the gap would be provided with an air-gap thickness of approximately 3/16 inch.

The reason for the difficulty in obtaining the necessary heat flow through the outer panel was due in part to the lack of heat available and in part to the low thermal conductance of the panel. This low conductance was caused by the relatively thick plastic layer of low thermal conductivity. Therefore, it is apparent that in the design of air-heated windshields attention should be directed to securing an outer panel of high thermal conductivity.

RESULTS AND ERRORS

A general summary of the calculated heated-air flows, skin-temperature rises, and air-pressure drops for the wing, horizontal stabilizer, and vertical-fin thermal systems is presented in figures 40, 41, and 42. Table VIII gives a summary of the calculated heat flows.

Aside from experimental errors involved in the determination of airfoil pressure distribution, the foregoing treatment of the analytical problem has introduced several errors which should be acknowledged.

An error was introduced in the use of the arithmetic average for obtaining $(t_2)_{av}$, the average air temperature in a corrugation between two points. A calculation of the air-temperature change through the upper corrugation at wing station 82 was made using small increments of corrugation length. This more exact calculation of t_2 is compared in figure 43 with the straight-line temperature gradient assumed in the analysis. The maximum deviation between the two curves was found to be 1.24 percent. A tabulation of the calculations made to obtain the more exact curve of the air-temperature change is presented in table IX.

The effects of radiation and conduction from the corrugation walls to the leading-edge skin were also neglected. However, since the corrugation ducts are 3/4 inch wide and are required to heat a 1-inch strip of skin, these errors tend to compensate each other.

Although the experimental distribution curve is for isothermal air flow and the calculated distribution is for a polytropic flow, the tests indicate that the desired air-flow distribution will be approximated at the design flight conditions.

DISCUSSION

The analytic procedure involved the employment of assumed atmospheric and flight conditions previously established as criteria in former design calculations of thermal ice-prevention systems. Tests of the equipment for the C-46 airplane will help to determine the completeness of the design criteria and the accuracy of the analytic methods, and possibly will permit their extension and refinement. The calculation of heat transfer from the airfoil surfaces to dry air was an expedient necessitated by a paucity of data on the water content and drop sizes in the atmosphere at various temperatures. Efforts are being made to determine from statistical researches of the atmosphere values of temperature, pressure, water content, drop size, and humidity, which may be used to establish the optimum design criteria for thermal ice prevention. When such data have been established, the heat required can be based on the combined transfer due to air convection and water-drop impingement on the airfoil surfaces.

The use of the method of utilizing the airfoil pressure distribution to obtain the required heat for thermal ice prevention appears entirely feasible in the design of future thermal ice-prevention systems. The pressure distribution for any airfoil may be calculated as well as determined experimentally. Methods of calculating the external heat-transfer coefficients in a turbulent boundary layer are available (references 10 and 11) in the event that the transition point from laminar to turbulent flow occurs within the heated region of the airfoil. Once the required heat flows based on a given surface-temperature rise are established, rough calculations can be made for various thermal-system designs to determine the optimum required heated-air flows. After the design has been decided upon, a complete analysis can be made.

Summarizing, the general procedure for analysis is as follows:

1. Determine the external heat-transfer coefficients from airfoil pressure distributions.

2. Determine the required heat flows through the airfoil leading edges for a given surface-temperature rise.

3. Determine the necessary heated-air flows and required heat-exchanger output, and correlate the air flows with the resulting air-pressure drops for a given thermal-system design.

Ames Aeronautical Laboratory,
National Advisory Committee for Aeronautics,
Moffett Field, Calif.

REFERENCES

1. Rodert, Lewis A., and Jackson, Richard: Preliminary Investigation and Design of an Air-Heated Wing for Lockheed 12A Airplane. NACA ARR, April 1942.

2. Jones, Alun R., and Rodert, Lewis A.: Development of Thermal Ice-Prevention Equipment for the B-24D Airplane. NACA ACR, Feb. 1943. (Classification changed to "Restricted," Aug. 1943.)

3. Jones, Alun R., and Rodert, Lewis A.: Development of Thermal Ice-Prevention Equipment for the B-17F Airplane. NACA ARR No. 3H24, 1943.

4. Corson, Blake W., Jr.: The Belt Method for Measuring Pressure Distribution. NACA RB, Feb. 1943.

5. Tribus, Myron, and Boelter, L. M. K.: An Investigation of Aircraft Heaters. II - Properties of Gases. NACA ARR, Oct. 1942.

6. von Kármán, Th., and Millikan, C. B.: On the Theory of Laminar Boundary Layers Involving Separation. Rep. No. 504, NACA, 1934.

7. Allen, H. Julian, and Look, Bonne C.: A Method for Calculating Heat Transfer in the Laminar Flow Region of Bodies. NACA RB, Dec. 1942.

8. McAdams, William H.: Heat Transmission. McGraw-Hill Book Co., Inc., 2d ed., 1942.

9. Kushnick, Jerome L.: Thermodynamic Design of Double-Panel, Air-Heated Windshields for Ice Prevention. NACA RB No. 3F24, 1943.

10. Frick, Charles W., Jr., and McCullough, George B.: A Method for Determining the Rate of Heat Transfer from a Wing or Streamline Body. NACA ACR, Dec. 1942. (Classification changed to "Restricted," Aug. 1943.)

11. Squire, H. B.: Heat Transfer Calculation for Aerofoils. NACA MRR No. 3E29, 1943.

A-52

TABLE I.- EXPERIMENTAL AIRFOIL PRESSURE DATA OBTAINED BY MEANS OF PRESSURE BELTS FROM FLIGHT TESTS OF THE C-46 AIRPLANE

$[1-P = 1-p_r/q_o]$

Station 92 q_o = 11.3 in. H_2O pressure altitude, 5000 ft		Station 157 q_o = 11.6 in. H_2O pressure altitude, 5000 ft		Station 292 q_o = 12.2 in. H_2O pressure altitude, 18,000 ft		Station 392 q_o = 12.4 in. H_2O pressure altitude, 19,000 ft	
Wing							
Percent chord	$1-P_{Upper}$	Percent chord	$1-P_{Upper}$	Percent chord	$1-P_{Upper}$	Percent chord	$1-P_{Upper}$
11.9	2.27	14.1	2.33	14.2	2.07	19.3	1.70
7.4	2.31	9.1	2.41	9.5	2.08	13.1	1.73
4.7	2.24	5.9	2.36	6.3	2.00	9.9	1.69
3.3	2.08	4.3	2.25	4.3	1.95	6.0	1.57
1.6	1.64	2.3	1.98	2.7	1.67	3.9	1.43
1.0	1.46	1.5	1.82	1.9	1.47	2.4	1.24
.4	1.02	.7	1.29	.9	1.13	1.3	1.00
.1	.58	.3	.90	.4	.79	.6	.75
-----	$1-P_{Lower}$	-----	$1-P_{Lower}$	.2	.55	.3	.49
.03	.08	.04	.08	0	.14	0	.08
.9	.27	.5	.29	----	$1-P_{Lower}$	----	$1-P_{Lower}$
1.1	.47	1.3	.54	.2	.28	.7	.90
2.1	.66	2.4	.93	.6	.97	1.4	1.23
3.3	.95	3.8	.93	1.4	.89	2.9	1.13
4.75	.98	5.8	1.03	2.5	1.22	4.0	1.19
6.6	1.03	7.7	1.10	3.9	1.19	6.2	1.21
9.1	1.06	10.8	1.15	6.0	1.25	9.6	1.11
13.0	1.16	15.0	1.21	9.4	1.22	11.9	1.15
-----	----	-----	-----	12.0	1.24	18.5	1.04
-----	----	-----	----	17.0	1.20	23.0	1.01

Station 72 q_o = 9.8 in. H_2O pressure altitude, 5000 ft		Station 127 q_o = 12.2 in. H_2O pressure altitude, 18,000 ft		Station 172 q_o = 12.4 in. H_2O pressure altitude, 19,000 ft		Station 122 q_o = 11.3 in. H_2O pressure altitude, 5000 ft		Station 172 q_o = 11.6 in. H_2O pressure altitude, 5000 ft	
Horizontal stabilizer						Vertical fin			
Percent chord	$1-P_{Upper}$	Percent chord	$1-P_{Upper}$	Percent chord	$1-P_{Upper}$	Percent chord	$1-P_{Left}$	Percent chord	$1-P_{Left}$
13.8	1.32	18.4	1.39	22.5	1.32	7.11	1.29	11.10	1.35
10.0	1.30	13.7	1.42	17.0	1.10	4.78	1.29	7.49	1.44
6.3	1.29	9.1	1.39	11.4	1.33	3.34	1.24	5.89	1.43
4.0	1.23	8.3	1.37	9.1	1.29	2.38	1.18	3.92	1.38
2.5	1.08	4.4	1.32	5.9	1.23	1.46	1.04	2.41	1.27
1.1	.92	2.9	1.19	3.9	1.12	1.03	.98	1.89	1.15
.4	.58	1.7	1.03	2.4	.99	.91	.90	1.36	1.03
.2	.25	1.3	.93	1.9	.93	.61	.82	1.04	.93
.01	.02	.8	.76	1.3	.92	.41	.72	.84	.74
-----	$1-P_{Lower}$	.4	.44	.7	.61	.11	.40	.14	.38
.01	.14	0	0	.03	-.06	0	.31	-----	$1-P_{Right}$
.5	.90	----	$1-P_{Lower}$	-----	$1-P_{Lower}$	---	$1-P_{Right}$	.02	.58
1.2	1.13	.5	1.03	.4	1.06	.03	.40	.17	.78
1.9	1.14	1.0	1.17	1.0	1.22	.11	.53	.42	.89
2.0	1.17	1.4	1.32	1.5	1.36	.23	.69	.69	.97
2.4	1.19	1.9	1.33	2.1	1.39	.61	.94	1.36	1.15
3.2	1.25	2.8	1.40	3.2	1.43	1.46	1.10	2.74	1.18
4.7	1.30	4.8	1.51	5.6	1.50	2.38	1.20	4.16	1.25
6.3	1.34	6.6	1.60	7.9	1.50	3.79	1.27	6.30	----
7.9	1.34	9.3	1.57	11.1	1.45	6.16	1.33	9.89	1.27
12.4	1.31	12.7	1.51	16.7	1.43	----	----	-----	----
16.2	1.30	17.4	1.55	22.2	1.41	----	----	-----	----

A-52

TABLE II.- DETERMINATION OF EXTERNAL HEAT-TRANSFER COEFFICIENTS FROM AIRFOIL PRESSURE-DISTRIBUTION MEASUREMENTS AT WING STATION 92 OF THE C-46 AIRPLANE

$s/c \times 100$	$x/c \times 100$	$1 - P$	V/V_o	$0.0000671 \frac{s_1/c}{V_1/V_o} \times 10^6$	$\frac{\int_0^{s_1/c} (V/V_o)^{3.17} d(s/c)}{(V_1/V_o)^{3.17} (s_1/c)}$	$\delta \times 10^6$ (ft)	λ	h_{s-t} [Btu/(hr)(sq ft)(°F)]	$(h_{s-t})_{corr}$ [Btu/(hr)(sq ft)(°F)]
Upper surface									
19.89	15.0	2.196	1.49	9.550	0.839	2.675	0.412	2.00	2.03
13.77	10.0	2.303	1.52	6.070	.598	1.903	.674	4.60	4.65
11.69	9.0	2.312	1.52	5.155	.511	1.622	.765	6.13	6.20
9.54	6.0	2.291	1.51	4.240	.423	1.338	.765	7.44	7.54
7.29	4.0	2.195	1.48	3.310	.324	1.033	.765	9.62	9.75
6.11	3.0	2.030	1.43	2.860	.317	.955	.765	10.41	10.55
5.47	2.5	1.930	1.39	2.640	.293	.860	.765	11.30	11.44
4.93	2.0	1.802	1.34	2.415	.265	.829	.765	12.00	12.15
4.12	1.5	1.650	1.29	2.155	.260	.748	.765	13.30	13.47
3.37	1.0	1.450	1.20	1.575	.241	.672	.765	14.80	15.00
2.51	.5	1.140	1.07	1.570	.233	.605	.765	16.43	16.64
.90	0	.250	.50	-----	-----	-----	.765	-----	-----
0	.1	0	----	-----	-----	.276	.765	36.00	36.50
Lower surface									
0.99	0.5	0.230	0.49	1.390	-----	-----	0.765	-----	-----
1.75	1.0	.425	.65	1.806	.375	.922	.765	12.10	12.27
2.41	1.5	.560	.75	2.165	.311	.919	.765	12.14	12.31
3.02	2.0	.661	.81	2.500	.251	.792	.765	12.55	12.71
3.58	2.5	.743	.86	2.792	.273	.874	.765	11.39	11.53
4.14	3.0	.913	.90	3.084	.280	.925	.795	10.75	10.90
5.21	4.0	.921	.96	3.640	.295	1.036	.765	9.60	9.73
7.31	6.0	1.024	1.01	4.850	.391	1.376	.765	7.22	7.31
9.36	9.0	1.065	1.03	6.070	.455	1.962	.765	5.97	6.05
11.39	10.0	1.077	1.04	7.36	.539	1.990	.765	5.00	5.06
16.45	15.0	1.160	1.09	10.27	.533	2.335	.765	4.26	4.31

TABLE III.- HEAT-FLOW AND SKIN-TEMPERATURE-RISE ANALYSIS FOR THE WING OUTER PANEL LEADING-EDGE THERMAL SYSTEM OF THE C-46 AIRPLANE

Station	Surface and percent chord		w (lb/hr per corrugation)	G [lb/(sec)(sq ft)]	$(t_s)_{av}$ (°F)	$\mu \times 10^6$ [lb/(sec)(ft)]	$\frac{GD_e}{\mu} \times 10^{-3}$	$\frac{h_{a-s} D_e}{k}$	k [Btu/(hr)(sq ft)(°F/ft)]	h_{a-s} [Btu/(hr)(sq ft)(°F)]	h_{s-t} [Btu/(hr)(sq ft)(°F)]	t_e Average skin temperature rise (°F)
82	Upper	0-3	5.00	2.13	248	1.52	2.69	10.9	0.0193	10.96	15.10	104
		3-7	5.00	2.13	198	1.42	2.99	11.5	.0179	10.71	8.55	104
		7-10	5.00	2.13	156	1.38	2.98	11.9	.0171	10.50	5.75	101
	Lower	0-3	5.20	2.22	250	1.52	2.90	11.3	0.0194	11.41	15.60	106
		3-7	5.20	2.22	192	1.43	2.98	11.8	.0180	11.07	8.53	109
		7-10	5.20	2.22	164	1.39	3.06	12.1	.0173	10.90	5.70	109
157	Upper	0-3	5.05	2.16	242	1.51	2.75	11.1	0.0192	11.10	18.60	91
		3-7	5.05	2.16	185	1.42	2.92	11.6	.0179	10.74	9.52	99
		7-10	5.05	2.16	157	1.38	3.00	11.9	.0172	10.67	9.55	97
	Lower	0-3	5.30	2.26	246	1.51	2.87	11.5	0.0193	11.57	19.60	101
		3-7	5.30	2.26	196	1.44	3.02	12.0	.0191	11.31	8.90	110
		7-10	5.30	2.26	170	1.40	3.10	12.2	.0175	11.11	9.42	109
292	Upper	0-3	5.50	2.35	243	1.51	2.99	11.9	0.0192	11.90	19.10	93
		3-7	5.50	2.35	202	1.45	3.11	12.2	.0182	11.58	10.43	106
		7-10	5.50	2.35	179	1.41	3.20	12.5	.0177	11.51	7.78	107
	Lower	0-3	5.85	2.50	246	1.51	3.19	12.4	0.0193	12.49	21.60	90
		3-7	5.85	2.50	209	1.46	3.29	12.7	.0194	12.17	9.75	118
		7-10	5.95	2.50	189	1.43	3.38	13.0	.0179	12.11	6.81	122
382	Upper	0-3	6.20	2.65	241	1.51	3.37	13.0	0.0192	13.00	20.50	94
		3-7	6.20	2.65	211	1.46	3.48	13.4	.0184	12.93	11.84	110
		7-10	6.20	2.65	122	1.43	3.56	13.6	.0189	12.74	8.70	114
	Lower	0-3	6.70	2.96	244	1.51	3.64	13.9	0.0192	13.90	23.00	92
		3-7	6.70	2.96	219	1.47	3.74	14.2	.0196	13.75	9.99	126
		7-10	6.70	2.96	203	1.45	3.76	14.3	.0193	13.62	6.10	148

TABLE IV.- HEATED-AIR PRESSURE-DROP ANALYSIS FOR WING OUTER PANEL CORRUGATIONS AND LEADING-EDGE DUCT OF THE C-46 AIRPLANE

Station and surface		T_1 (°F absolute)	v_1 (cu ft/lb)	T_3 (°F absolute)	v_3 (cu ft/lb)	v_{av} (cu ft/lb)	G [lb/(sec)(sq ft)]	$\left(\frac{GD_e}{\mu}\right)_{av} \times 10^{-3}$	f	N (ft)	$\frac{G^2(v_3 - v_1)}{g}$ (lb/sq ft)	$\frac{fNG^2 v_{av}}{2gm}$ (lb/sq ft)	$p_1 - p_3$ (lb/sq ft)	$p_1 - p_3$ (in. H_2O)
Pressure drop in corrugations														
82	Upper	750	37.8	607	30.6	34.20	2.13	2.88	0.0114	1.893	-1.015	10.85	9.835	1.89
	Lower	750	37.8	615	31.0	34.40	2.22	2.98	.0112	1.778	-1.040	10.91	9.870	1.90
157	Upper	740	37.3	607	30.6	33.95	2.16	2.92	0.0114	1.648	-0.970	9.64	8.670	1.67
	Lower	740	37.3	621	31.4	34.35	2.26	3.02	.0112	1.536	-.936	9.75	8.814	1.69
292	Upper	730	36.8	631	31.8	34.30	2.35	3.11	0.0111	1.203	-0.856	8.20	7.344	1.41
	Lower	730	36.8	642	32.4	34.60	2.50	3.29	.0108	1.097	-.855	8.28	7.425	1.43
382	Upper	720	36.3	646	32.6	34.45	2.65	3.48	0.0107	0.912	-0.806	7.66	6.854	1.32
	Lower	720	36.3	659	33.3	34.75	2.86	3.74	.0104	.819	-.789	7.80	7.011	1.35

Station	$(w)_{av}$ Upper (lb/hr per corrugation)	$(w)_{av}$ Lower (lb/hr per corrugation)	$(w)_{av}$ Upper plus Lower (lb/hr per corrugation)	$(W_a)_L$ Total air lost (lb/hr)	W_a Flow rate (lb/hr)	A Duct area (sq ft)	G [lb/(sec)(sq ft)]	m (ft)	D_e (ft)	t_1 (°F)	$\mu \times 10^8$ [lb/(sec)(ft)]	$\frac{GD_e}{\mu} \times 10^{-4}$	f	$(v_1)_{av}$ (cu ft/lb)	Δp_1 (lb/sq ft per ft)	Δp_1 (in. H_2O/ft)
Pressure drop in leading-edge duct																
11	0	0	0	0	4130	0.511	1.878	0.181	0.724	300	1.60	8.49	0.00483	38.3	0.0560	0.01075
82	5.00	5.15	10.15	670	3460	.458	2.100	.160	.640	290	1.58	8.50	.00483	37.8	.0781	.01501
157	5.00	5.21	10.21	1380	2750	.344	2.220	.140	.560	280	1.57	7.92	.00491	37.3	.1002	.01930
220	5.05	5.28	10.33	1994	2136	.261	2.275	.123	.492	275	1.56	7.17	.00500	37.0	.1210	.02325
292	5.12	5.40	10.52	2725	1405	.184	2.120	.104	.416	270	1.55	5.70	.00525	36.8	.1291	.02483
382	5.30	5.65	10.95	3740	309	.098	1.107	.081	.324	260	1.54	2.33	.00650	36.3	.0550	.01060

A-52

TABLE V.- HEAT-FLOW AND SKIN-TEMPERATURE-RISE ANALYSIS FOR HORIZONTAL STABILIZER LEADING-EDGE THERMAL SYSTEM OF THE C-46 AIRPLANE

Station	Surface and percent chord		w (lb/hr per corrugation)	G [lb/(sec)(sq ft)]	$(t_a)_{av}$ (^{o}F)	$\mu \times 10^5$ [lb/(sec)(ft)]	$\frac{GD_e}{\mu} \times 10^{-3}$	$\frac{h_{a-e}D_e}{k}$	k [Btu/(hr)(sq ft)(^{o}F/ft)]	$(h_{a-e})_{av}$ [Btu/(hr)(sq ft)(^{o}F)]	$(h_{6-7})_{av}$ [Btu/(hr)(sq ft)(^{o}F)]	t_s Average skin temperature rise (^{o}F)
72	Upper	0-3	8.5	3.62	255	1.53	4.54	16.6	0.0195	16.87	17.10	127
		3-7	8.5	3.62	231	1.49	4.66	16.9	.0189	16.63	9.98	144
		7-10	8.5	3.62	215	1.47	4.73	17.1	.0185	16.49	7.13	150
	Lower	0-3	8.5	3.62	253	1.52	4.57	16.7	0.0194	16.89	23.80	105
		3-7	8.5	3.62	227	1.49	4.66	16.9	.0188	16.54	9.51	144
		7-10	8.5	3.62	213	1.46	4.76	17.1	.0185	16.49	6.68	152
127	Upper	0-3	8.6	3.67	245	1.51	4.64	16.9	0.0193	17.00	28.80	91
		3-7	8.6	3.67	222	1.48	4.76	17.1	.0187	16.67	12.23	128
		7-10	8.6	3.67	208	1.46	4.83	17.4	.0184	16.69	8.40	138
	Lower	0-3	8.6	3.67	246	1.51	4.64	16.9	0.0193	17.00	25.90	98
		3-7	8.6	3.67	223	1.48	4.76	17.1	.0187	16.67	11.26	133
		7-10	8.6	3.67	210	1.46	4.83	17.4	.0184	16.69	7.75	143
172	Upper	0-3	9.3	3.96	239	1.50	5.06	18.1	0.0191	18.00	25.40	99
		3-7	9.3	3.96	220	1.47	5.16	18.3	.0187	17.82	13.10	127
		7-10	9.3	3.96	209	1.46	5.20	18.5	.0184	17.72	9.41	137
	Lower	0-3	9.3	3.96	239	1.50	5.06	18.1	0.0191	18.00	25.20	100
		3-7	9.3	3.96	222	1.48	5.14	18.3	.0187	17.82	11.21	136
		7-10	9.3	3.96	212	1.46	5.20	18.5	.0185	17.82	7.25	151

A-52

TABLE VI.- HEATED-AIR PRESSURE-DROP ANALYSIS FOR HORIZONTAL STABILIZER CORRUGATIONS AND LEADING-EDGE DUCT OF THE C-46 AIRPLANE

Station and surface		T_1 (°F absolute)	v_1 (cu ft/lb)	T_3 (°F absolute)	v_3 (cu ft/lb)	v_{av} (cu ft/lb)	G [lb/(sec)(sq ft)]	$\left(\frac{GD_e}{\mu}\right)_{av} \times 10^{-3}$	f	N (ft)	$\frac{G^2(v_3-v_1)}{g}$ (lb/sq ft)	$\frac{fNG^2v_{av}}{2gm}$ (lb/sq ft)	p_1-p_3 (lb/sq ft)	p_1-p_3 (in. H_2O)
Pressure drop in corrugations														
72	Upper	[illegible]	36.8	670	33.8	35.3	3.62	4.66	0.0099	0.925	-1.22[illegible]	[illegible]	[illegible]	[illegible]
	Lower	730	36.8	668	33.6	35.2	3.62	4.66	.0099	.925	[illegible]	[illegible]	[illegible]	[illegible]
127	Upper	720	36.3	663	33.4	34.85	3.67	4.76	0.0096	0.76[illegible]	[illegible]	[illegible]	[illegible]	[illegible]
	Lower	720	36.3	666	33.6	34.95	3.67	4.76	.0098	[illegible]	[illegible]	[illegible]	[illegible]	1.56
172	Upper	710	35.8	665	33.5	34.65	3.96	5.16	0.0096	0.640	[illegible]	[illegible]	[illegible]	1.89
	Lower	710	35.8	669	33.7	34.75	3.96	5.14	.0096	.640	-1.0[illegible]	[illegible]	[illegible]	[illegible]

Station	$(w)_{av}$ Upper and Lower (lb/hr per corrugation)	$(w)_{av}$ Upper plus Lower (lb/hr per corrugation)	$(W_a)_L$ Total air lost (lb/hr)	W_a Flow rate (lb/hr)	A Duct area (sq ft)	G [lb/(sec)(sq ft)]	m (ft)	D_e (ft)	t_1 (°F)	$\mu \times 10^5$ [lb/(sec)(ft)]	$\frac{GD_e}{\mu} \times 10^{-4}$	f	v_{av} (cu ft/lb)	Δp_1 (lb/sq ft per ft)	Δp_1 (in. H_2O/ft)
Pressure drop in leading-edge duct															
47	0	0	0	2514	0.184	3.795	0.1062	0.4248	275	1.56	10.33	0.00463	37.00	0.360	0.0692
72	8.49	16.98	424	2090	.157	3.690	.0988	.3952	270	1.55	9.40	.00472	36.80	.372	.0715
100	8.50	17.00	901	1613	.129	3.475	.0896	.3584	265	1.54	7.86	.00491	36.55	.376	.0722
127	8.53	17.06	1364	1150	.104	3.065	.0803	.3212	260	1.54	6.39	.00515	36.30	.340	.0655
172	8.66	17.36	2168	346	.069	1.389	.0650	.2600	250	1.52	2.38	.00648	35.80	.107	.0206

A-52

TABLE VII.- HEAT-FLOW AND SKIN-TEMPERATURE-RISE ANALYSIS AND HEATED-AIR PRESSURE-DROP ANALYSIS FOR VERTICAL FIN LEADING-EDGE THERMAL SYSTEM OF THE C-46 AIRPLANE

Station	Percent chord	w (lb/hr per corrugation)	G [lb/(sec) (sq ft)]	$(t_s)_{av}$ (°F)	$\mu \times 10^8$ [lb/(sec)(ft)]	$\frac{GD_e}{\mu} \times 10^{-3}$	$\frac{b_{a-s} D_e}{k}$	k [Btu/(hr)(sq ft)(°F/ft)]	$(b_{a-s})_{av}$ [Btu/(hr)(sq ft)(°F)]	$(b_{s-v})_{av}$ [Btu/(hr)(sq ft)(°F)]	t_s average skin temperature rise (°F)
Heat flow											
122	0-3	6.00	2.56	244	1.51	3.25	12.7	0.0192	12.70	18.70	99
	3-7	6.00	2.56	203	1.45	3.39	13.1	.0183	12.49	7.85	125
	7-10	6.00	2.56	182	1.42	3.46	13.3	.0178	12.32	4.62	132
172	0-3	7.55	3.22	243	1.51	4.09	15.2	0.0192	15.20	22.00	99
	3-7	7.55	3.22	217	1.47	4.20	15.5	.0186	15.00	10.05	130
	7-10	7.55	3.22	202	1.45	4.26	15.7	.0182	14.89	6.25	142

Station	T_1 (°F absolute)	v_1 (cu ft/lb)	T_s (°F absolute)	v_s (cu ft/lb)	v_{av} (cu ft/lb)	G [lb/(sec)(sq ft)]	$\left(\frac{GD_e}{\mu}\right)_{av} \times 10^{-3}$	f	M (ft)	$\frac{G^2(v_s-v_1)}{g}$ (lb/sq ft)	$\frac{fMG^2 v_{av}}{2gm}$ (lb/sq ft)	$P_1 - P_s$ (lb/sq ft)	$P_1 - P_s$ (in. H_2O)
Pressure drop in corrugations													
122	730	36.8	635	32.1	34.5	2.56	3.39	0.0108	1.374	-0.956	10.90	9.944	1.91
172	720	36.3	657	33.1	34.7	3.22	4.20	.0101	.922	-1.038	10.83	9.792	1.88

Station	$(w)_{av}$ Right (lb/hr per corrugation)	$(w)_{av}$ Left (lb/hr per corrugation)	$(w)_{av}$ Right plus Left (lb/hr per corrugation)	$(W_a)_L$ Total air lost (lb/hr)	W_a Flow rate (lb/hr)	A Duct area (sq ft)	G [lb/(sec)(sq ft)]	m (ft)	D_e (ft)	t_1 (°F)	$\mu \times 10^8$ [lb/(sec)(ft)]	$\frac{GD_e}{\mu} \times 10^{-4}$	f	v_{av} (cu ft/lb)	Δp_1 (lb/sq ft per ft)	Δp_1 (in. H_2O/ft)
Pressure drop in leading-edge duct																
112	0	0	0	0	1120	0.335	0.929	0.1475	0.5900	270	1.55	3.54	0.00590	36.8	0.0187	0.00379
122	5.96	5.96	11.92	119	1001	.301	.925	.1360	.5520	270	1.55	3.30	.00599	36.8	.0212	.00408
147	6.15	6.15	12.30	431	689	.215	.890	.1142	.4568	265	1.54	2.64	.00630	36.55	.0248	.00476
172	6.50	6.50	13.00	780	340	.130	.728	.0908	.3624	260	1.54	1.71	.00700	36.3	.0230	.00442

A-52

TABLE VIII.- SUMMARY OF HEAT-FLOW CALCULATIONS FOR THE WING, HORIZONTAL STABILIZER, AND VERTICAL FIN THERMAL SYSTEMS OF THE C-46 AIRPLANE

Leading-edge surface	W_a (lb/hr)	Δt air temperature rise (°F)	Q Total heat supplied to leading-edge thermal system above 0° F (Btu/hr)	Q_R Total heat removed from leading-edge surface (Btu/hr)
Wing	4130	300	301,000	115,500
Stabilizer	2514	275	167,000	32,640
Fin	1120	270	73,000	19,860

Leading-edge surface	$\frac{Q_R}{Q} \times 100$ Percent heat removed from leading edge	S Total heated leading-edge surface (sq ft)	Q_R/S Average heat removed from leading-edge surface [Btu/(hr)(sq ft)]
Wing	38	94.5	1220
Stabilizer	20	18.9	1730
Fin	27	14.7	1350

TABLE IX.- CALCULATION OF HEATED-AIR TEMPERATURE CHANGE THROUGH UPPER CORRUGATION AT WING STATION 82 OF THE C-46 AIRPLANE

w = 5.0 pounds per hour per corrugation
G = 2.13 pounds per second, square foot
c = 14.51 feet

$s/c \times 100$	$(t_a)_{av}$	$\mu \times 10^8$ [lb/(sec)(ft)]	$\frac{GD_e}{\mu} \times 10^{-3}$	$\frac{h_{a-e}D_e}{k}$	k [Btu/(hr)(sq ft)(°F/ft)]	$(h_{a-e})_{av}$ [Btu/(hr)(sq ft)(°F)]	$(h_{e-7})_{av}$ [Btu/(hr)(sq ft)(°F)]	t_e Average skin temperature rise (°F)
0.80-1	288	1.58	2.59	10.5	0.0202	11.04	21.73	97.0
1-2	276	1.56	2.62	10.7	.0200	11.14	19.57	100.1
2-3	257.5	1.53	2.67	10.9	.0195	11.08	16.62	103.0
3-4	241.5	1.51	2.71	11.0	.0192	11.00	14.57	104.0
4-5	227.5	1.49	2.74	11.1	.0188	10.87	12.90	104.0
5-6	215	1.47	2.78	11.2	.0185	10.79	11.50	104.0
6-7	203.5	1.45	2.82	11.4	.0183	10.87	10.28	104.5
7-8	193	1.43	2.86	11.5	.0180	10.79	9.21	104.0
8-9	183.5	1.42	2.88	11.6	.0178	10.75	8.31	103.6
9-10	175	1.40	2.92	11.7	.0176	10.72	7.56	102.8
10-11	167.5	1.40	2.92	11.7	.0174	10.60	6.91	101.2
11-12	161	1.38	2.96	11.8	.0173	10.62	6.30	101.1
12-13	155	1.37	2.98	11.8	.0171	10.50	5.60	101.1
13-13.77	150	1.37	2.98	11.8	.0170	10.44	4.96	101.8

Figure 1.- The C-46 airplane in which the thermal ice-prevention equipment was installed.

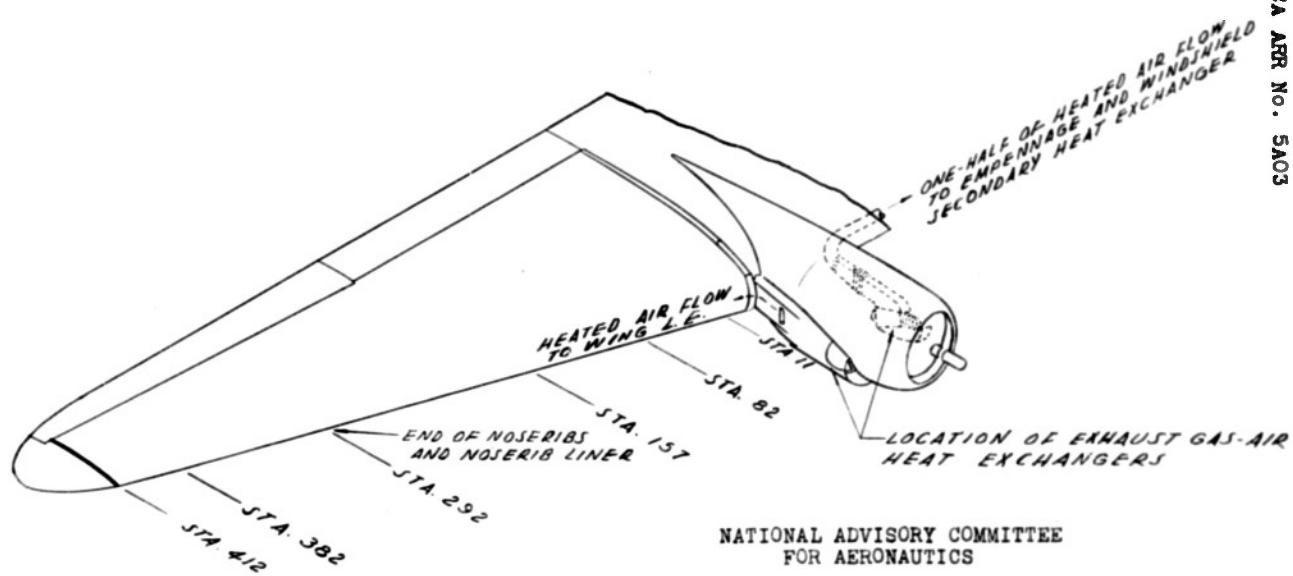

NATIONAL ADVISORY COMMITTEE
FOR AERONAUTICS

FIGURE 2.- THE RIGHT WING OUTER PANEL OF THE C-46 AIRPLANE SHOWING THE THERMAL ICE-PREVENTION SYSTEM AND THE STATIONS ANALYZED

41

A-52

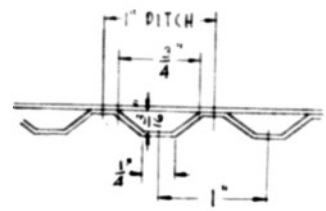

CORRUGATION DIMENSIONS

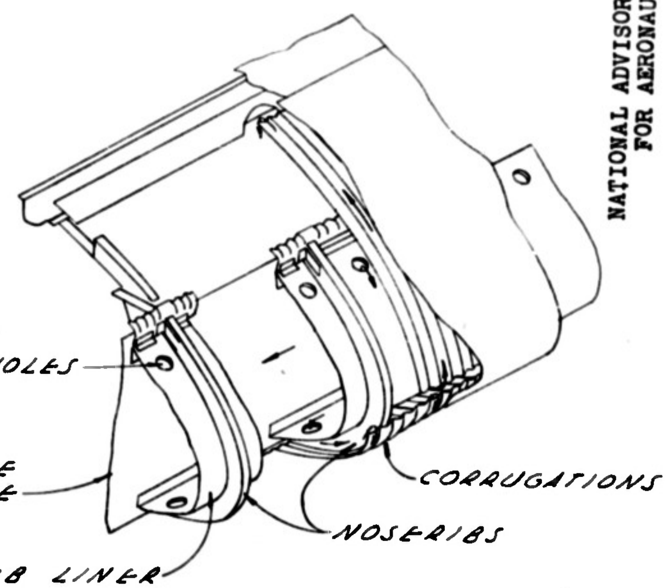

NOTE: NOSERIBS AND NOSERIB LINER END AT STATION 292.

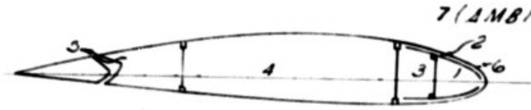

REGIONS OF ANALYSIS

FIGURE 3.- DETAILS OF THE WING LEADING-EDGE THERMAL SYSTEM OF THE C-46 AIRPLANE.

A-52

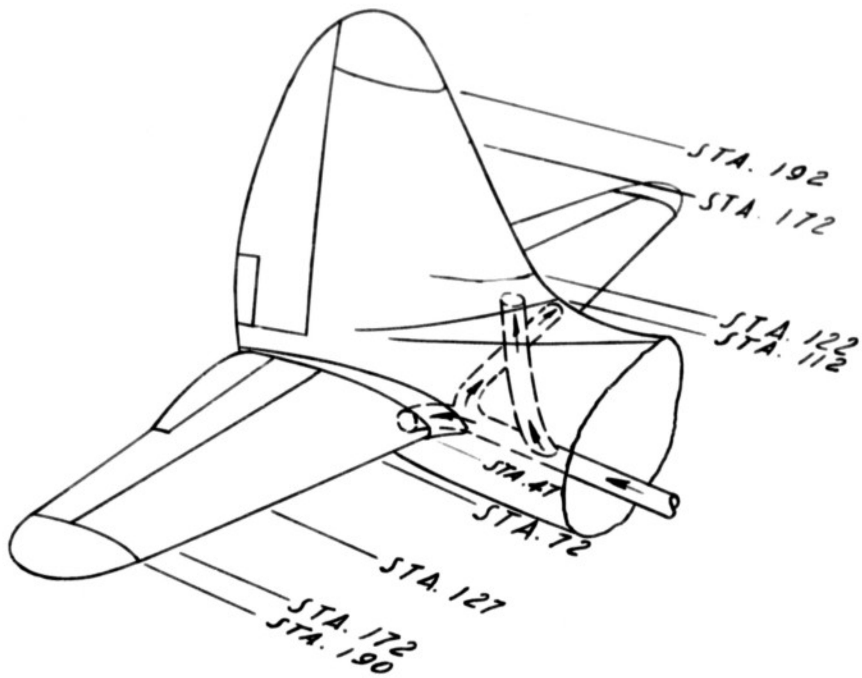

NATIONAL ADVISORY COMMITTEE
FOR AERONAUTICS

FIGURE 4.- THE EMPENNAGE OF THE C-46 AIRPLANE SHOWING THE THERMAL ICE-PREVENTION SYSTEM AND THE STATIONS ANALYZED.

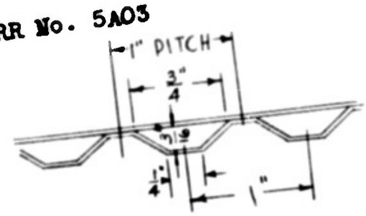

CORRUGATION DIMENSIONS

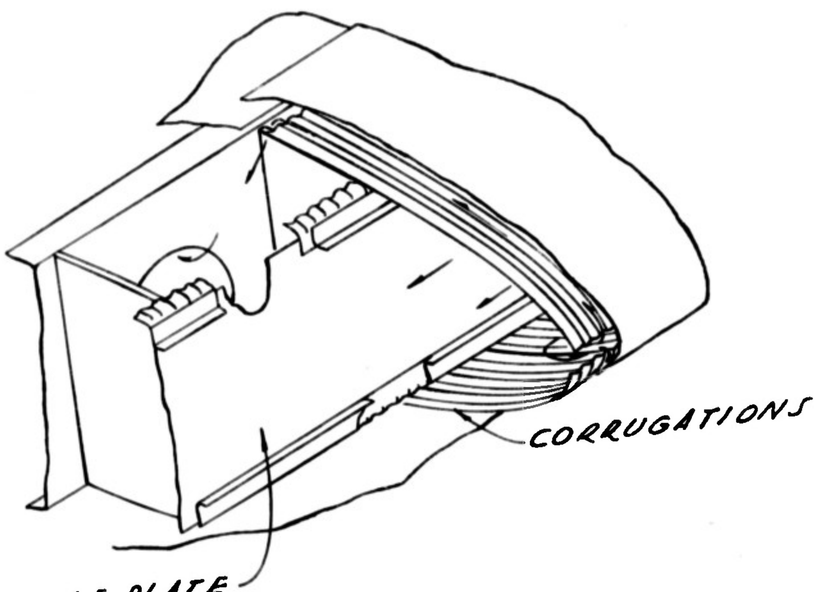

NATIONAL ADVISORY COMMITTEE
FOR AERONAUTICS

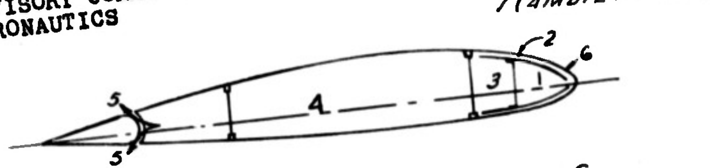

REGIONS OF ANALYSIS

FIGURE 5.- DETAILS OF THE LEADING-EDGE THERMAL SYSTEM FOR THE HORIZONTAL-STABILIZER AND VERTICAL FIN OF THE C-46 AIRPLANE.

A-52

NATIONAL ADVISORY COMMITTEE
FOR AERONAUTICS

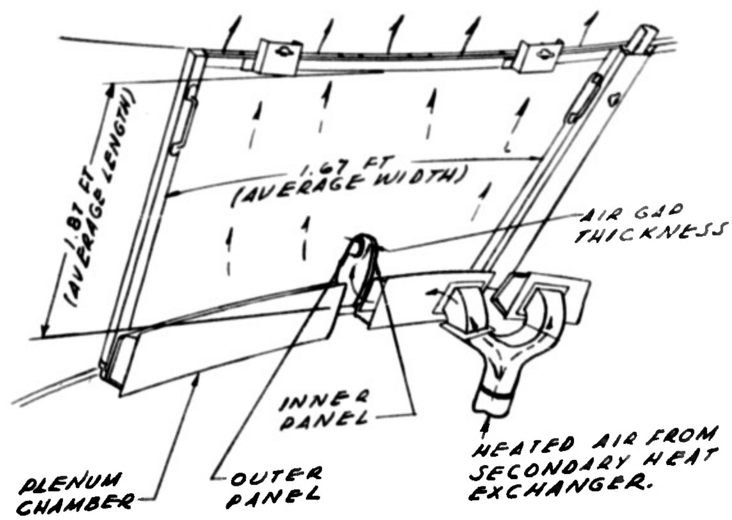

FIGURE 6. DETAILS OF THE WINDSHIELD THERMAL SYSTEM OF THE C-46 AIRPLANE

A-52

Figure 7.- Pressure belt mounted on the C-46 wing for measuring the pressure distribution over the leading edge.

A-52

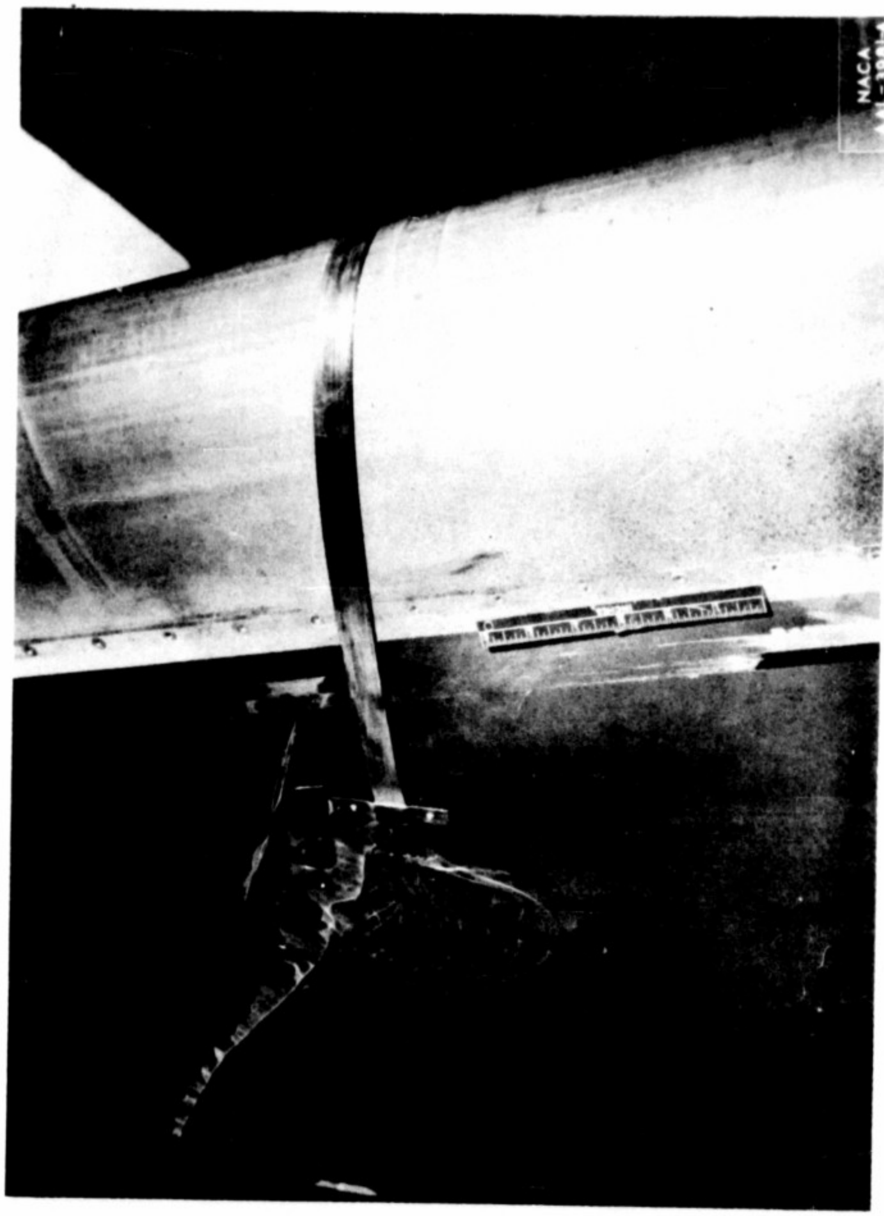

Figure 8.- Pressure belt mounted on the C-46 vertical fin leading edge for measuring the pressure distribution over the leading edge of the fin.

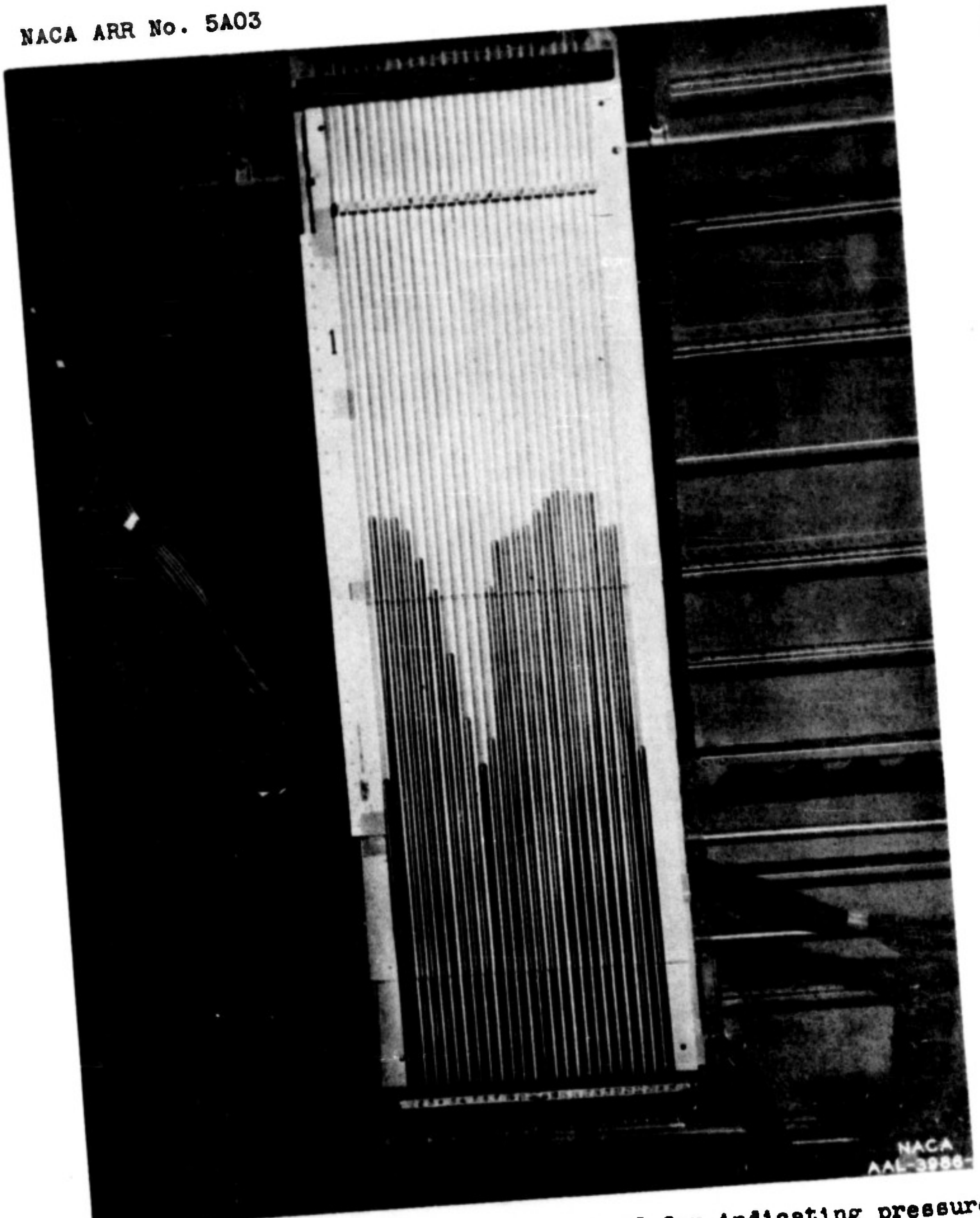

Figure 9.- The water manometer used for indicating pressures at the empennage pressure belts, with a typical pressure indication, C-46 airplane.

A-52

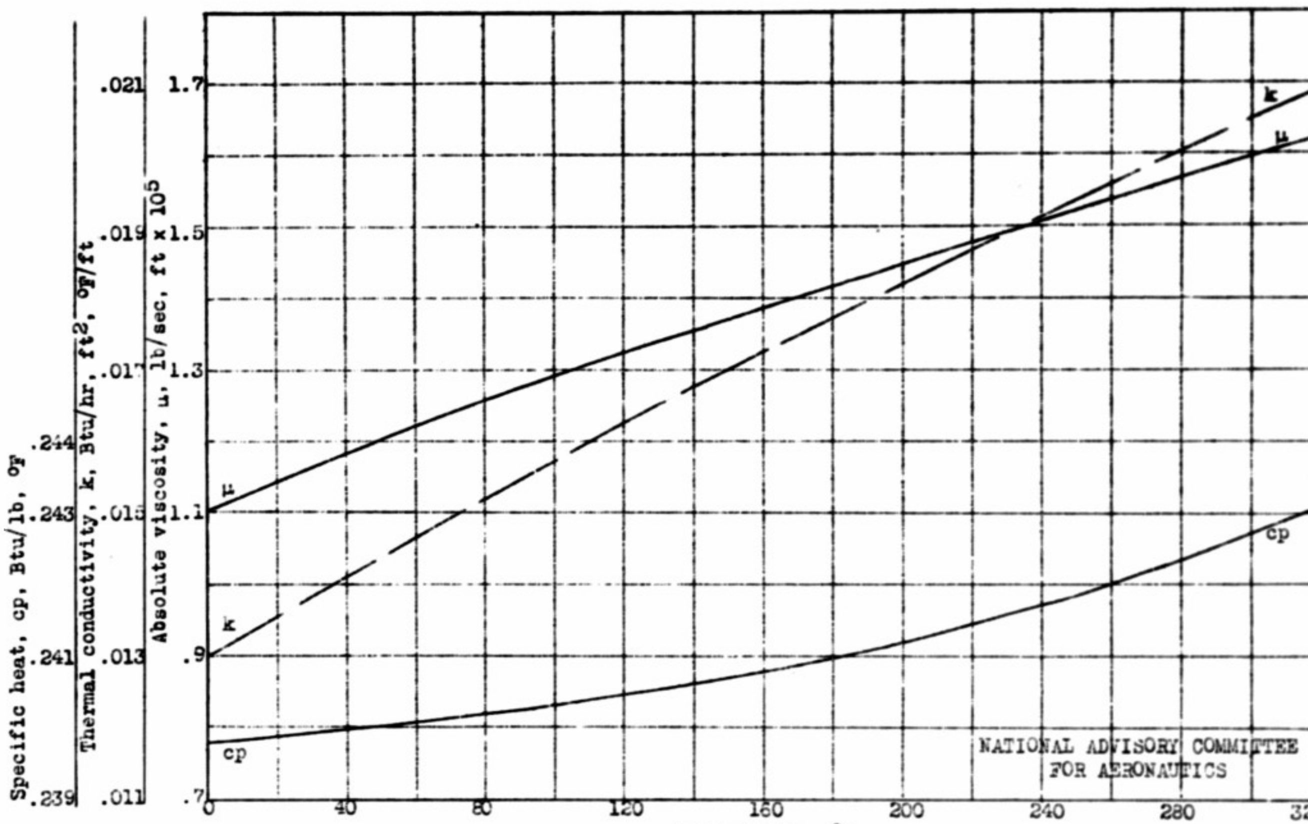

Figure 10.- Properties of air obtained from reference 5, as employed in the analysis of the thermal ice-prevention equipment for the C-46 airplane.

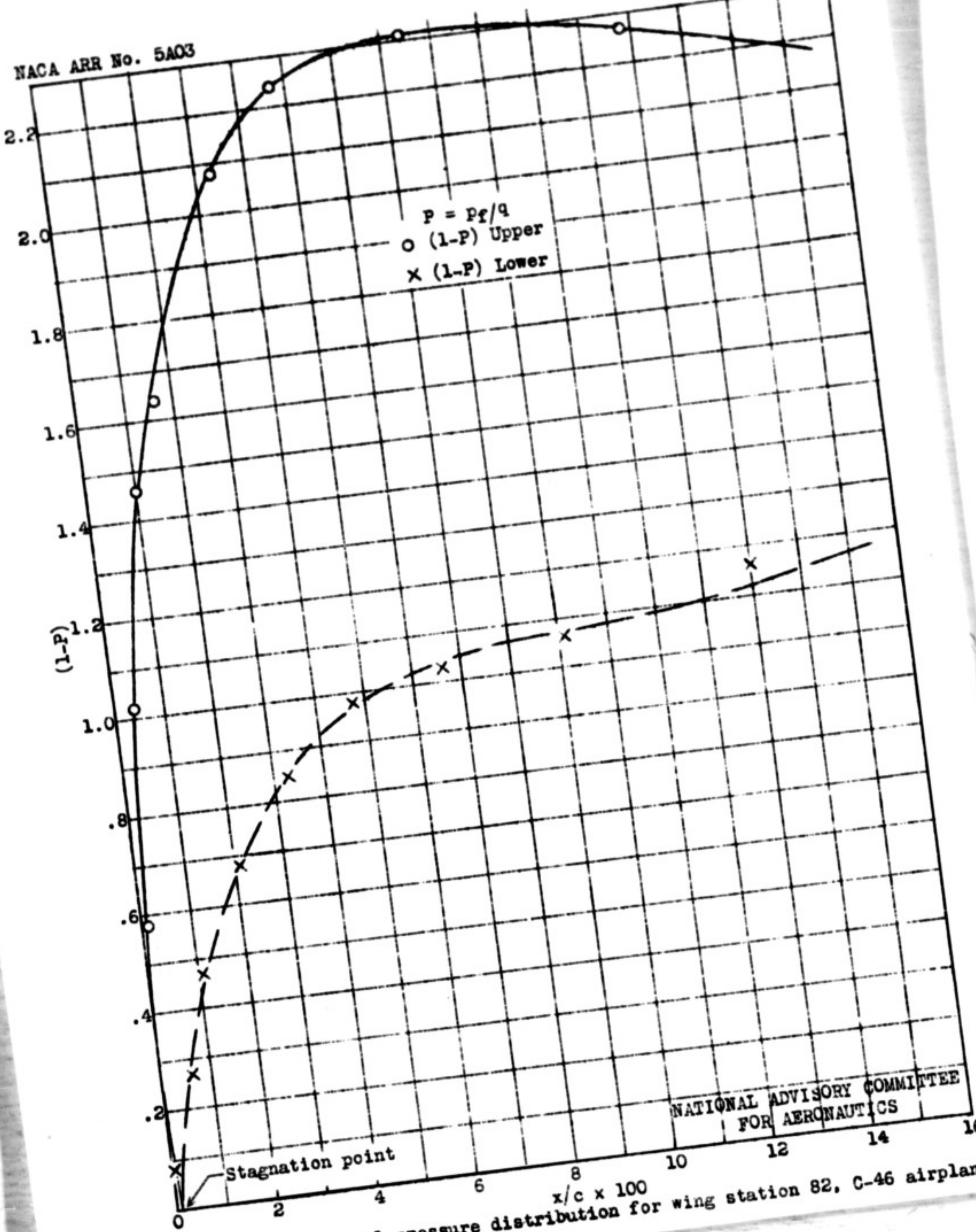

Figure 11.- The airfoil pressure distribution for wing station 82, C-46 airplane.

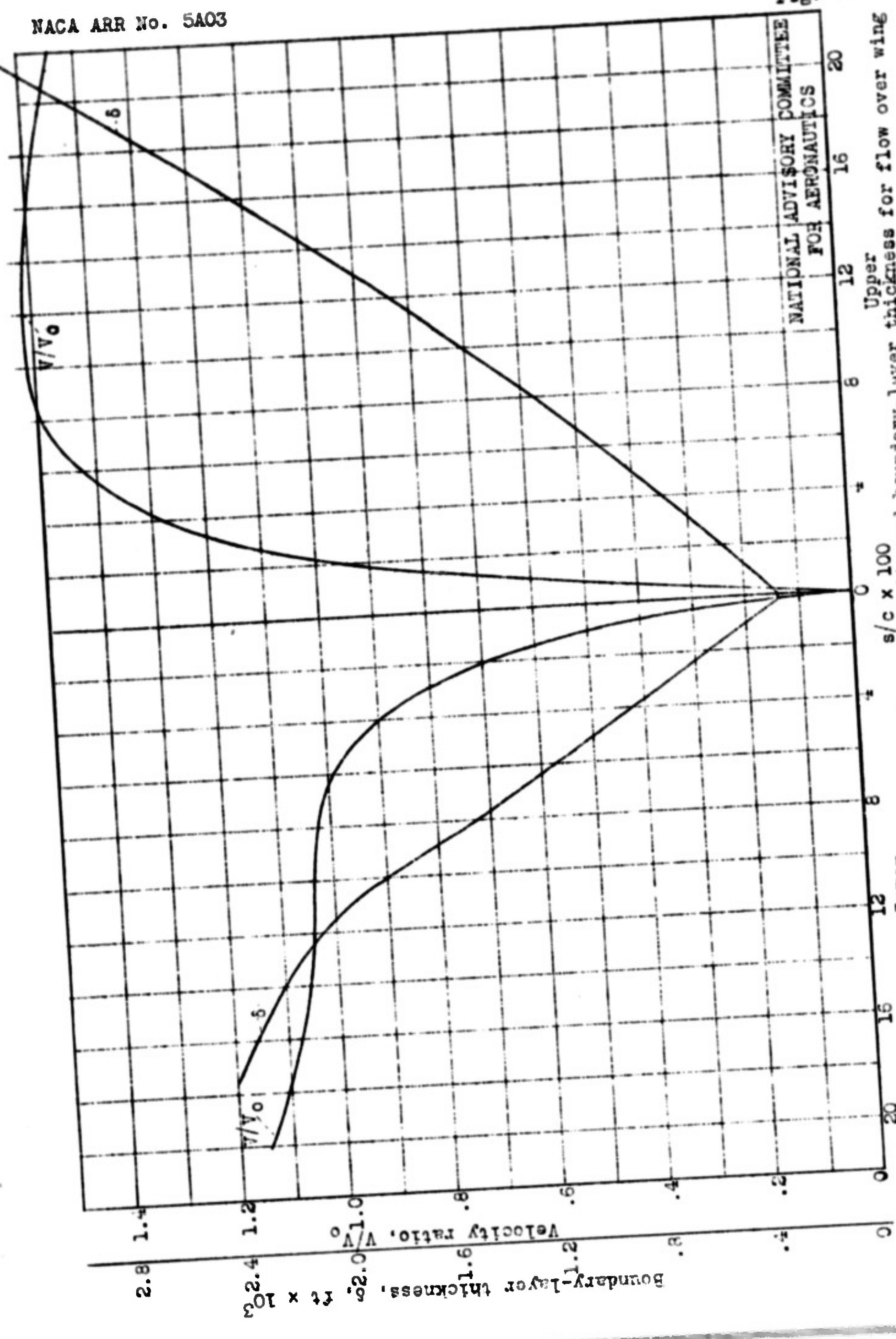

Figure 12.- Ratio of local air velocity to free-stream velocity and boundary-layer thickness for flow over wing station 82, C-46 airplane.

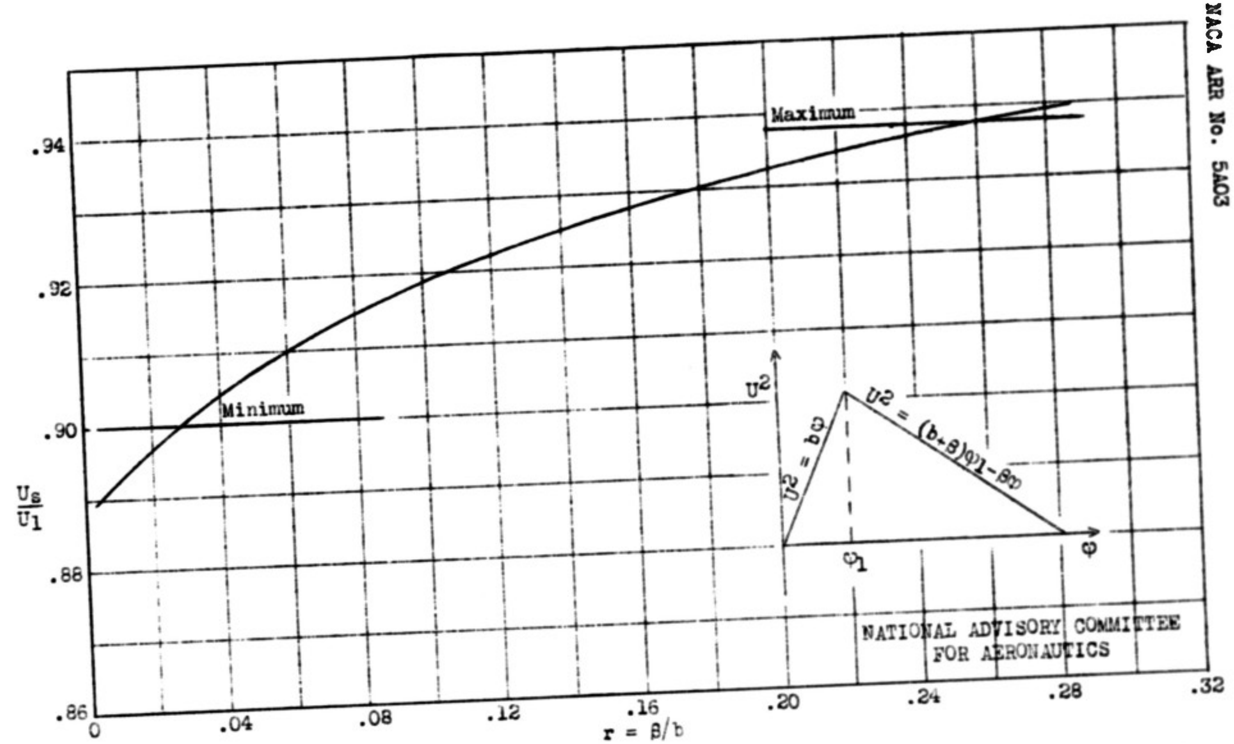

Figure 13.- Ratio of the local velocity at laminar separation, U_s, to the maximum local velocity, U_1, as a function of the slopes of the double-roof velocity profile. (Values obtained from reference 6.) C-46 airplane.

51

A-52

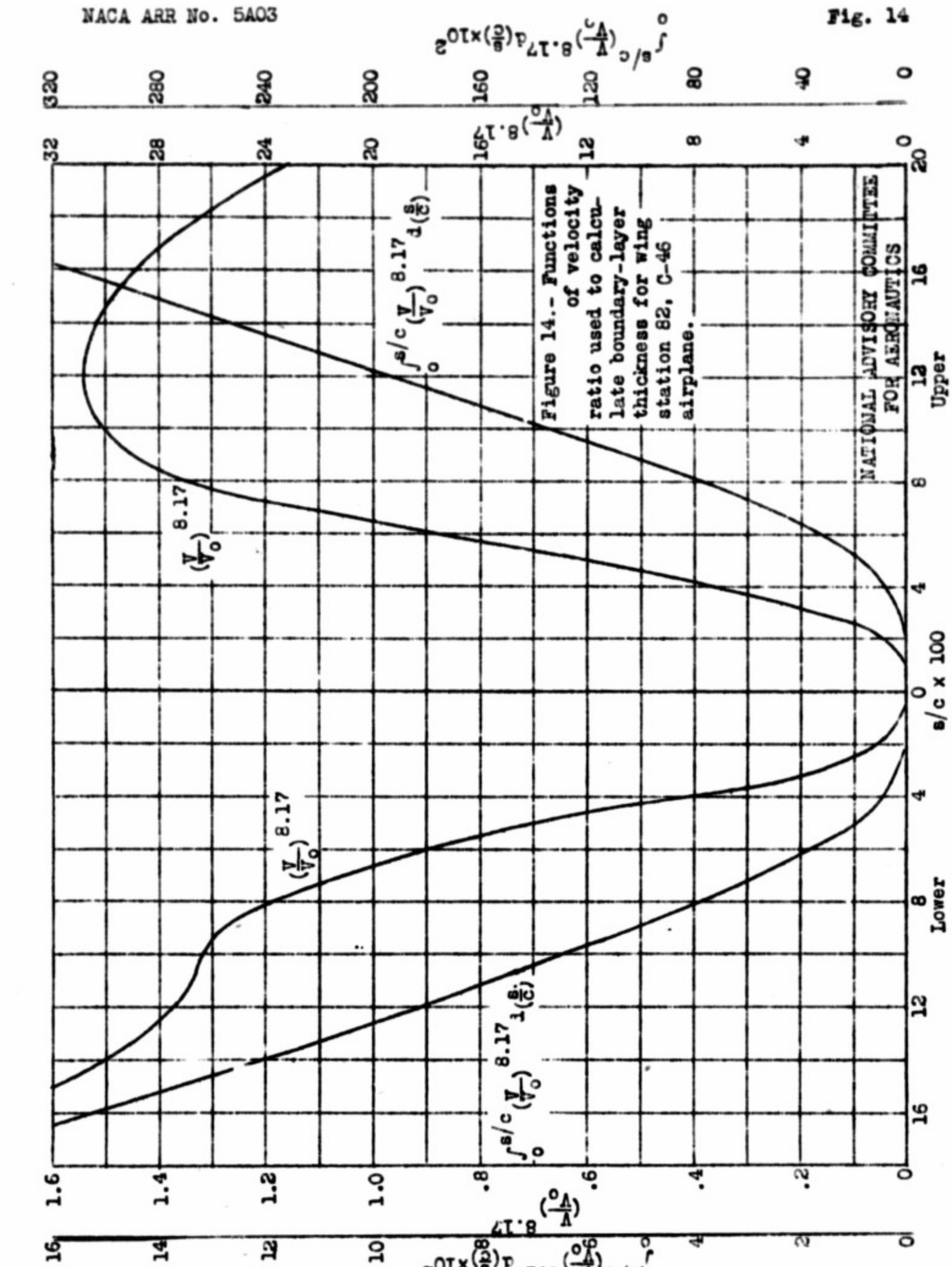

Figure 14.- Functions of velocity ratio used to calculate boundary-layer thickness for wing station 82, C-46 airplane.

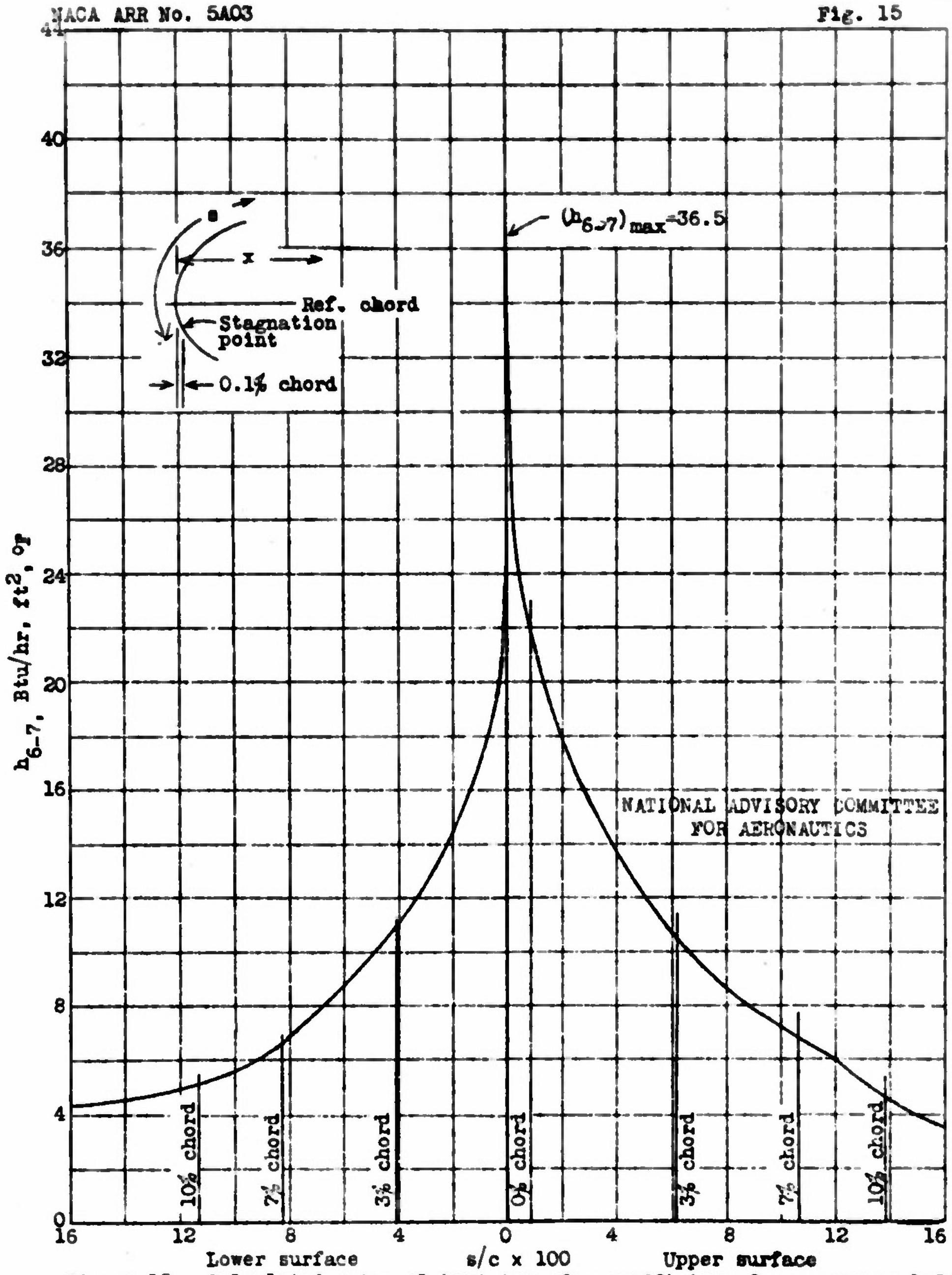

Figure 15.- Calculated external heat-transfer coefficient from pressure-belt data for wing station 82, C-46 airplane.

A-52

34

A-52

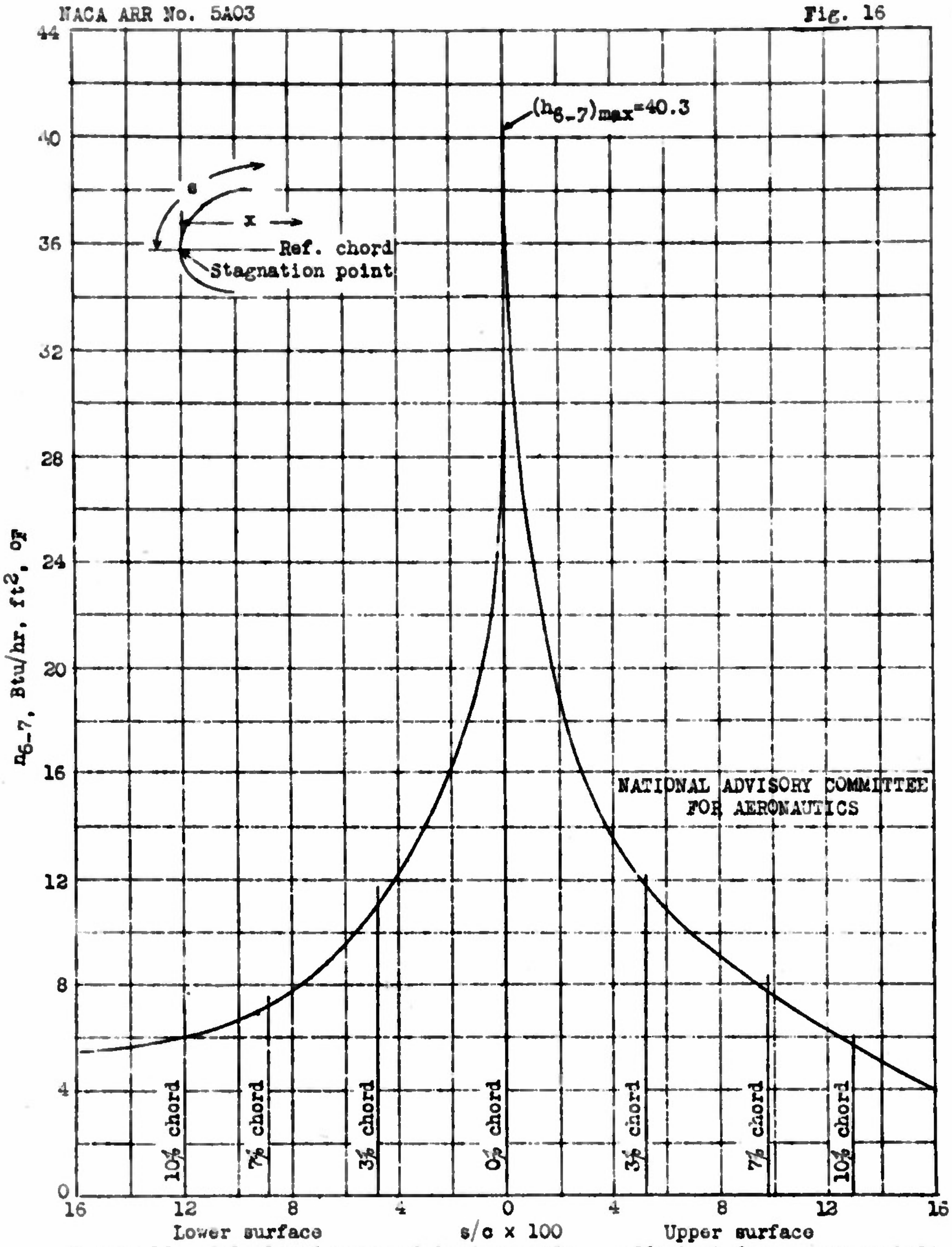

Figure 16.- Calculated external heat-transfer coefficient from pressure-belt data for wing station 157, C-46 airplane.

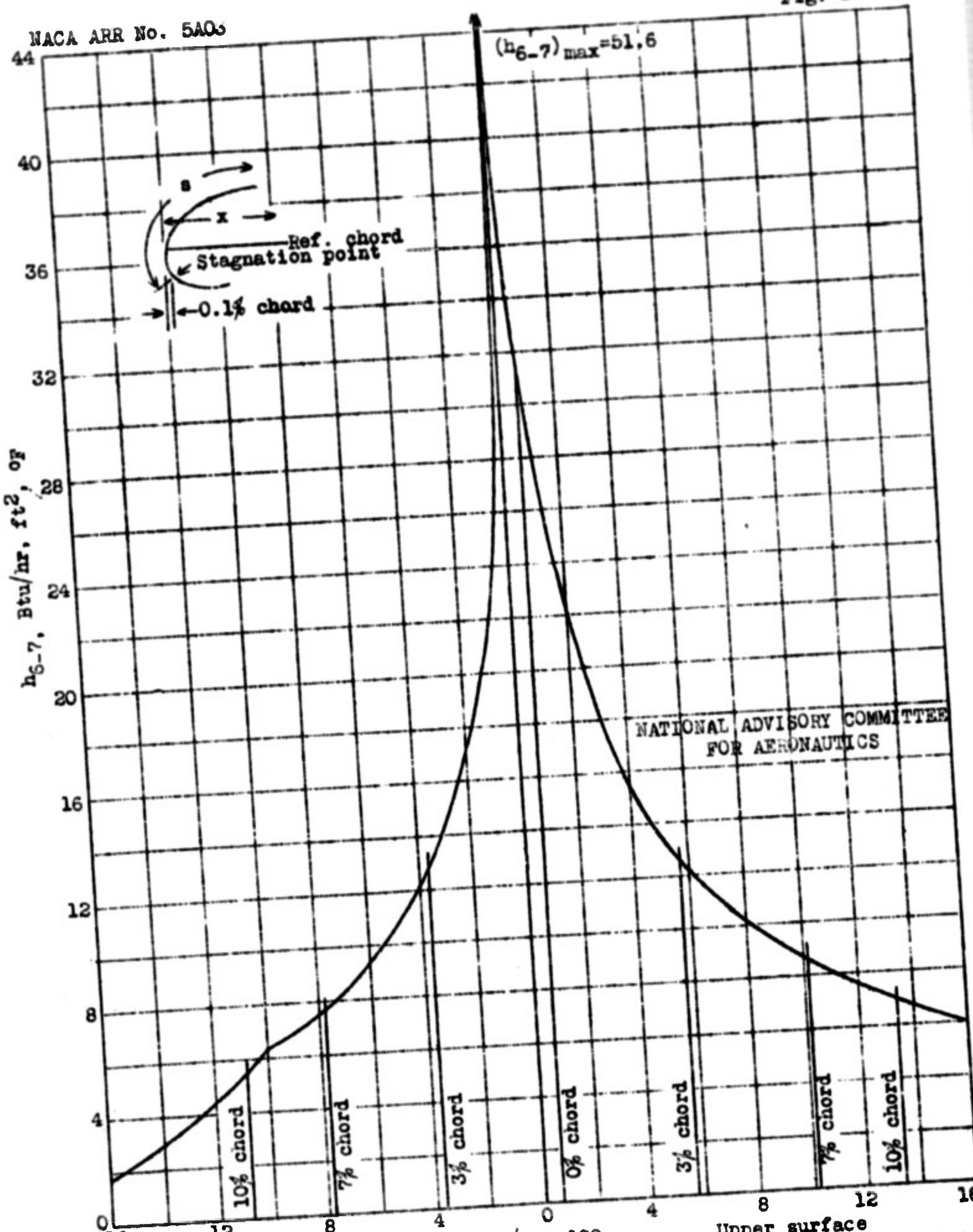

Figure 17.- Calculated external heat-transfer coefficient from pressure-belt data for wing station 292, C-46 airplane.

56

A-52

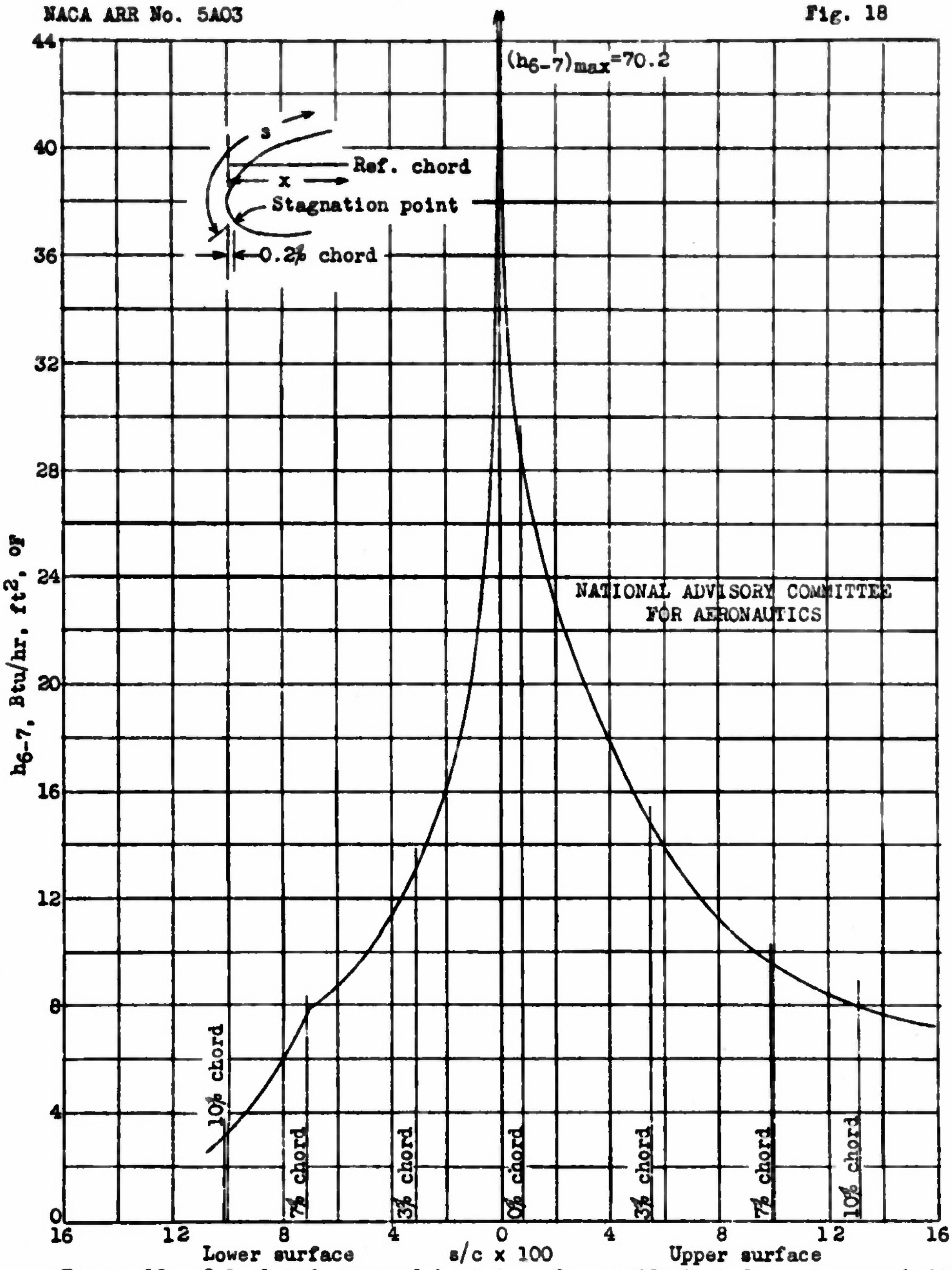

Figure 18.- Calculated external heat-transfer coefficient from pressure-belt data for wing station 382, C-46 airplane.

A-52

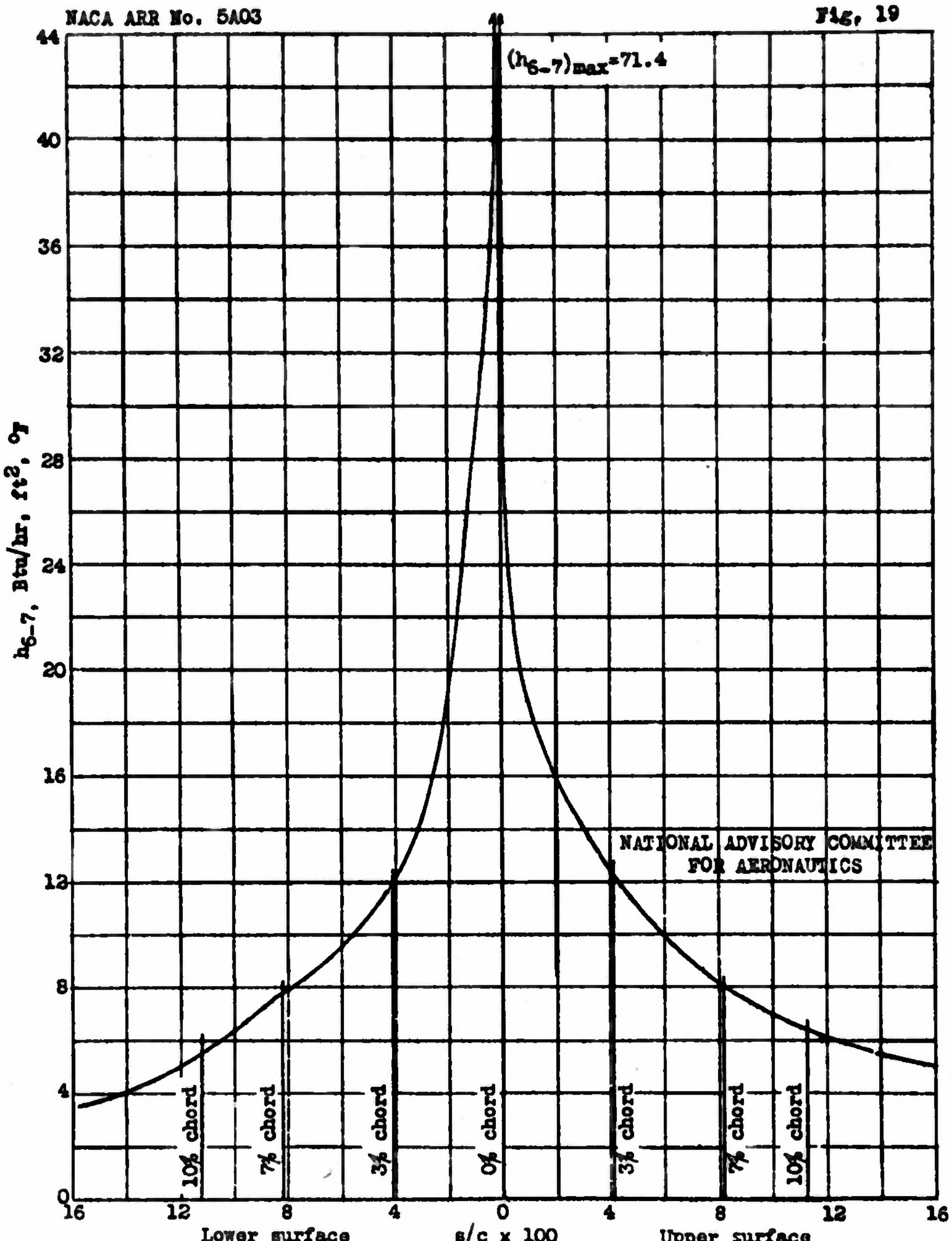

Figure 19.- Calculated external heat-transfer coefficient from pressure-belt data for horizontal stabilizer station 72, C-46 airplane.

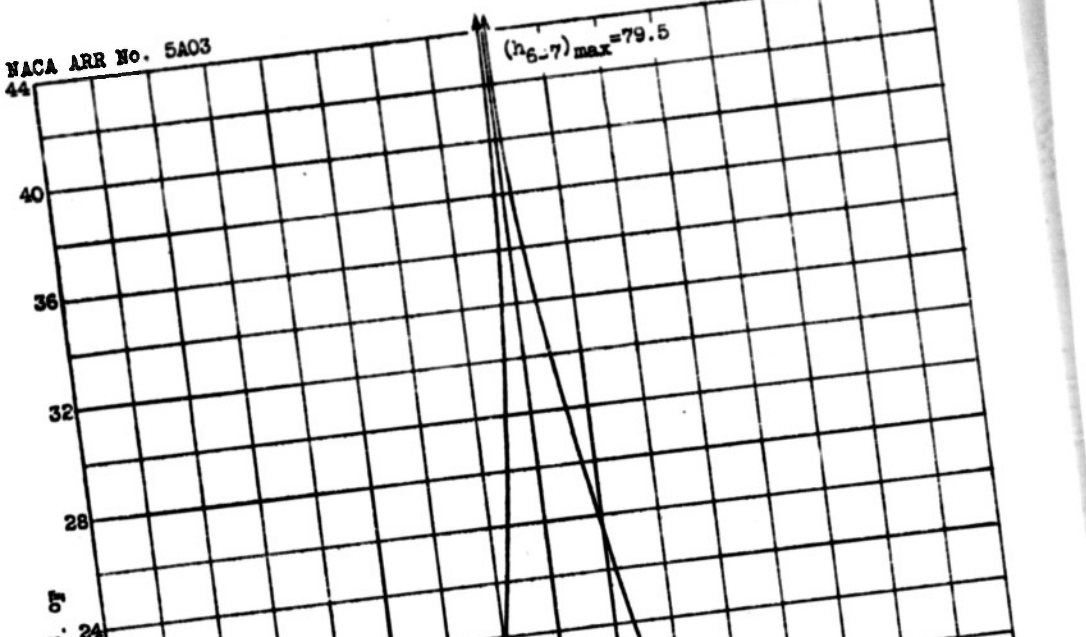

Figure 20.- Calculated external heat-transfer coefficient from pressure-belt data for horizontal-stabilizer station 127, C-46 airplane.

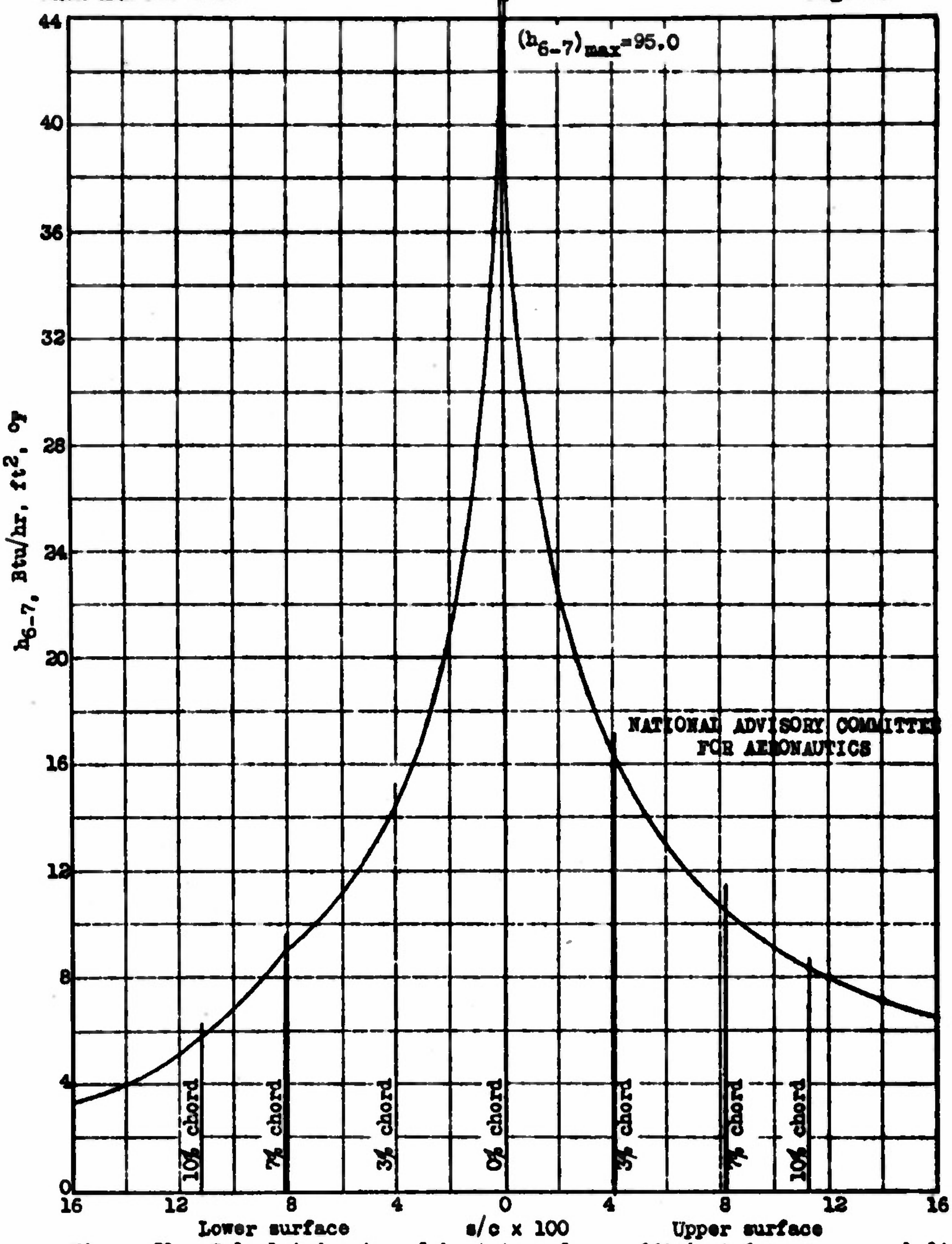

Figure 21.- Calculated external heat-transfer coefficient from pressure-belt data for horizontal-stabilizer station 172, C-46 airplane.

60

A-52

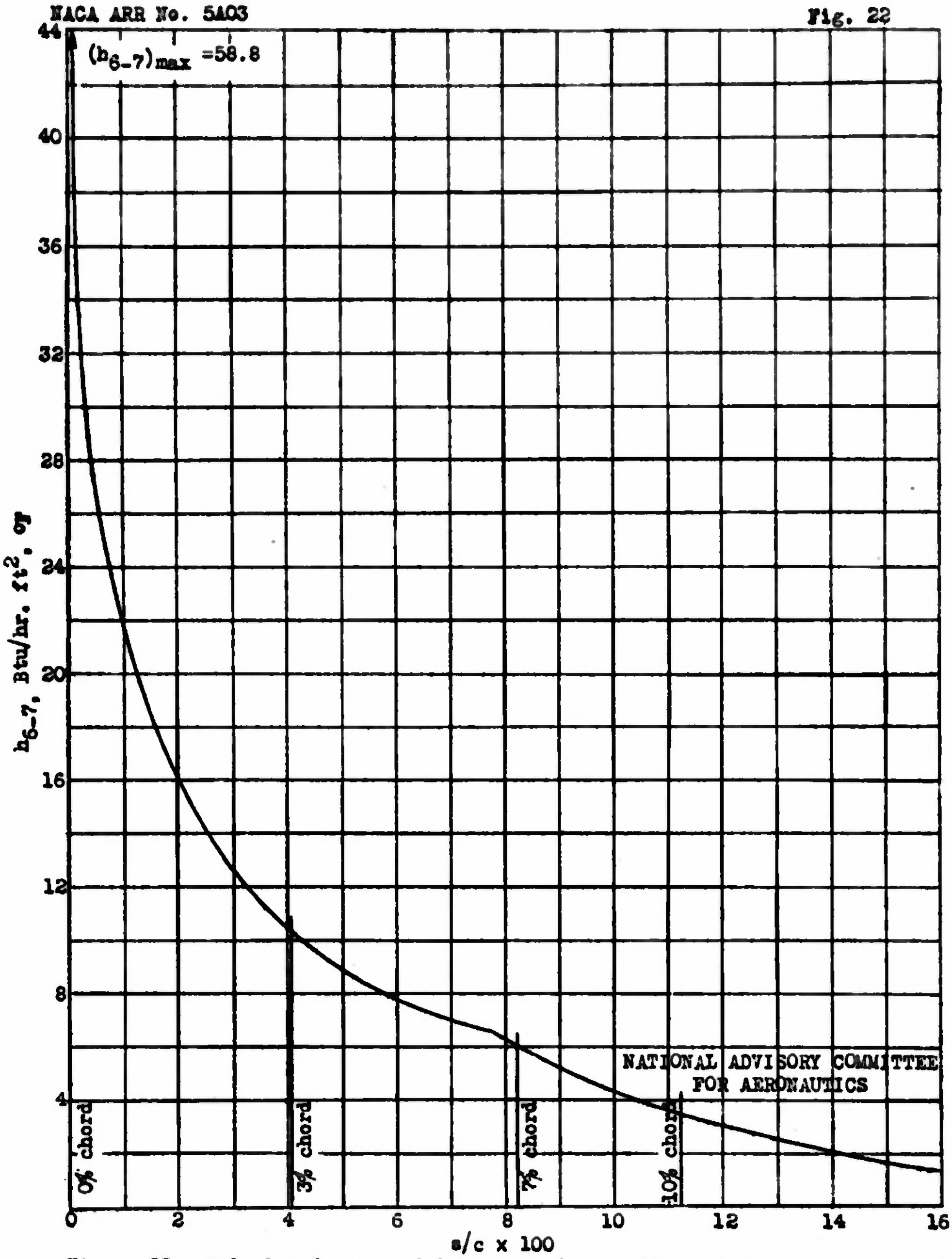

Figure 22.- Calculated external heat-transfer coefficient from pressure-belt data for vertical-fin station 122, C-46 airplane.

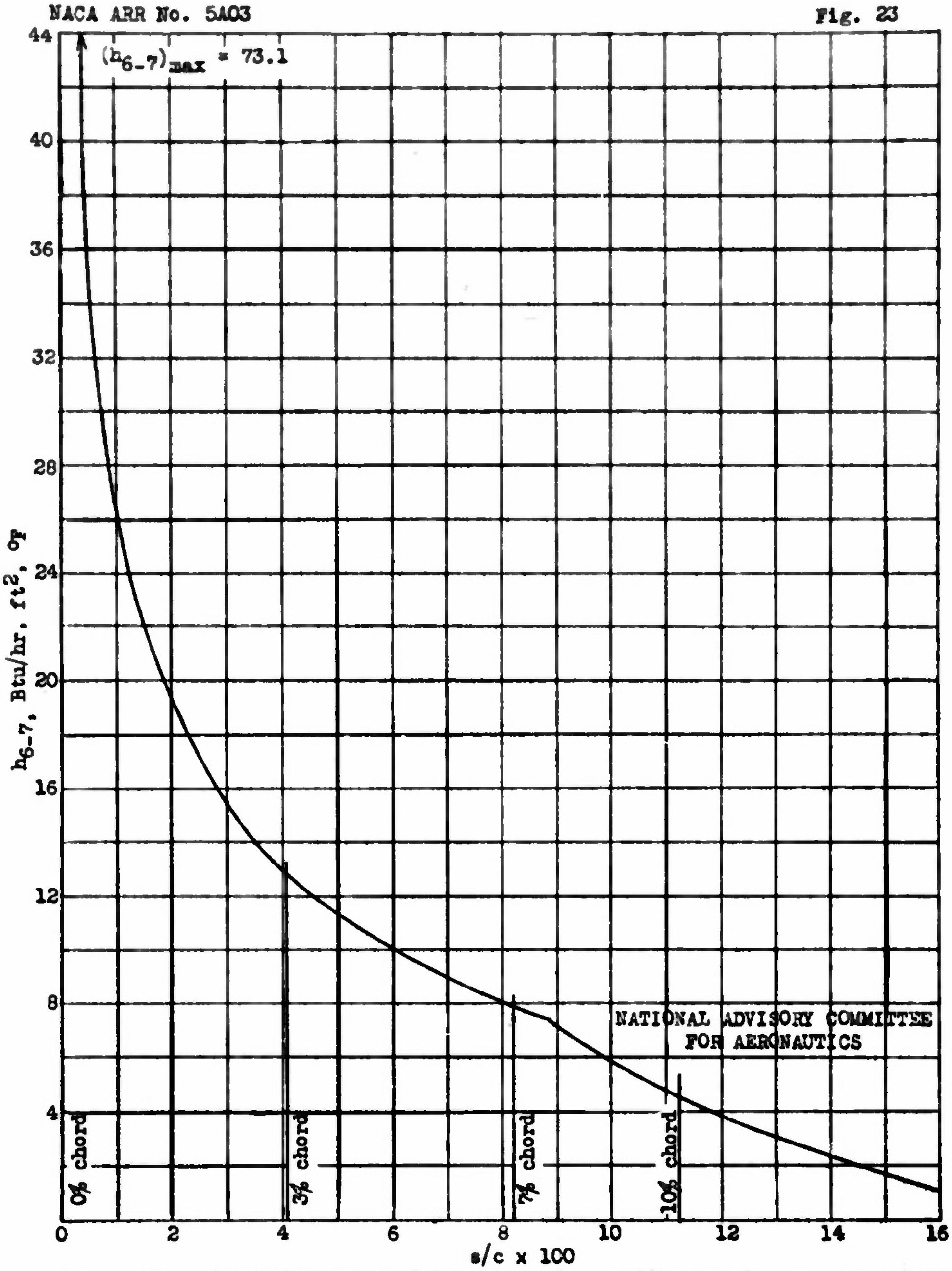

Figure 23.- Calculated external heat-transfer coefficient from pressure-belt data for vertical-fin station 172, C-46 airplane.

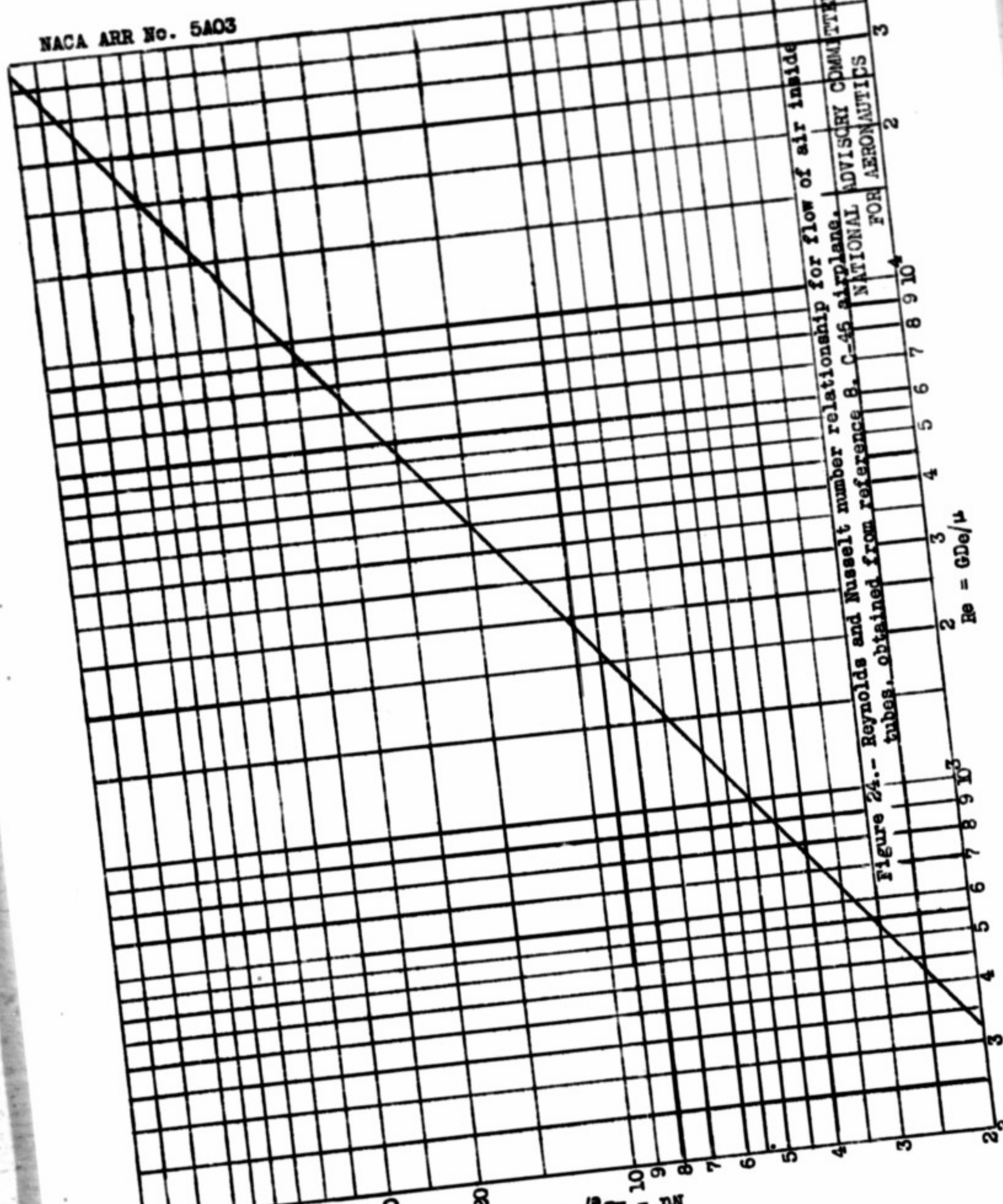

Figure 24.- Reynolds and Nusselt number relationship for flow of air inside tubes, obtained from reference 8. C-46 airplane.

NATIONAL ADVISORY COMMITTEE FOR AERONAUTICS

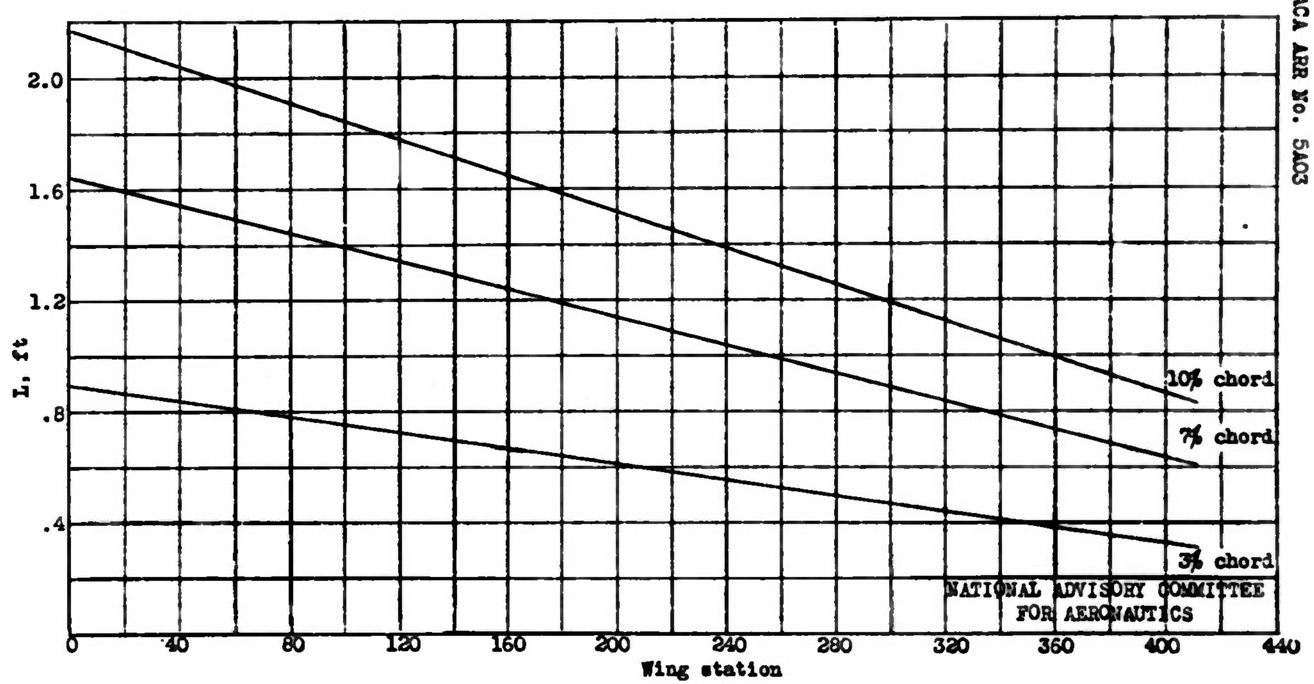

Figure 25.- Distance around leading edge measured chordwise from 0 percent chord point for wing upper surface, C-46 airplane.

A-52

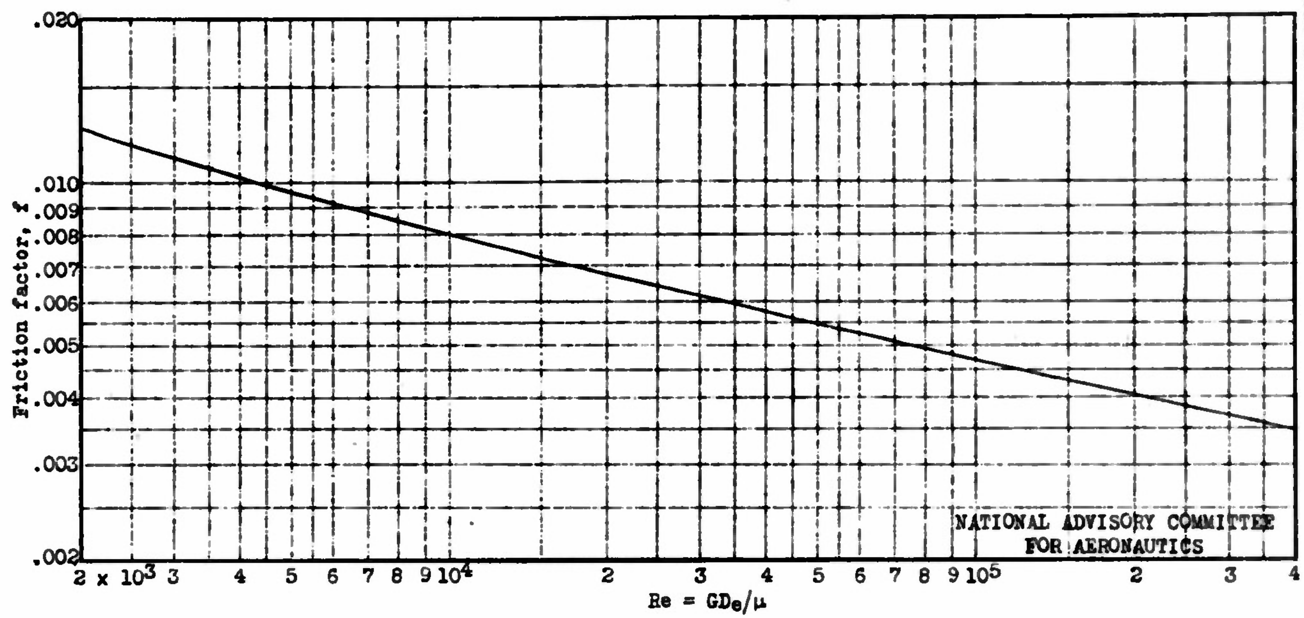

Figure 26.- Friction factors for isothermal flow of air in smooth tubes, obtained from reference 8. C-46 airplane.

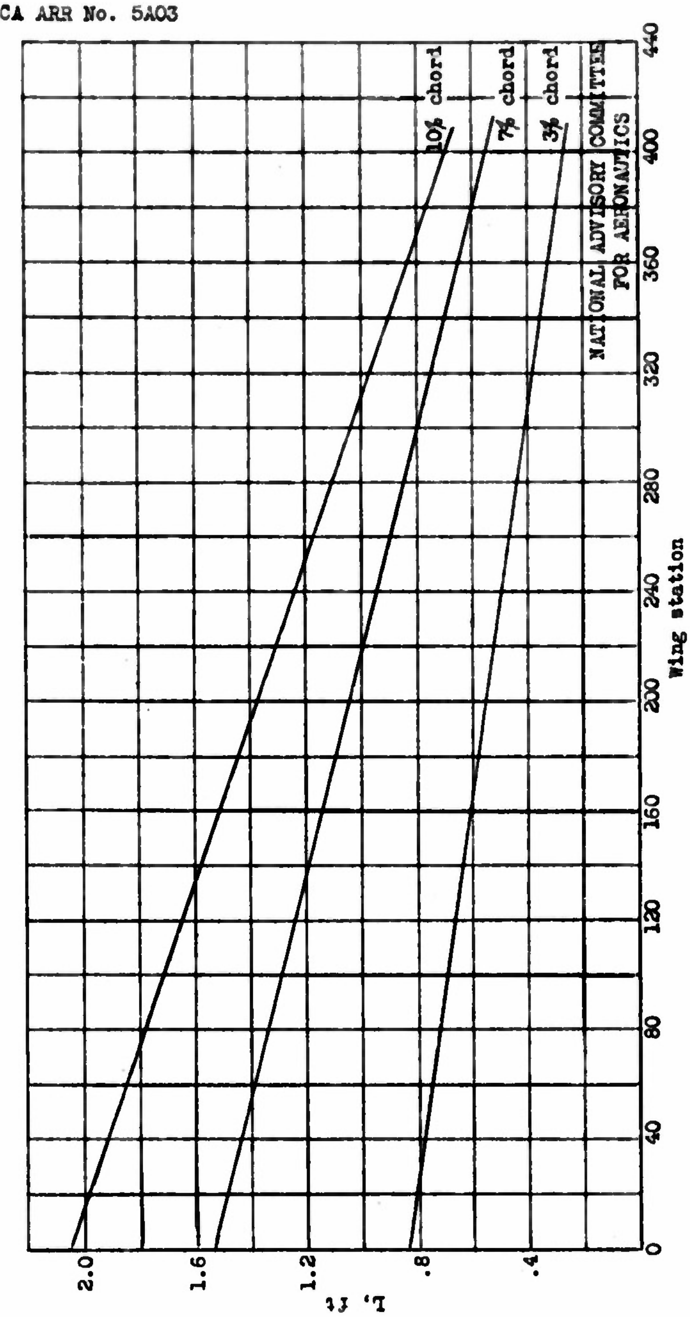

Figure 27.- Distance around leading edge measured chordwise from 0 percent chord point for wing lower surface, C-46 airplane.

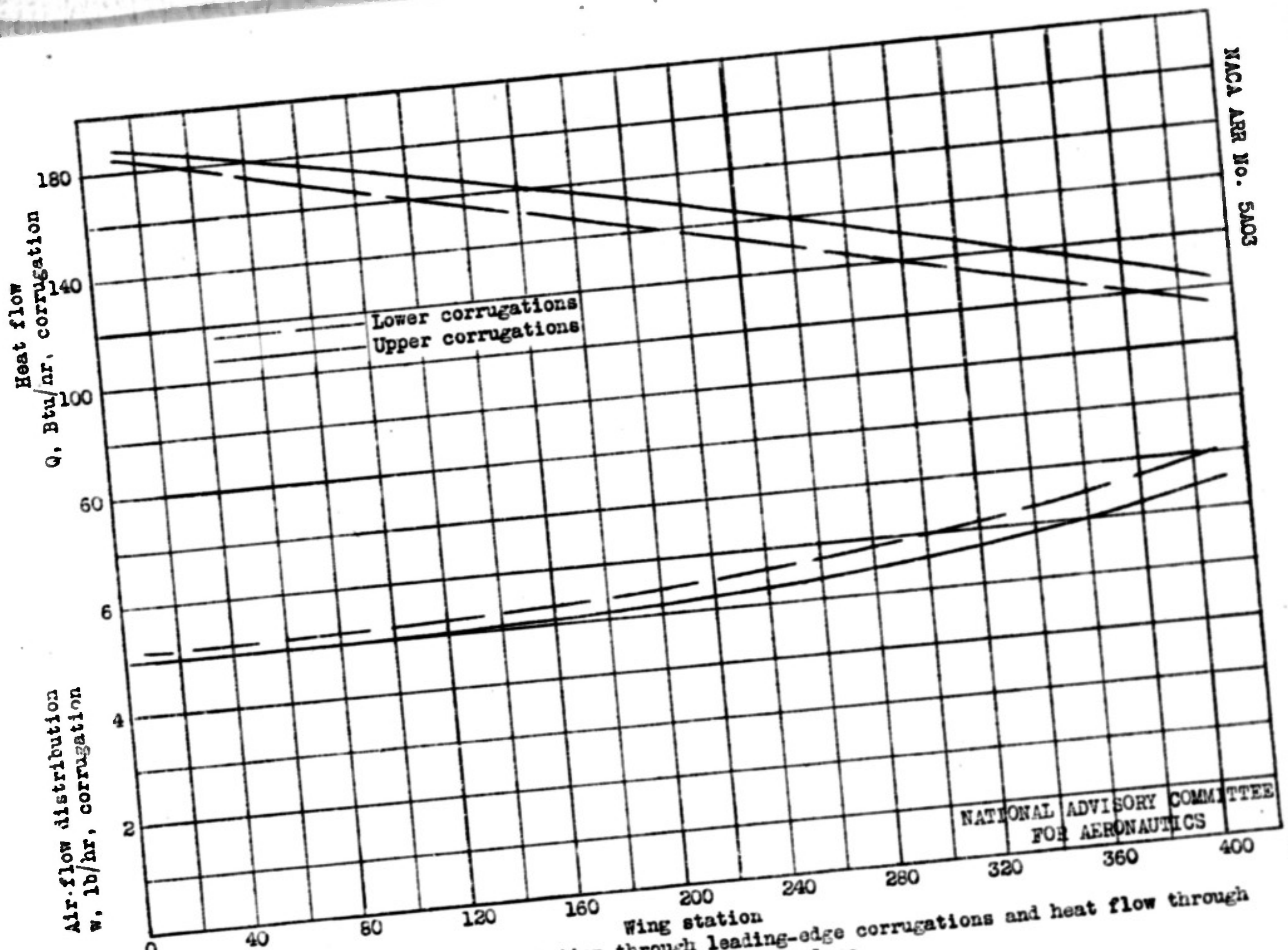

Figure 28.- Heated-air-flow distribution through leading-edge corrugations and heat flow through heated surface of wing leading edge, C-46 airplane.

66

67

A-52

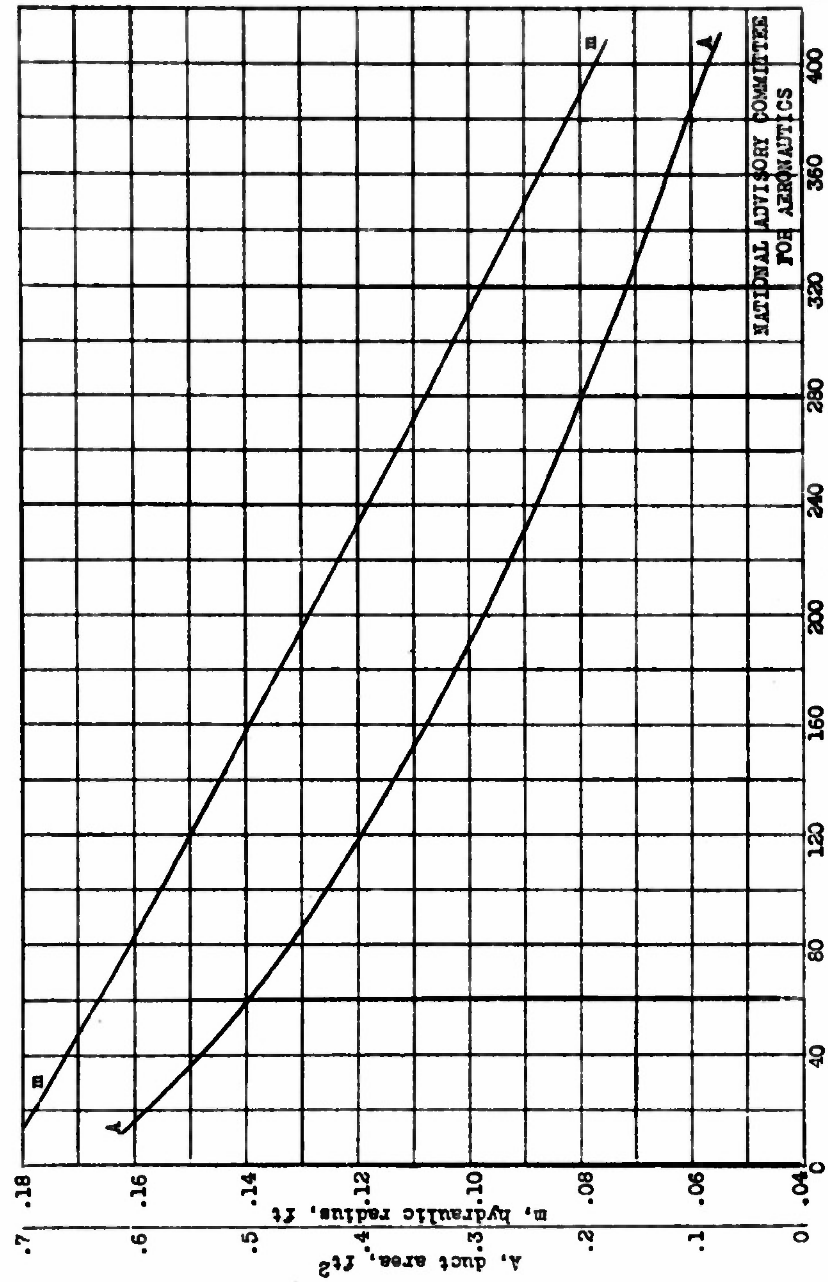

Figure 29.- Wing leading-edge-duct area and hydraulic radius, C-46 airplane.

68

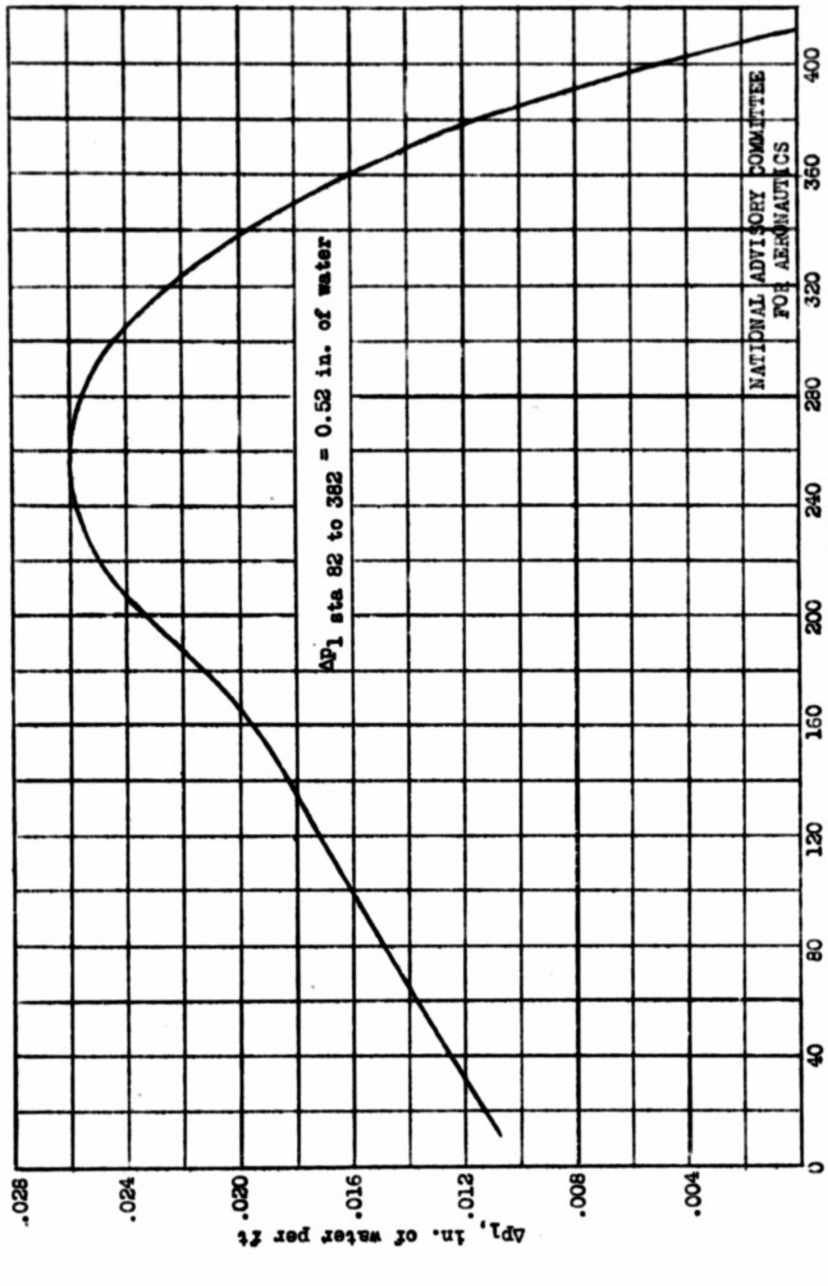

Figure 30.- Heated-air-pressure drop through wing leading-edge duct, C-46 airplane.

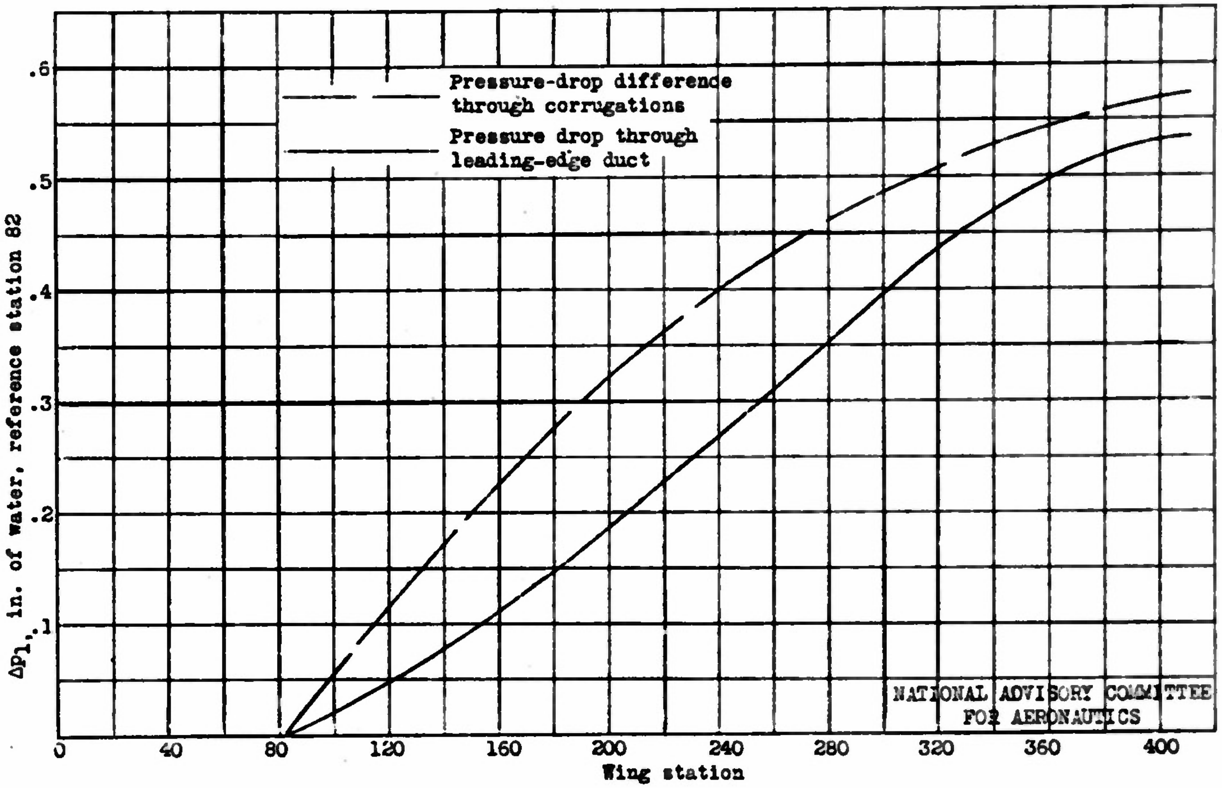

Figure 31.- Comparison of air-pressure drop through corrugations with air-pressure drop through wing leading-edge duct, C-46 airplane.

A-52

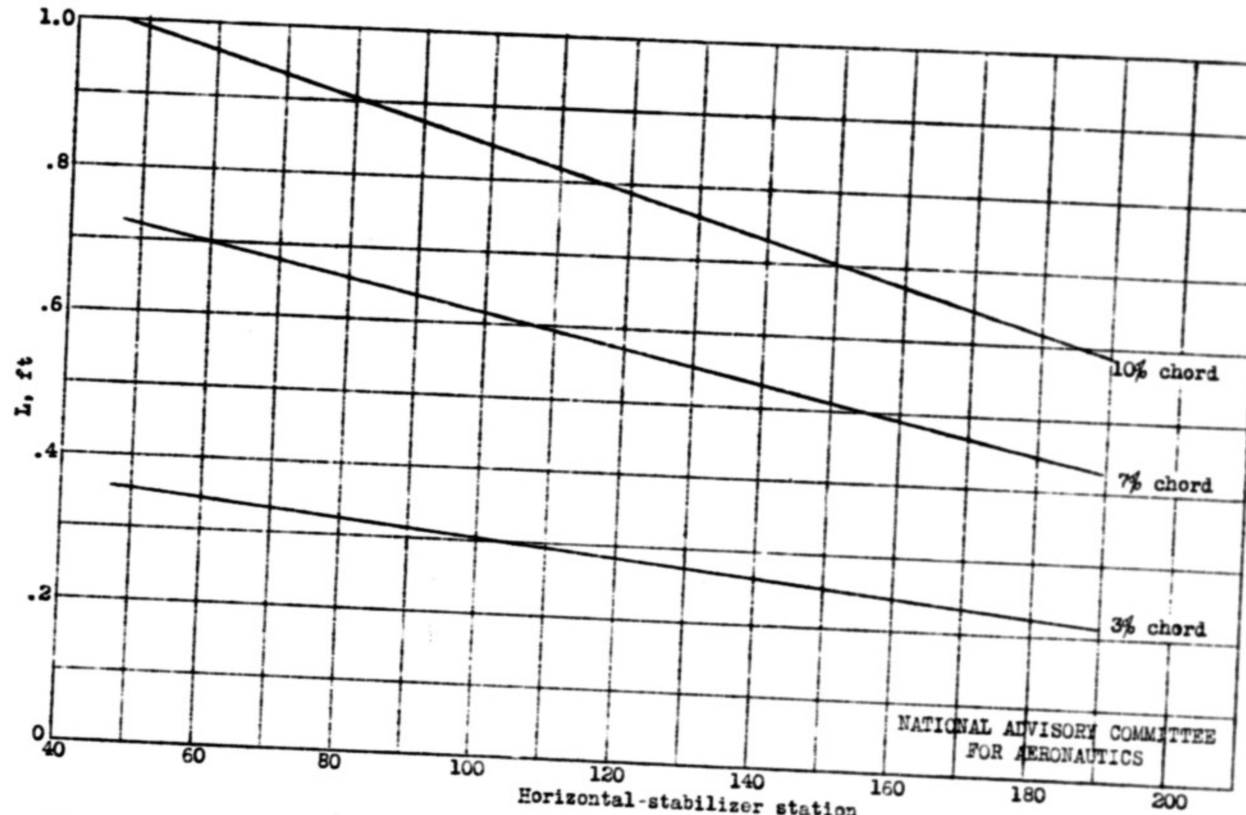

Figure 32.- Distance around leading edge measured chordwise from 0 percent chord point for horizontal-stabilizer upper and lower surfaces, C-46 airplane.

70

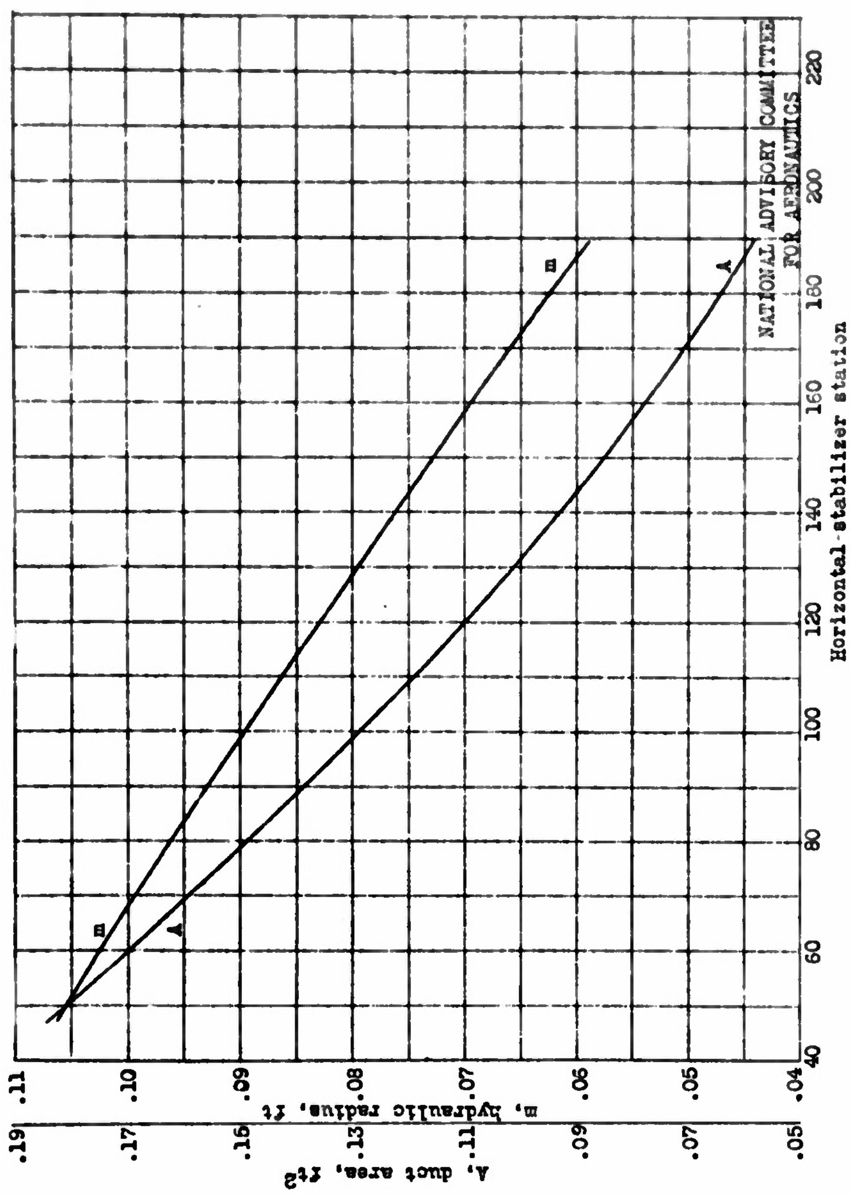

Figure 33.- Horizontal-stabilizer leading-edge-duct area and hydraulic radius, C-46 airplane.

A-52

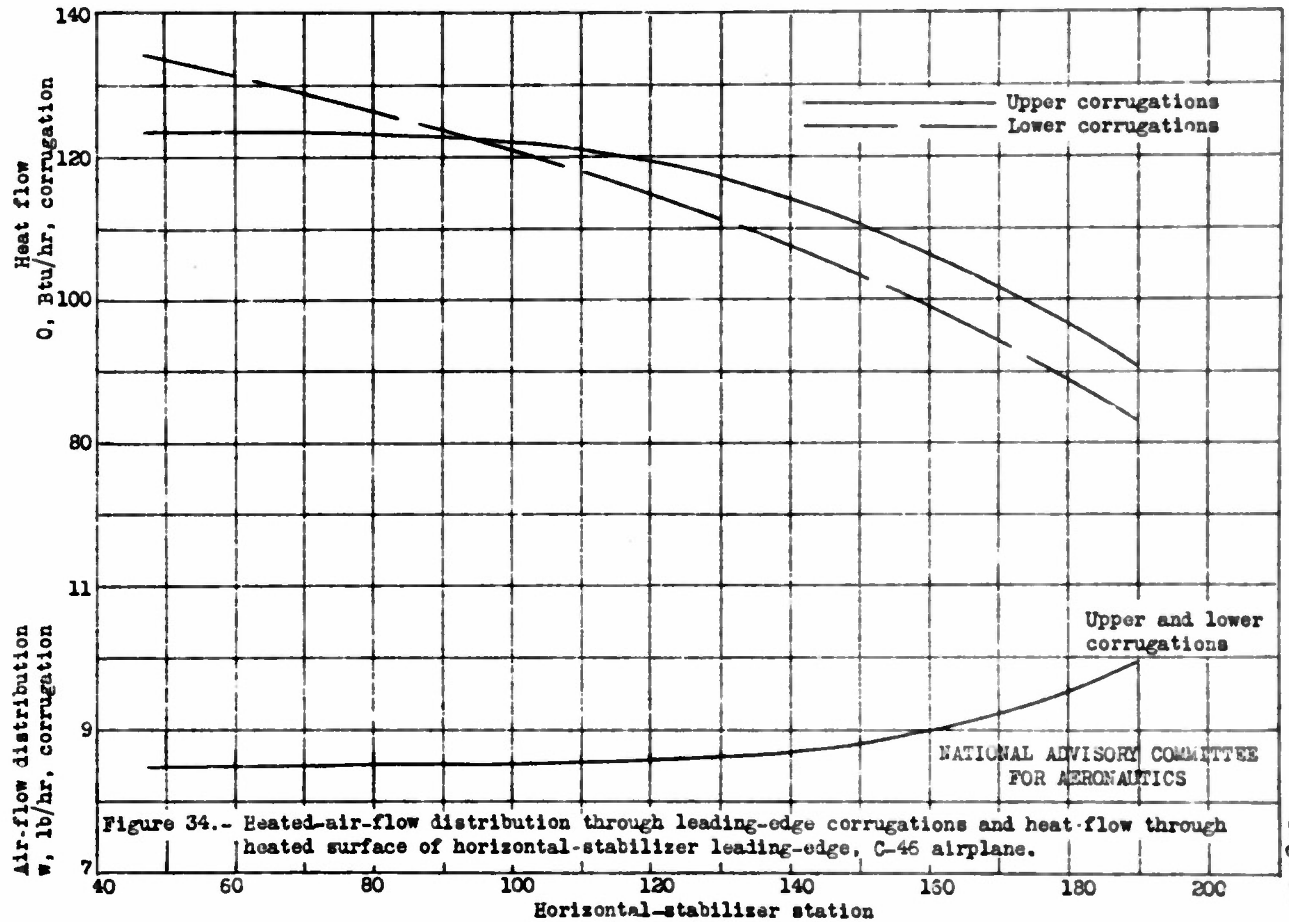

Figure 34.- Heated-air-flow distribution through leading-edge corrugations and heat flow through heated surface of horizontal-stabilizer leading-edge, C-46 airplane.

77

A-52

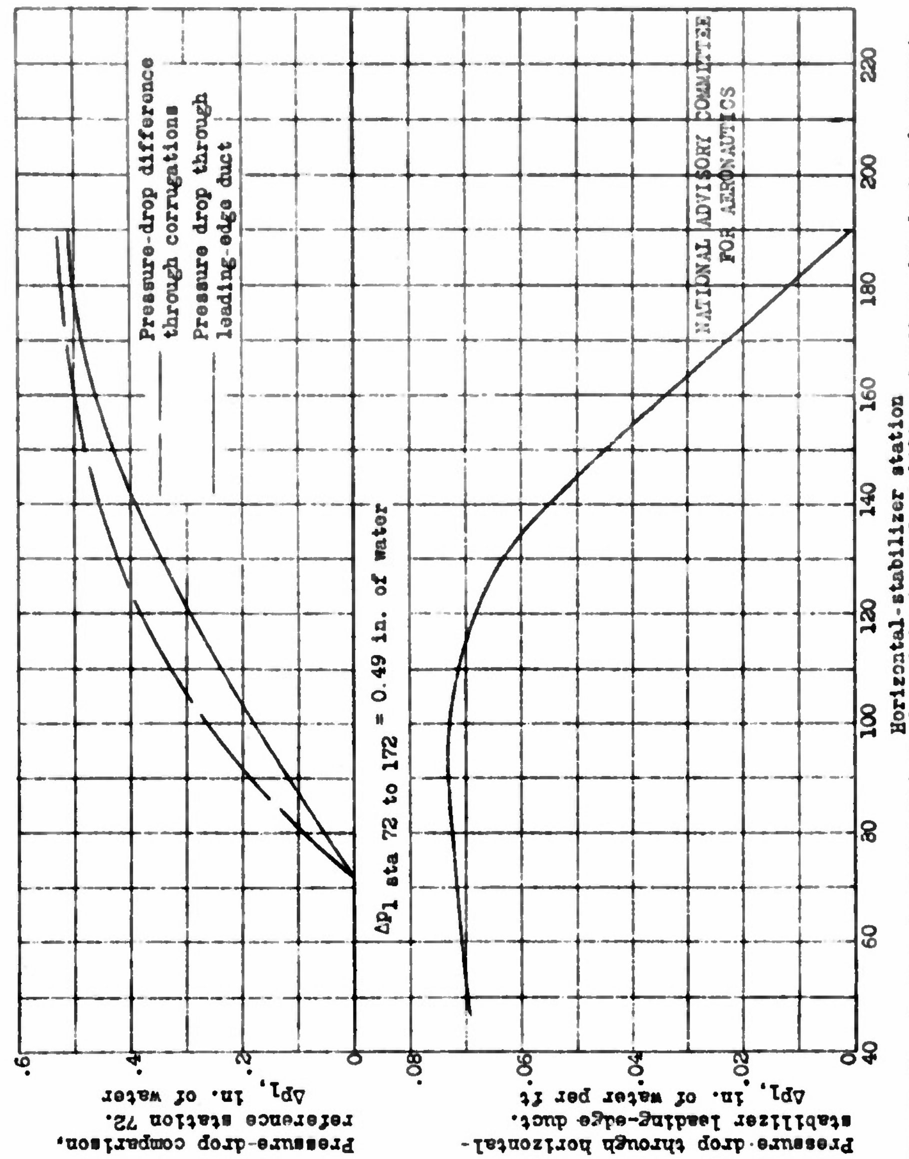

Figure 35.- Heated-air-pressure drop through horizontal-stabilizer leading-edge duct and comparison of calculated air-pressure drop through corrugations with air-pressure drop through leading-edge duct, C-46 airplane.

74

A-52

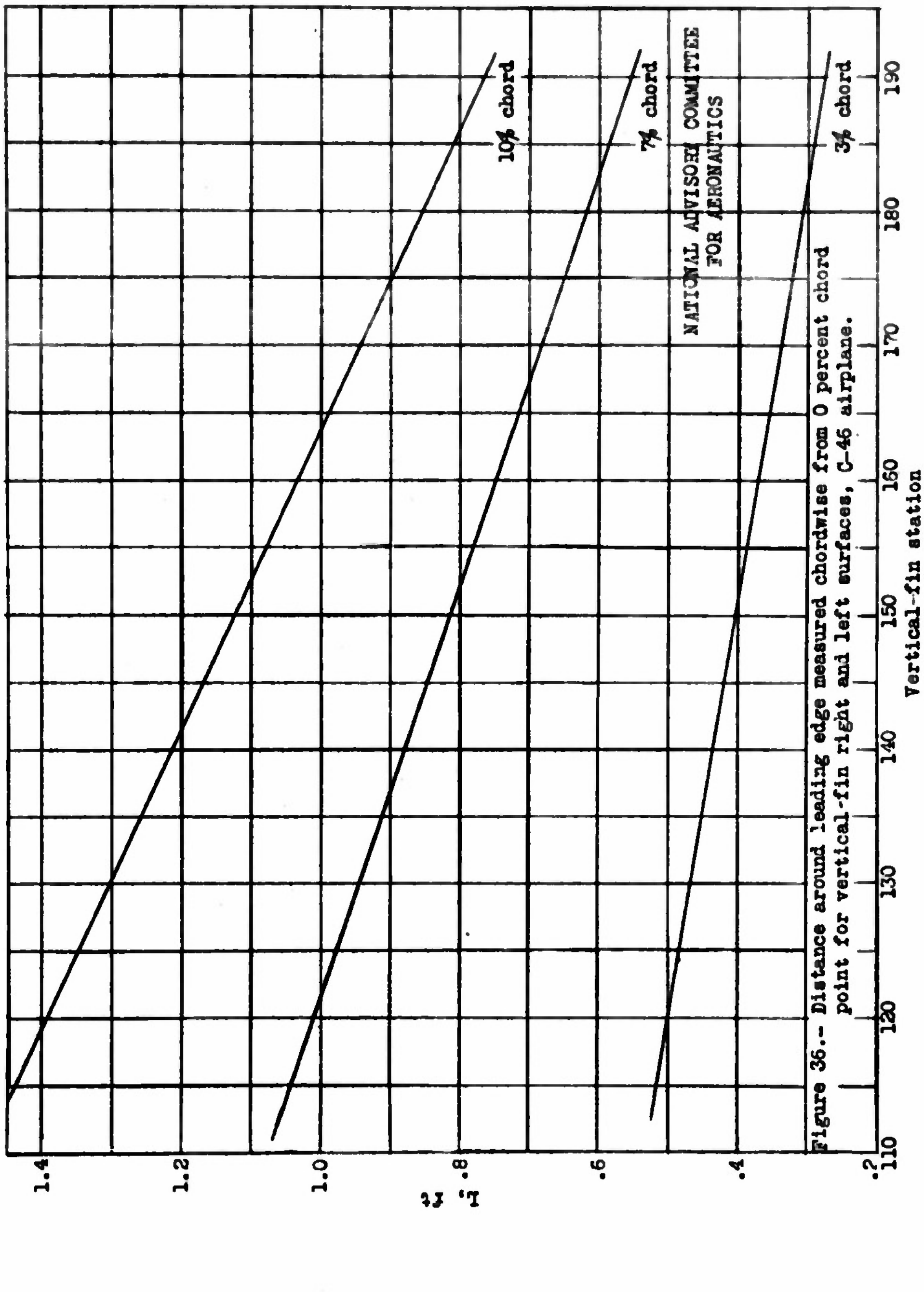

Figure 36.- Distance around leading edge measured chordwise from 0 percent chord point for vertical-fin right and left surfaces, C-46 airplane.

A-52

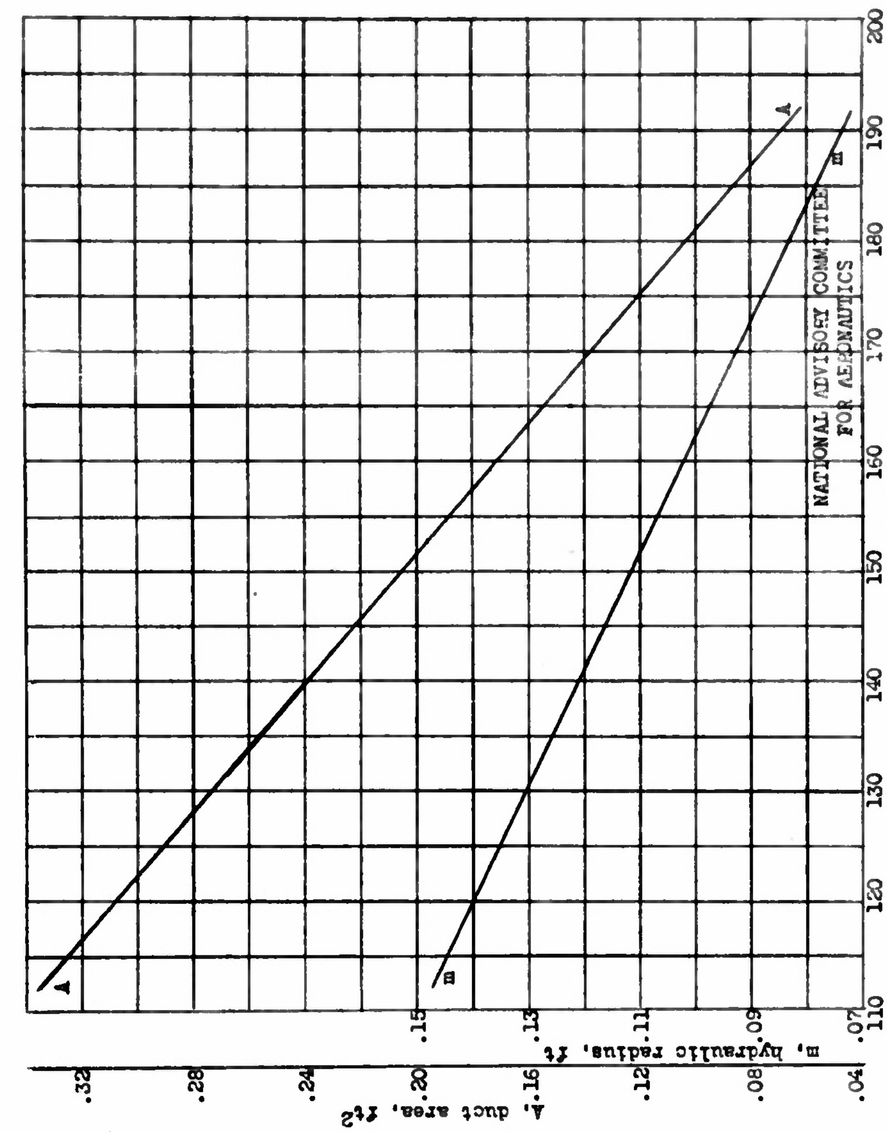

Figure 37.- Vertical-fin leading-edge-duct area and hydraulic radius, C-46 airplane.

A-52

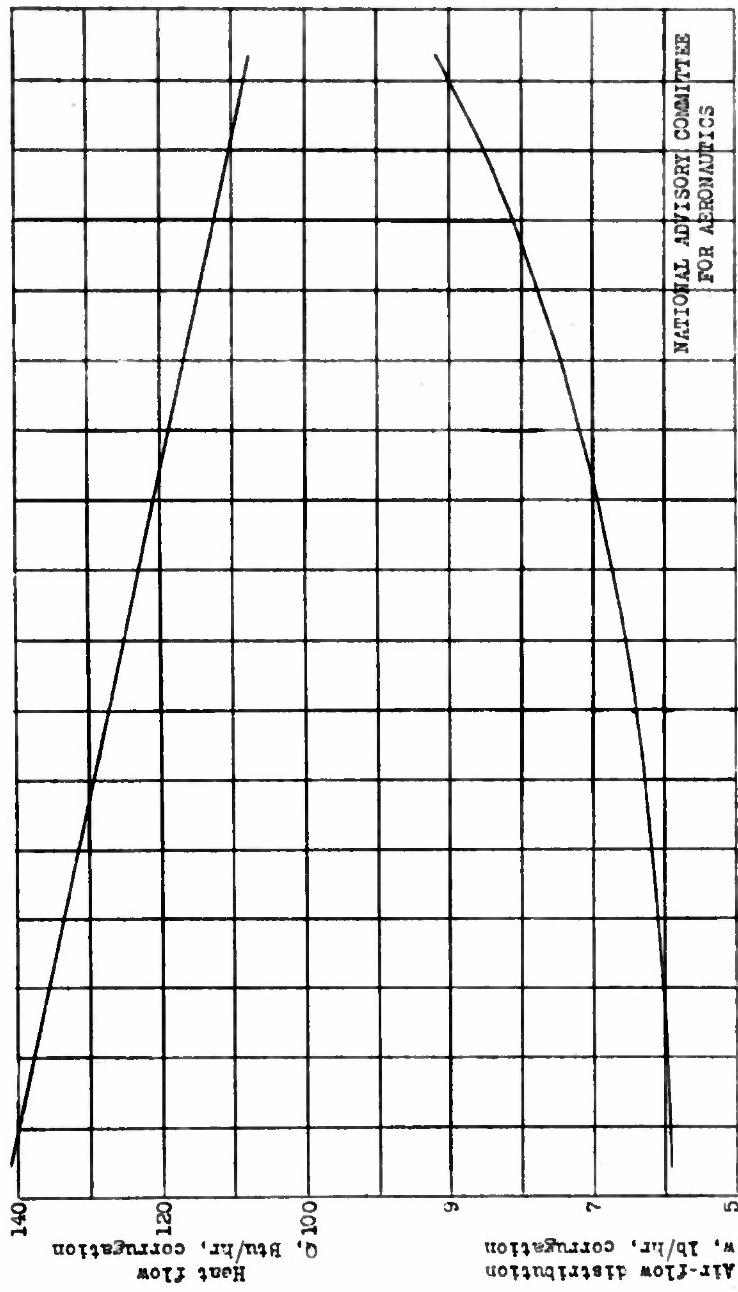

Figure 38.- Heated-air-flow distribution through leading-edge corrugations and heat flow through heated surface of vertical-fin leading edge, for one side only, C-46 airplane.

71

A-52

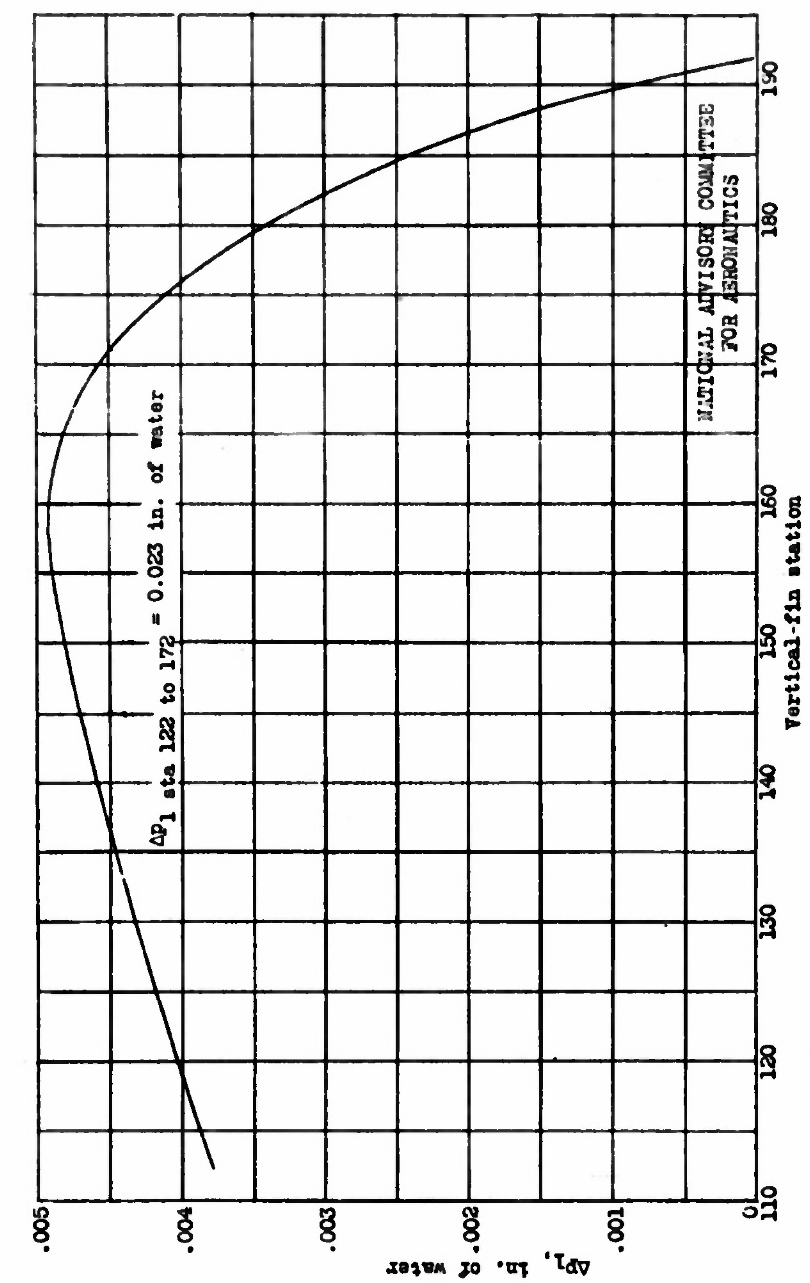

Figure 39.- Heated-air-pressure drop through vertical-fin leading-edge duct, C-46 airplane.

A-52

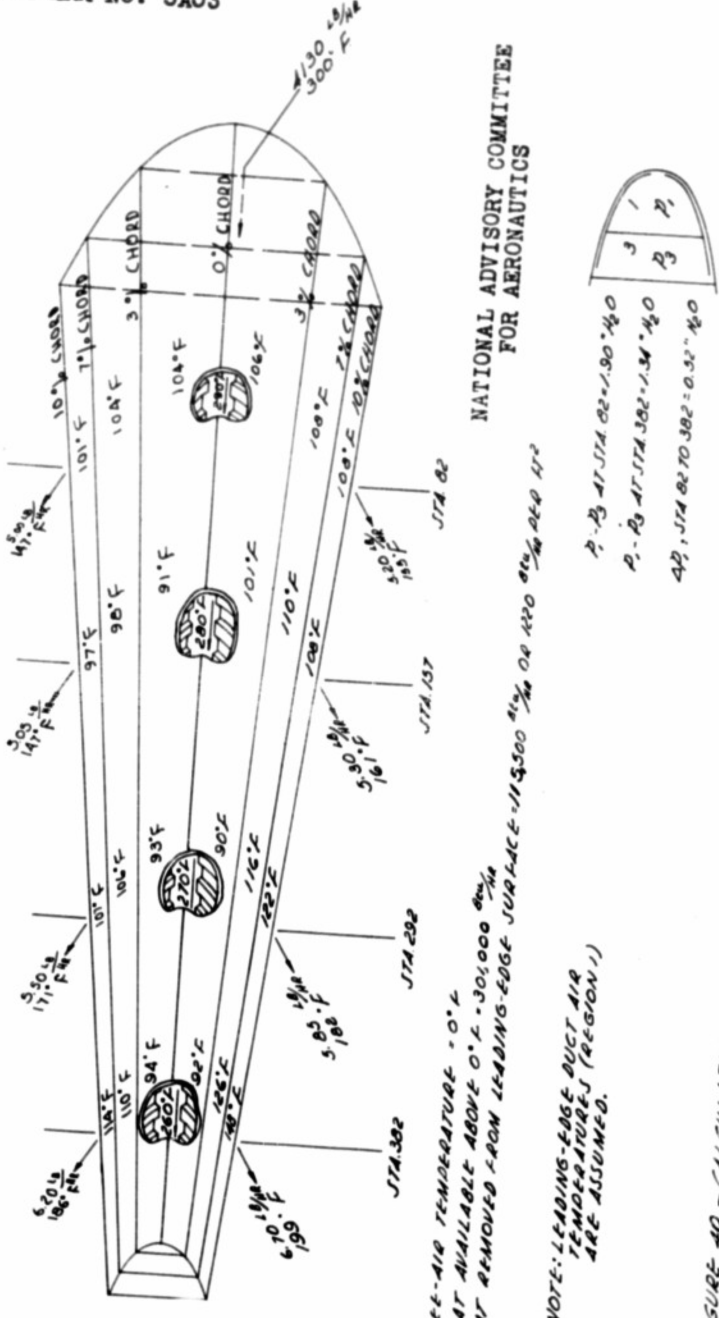

NATIONAL ADVISORY COMMITTEE
FOR AERONAUTICS

FIGURE 40.- CALCULATED HEAT AND AIR-FLOWS AND LEADING-EDGE SKIN TEMPERATURE RISES FOR THE WING THERMAL ICE-PREVENTION SYSTEM OF THE C-46 AIRPLANE.

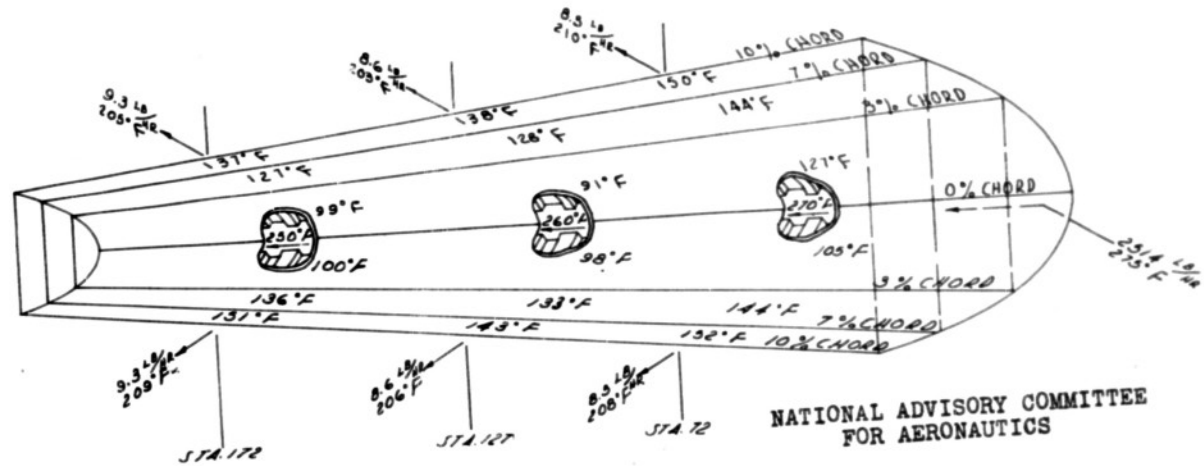

NATIONAL ADVISORY COMMITTEE
FOR AERONAUTICS

FREE-AIR TEMPERATURE = 0° F
HEAT AVAILABLE ABOVE 0° F = 167,000 BTU/HR
HEAT REMOVED FROM LEADING-EDGE SURFACE = 32,610 BTU/HR OR 1730 BTU/HR PER FT²

NOTE: LEADING-EDGE DUCT AIR TEMPERATURES (REGION 1) ARE ASSUMED.

$P_1 - P_3$ AT STA. 72 = 2.39" H_2O

$P_1 - P_3$ AT STA. 172 = 1.88" H_2O

ΔP_1, STA. 72 TO 172 = 0.49" H_2O

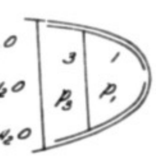

FIGURE 41.- CALCULATED HEAT AND AIR-FLOWS AND LEADING-EDGE SKIN TEMPERATURE RISES FOR THE HORIZONTAL STABILIZER THERMAL ICE-PREVENTION SYSTEM OF THE C-46 AIRPLANE.

A-52

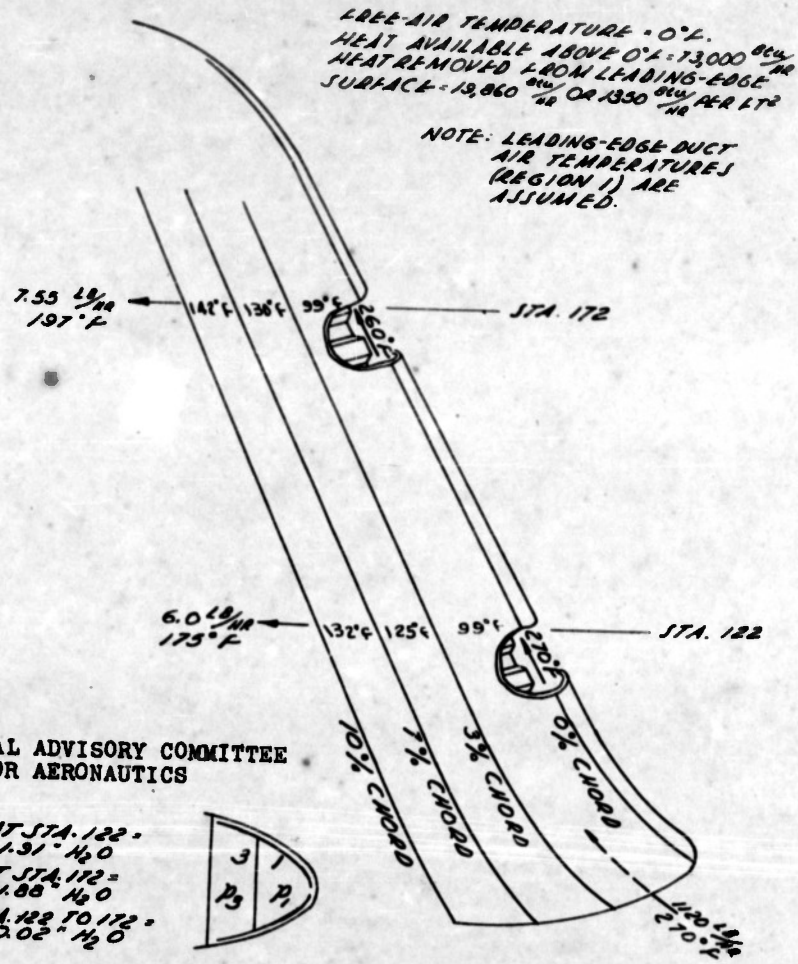

NATIONAL ADVISORY COMMITTEE
FOR AERONAUTICS

$P_1 - P_3$ AT STA. 122 = 1.91" H_2O
$P_1 - P_3$ AT STA. 172 = 1.88" H_2O
ΔP_1, STA. 122 TO 172 = 0.02" H_2O

FIGURE 42.- CALCULATED HEAT AND AIR-FLOWS AND LEADING-EDGE TEMPERATURE RISES FOR THE VERTICAL FIN THERMAL ICE-PREVENTION SYSTEM OF THE C-46 AIRPLANE.

A-52

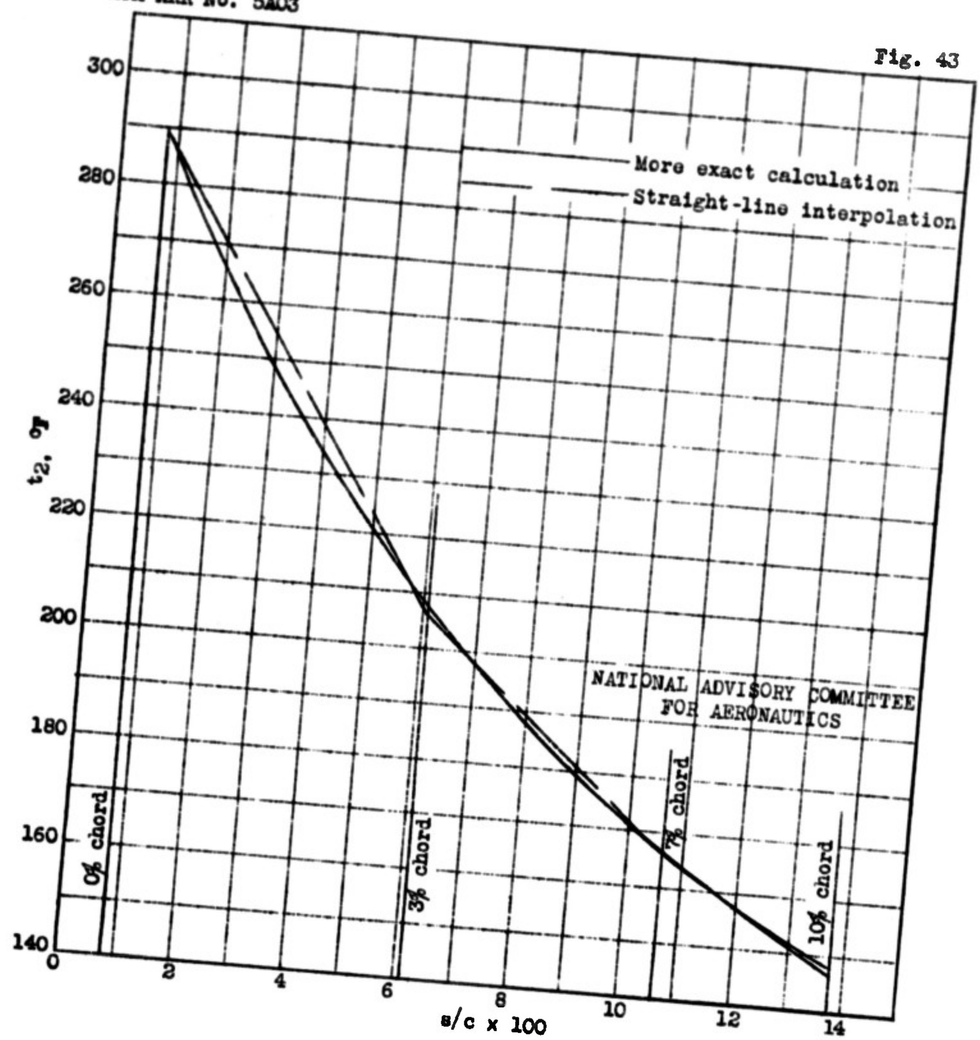

Figure 43.- A comparison of the straight-line interpolation of the heated-air-temperature change as used in the analysis with a more exact calculation for air in the upper corrugation at wing station 82, C-46 airplane.

A-52

87

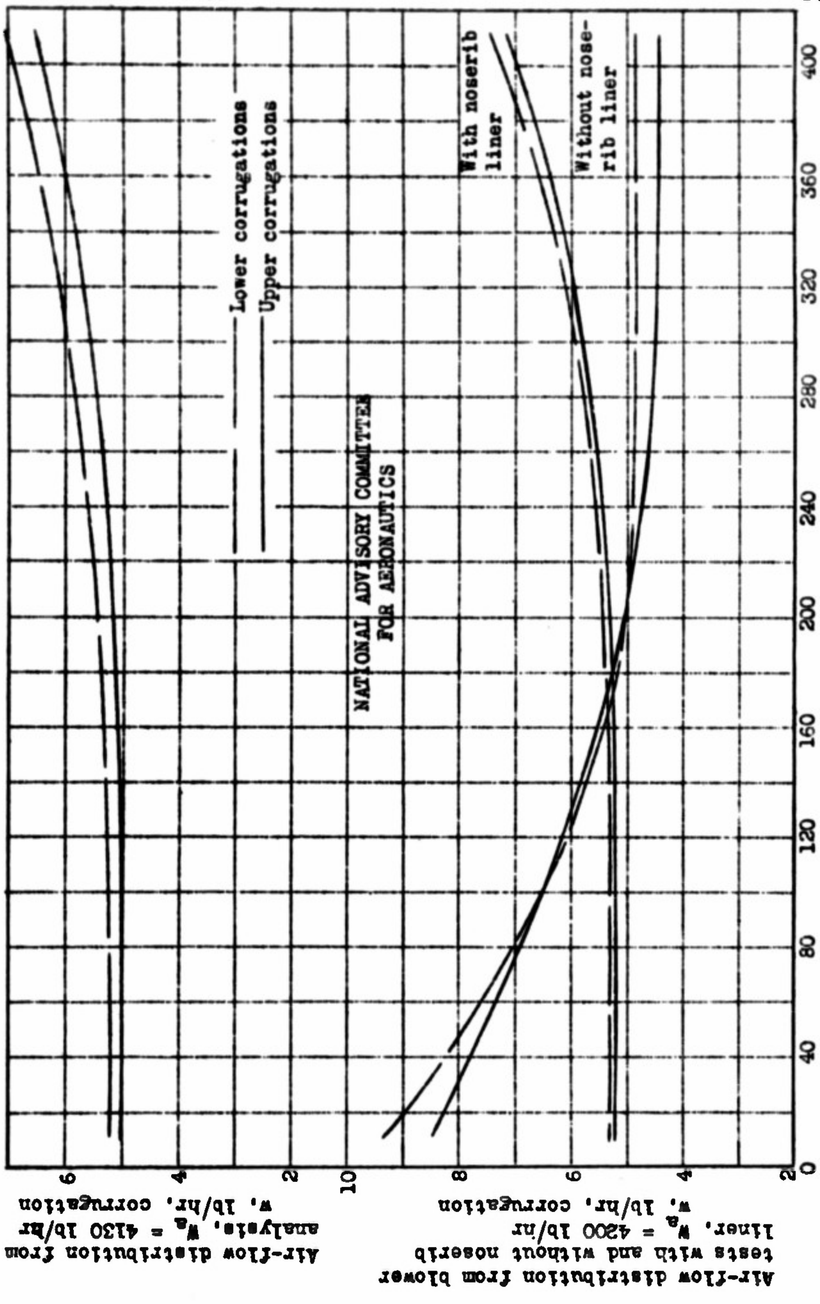

Figure 44.- Comparison of analytical heated-air distribution through corrugations with isothermal blower tests of wing leading-edge thermal system with and without noserib liner, C-46 airplane.

REEL – C

349

A.T.I.

8949

TITLE: An Investigation of a Thermal Ice-Prevention System for a C-46 Cargo Airplane - I - Analysis of the Termal Design for Wings, Empennage, and Windshield	ATI- 8949
AUTHOR(S) : Neel, Carr B.	REVISION (None)
ORIG. AGENCY : Ames Aeronautical Lab., Moffet Field, Calif.	ORIG. AGENCY NO. ARR-5A03
PUBLISHED BY : National Advisory Committee for Aeronautics, Washington, D. C.	PUBLISHING AGENCY NO. (Same)

DATE	DOC. CLASS.	COUNTRY	LANGUAGE	PAGES	ILLUSTRATIONS
Feb '45	Unclass.	U.S.	English	82	photos, tables, graphs, drwgs

ABSTRACT:

Purpose of analysis was to establish thermal requirements for C-46 ice-prevention equipment on basis of certain temperature rise for all points on heated surfaces of wings and empennage, and of a specified heat flow through outer panel of windshield. Design analysis showed that thermal requirements for anti-icing system of wings, empennage, and windshield were within limits of practicability, although complete protection of windshield could not be accomplished in specific application when utilizing a secondary heat exchanger.

DISTRIBUTION: SPECIAL. All requests for copies must be addressed to: Publishing Agency.

DIVISION: Operating Problems (31) SECTION: Icing (1)	SUBJECT HEADINGS: De-icing (28891)

ATI SHEET NO.:

Central Air Documents Office Wright-Patterson Air Force Base, Dayton, Ohio	AIR TECH. INDEX

ATI- 8949

REVISION (None)

ORIG. AGENCY NO. ARR-5A03

PUBLISHING AGENCY NO. (Same)

TITLE: An Investigation of a Thermal Ice-Prevention System for a C-46 Cargo Airplane - I - Analysis of the Termal Design for Wings, Empennage, and Windshield

AUTHOR(S) : Neel, Carr B.

ORIG. AGENCY : Ames Aeronautical Lab., Moffet Field, Calif.

PUBLISHED BY : National Advisory Committee for Aeronautics, Washington, D. C.

DATE	DOC. CLASS.	COUNTRY	LANGUAGE	PAGES	ILLUSTRATIONS
Feb '45	Unclass.	U.S.	English	82	photos, tables, graphs, drwgs

ABSTRACT:

Purpose of analysis was to establish thermal requirements for C-46 ice-prevention equipment on basis of certain temperature rise for all points on heated surfaces of wings and empennage, and of a specified heat flow through outer panel of windshield. Design analysis showed that thermal requirements for anti-icing system of wings, empennage, and windshield were within limits of practicability, although complete protection of windshield could not be accomplished in specific application when utilizing a secondary heat exchanger.

DISTRIBUTION: SPECIAL. All requests for copies must be addressed to: Publishing Agency.

DIVISION: Operating Problems (31)

SECTION: Icing (1)

SUBJECT HEADINGS: De-icing (28891)

ATI SHEET NO.:

Unclassified per authority:
Index of NACA Technical
Publication Dated 31
December 1947